SYNCHRONIZATION AND RESOURCE ALLOCATION IN DOWNLINK OFDM SYSTEMS

DOCTOR OF PHILOSOPHY

FAN WU

2010

Copyright Statement

SYNCHRONIZATION AND RESOURCE ALLOCATION IN DOWNLINK OFDM SYSTEMS

by

FAN WU

A PhD thesis submitted to the University of Plymouth

in partial fulfilment for the degree of

DOCTOR OF PHILOSOPHY

Centre for Security, Communications and Network Research

School of Computing and Mathematics

Faculty of Science and Technology

August 2010

Authorization

I hereby declare that I am the sole author of the thesis. I authorize the University of Plymouth to lend this thesis, or reproduce the thesis by photocopying or by other means in total or in part, to other institutions or individuals for the purpose of scholarly research.

Acknowledgements

First of all, I am deeply indebted to my supervisors Dr Mosa Ali Abu-Rgheff for his patient guidance, continuous support and deep insights in this project, and Dr Mohammed Zaki Ahmed for his valuable discussion and advice. Their valuable suggestions and comments helped me identify the right research topic and keep in the right track.

I am sincerely grateful to Mr Harold Wilkin from RONDO and University of Plymouth for their finance support during these years. I wish also thank the staff at the School of Computing and Mathematics and Faculty of Science and Technology for their support and help.

Finally, I would like to thank my dear parents Weijian Wu and Xujing Huang, my beloved wife Miaorui Li, and my genuine friends for their encouragement, understanding, support and patience in the whole journey.

Synchronization and Resource Allocation in Downlink OFDM systems

Fan Wu

Abstract

The next generation (4G) wireless systems are expected to provide universal personal and multimedia communications with seamless connection and very high rate transmissions and without regard to the users' mobility and location. OFDM technique is recognized as one of the leading candidates to provide the wireless signalling for 4G systems. The major challenges in downlink multiuser OFDM based 4G systems include the wireless channel, the synchronization and radio resource management. Thus algorithms are required to achieve accurate timing and frequency offset estimation and the efficient utilization of radio resources such as subcarrier, bit and power allocation.

The objectives of the thesis are of two fields. Firstly, we presented the frequency offset estimation algorithms for OFDM systems. Building our work upon the classic single user OFDM architecture, we proposed two FFT-based frequency offset estimation algorithms with low computational complexity. The computer simulation results and comparisons show that the proposed algorithms provide smaller error variance than previous well-known algorithm.

Secondly, we presented the resource allocation algorithms for OFDM systems. Building our work upon the downlink multiuser OFDM architecture, we aimed to minimize the total transmit power by exploiting the system diversity through the management of subcarrier allocation, adaptive modulation and power allocation. Particularly, we focused on the dynamic resource allocation algorithms for multiuser OFDM system and multiuser MIMO-OFDM system. For the multiuser OFDM system, we proposed a low-

complexity channel gain difference based subcarrier allocation algorithm. For the multiuser MIMO-OFDM system, we proposed a unit-power based subcarrier allocation algorithm. These proposed algorithms are all combined with the optimal bit allocation algorithm to achieve the minimal total transmit power. The numerical results and comparisons with various conventional non-adaptive and adaptive algorithmic approaches are provided to show that the proposed resource allocation algorithms improve the system efficiencies and performance given that the Quality of Service (QoS) for each user is guaranteed.

The simulation work of this project is based on hand written codes in the platform of the MATLAB R2007b.

Table of Content

List of Figures

List of Tables

Abbreviations

ACG	Amplitude Craving Greedy
AWGN	Additive White Gaussian Noise
BER	Bit Error Rate
BW	Bandwidth
BS	Basestation
BLAST	Bell Laboratories Layered Space-Time
CDMA	Code Division Multiple Access
CDPD:	Cellular Digital Packet Data
CP	Cyclic Prefix
CAZAC	Constant Amplitude Zero Auto Correlation
CSI	Channel State Information
DFT	Discrete Fourier Transform
DVB	Digital Video Broadcasting
DAB	Digital Audio Broadcasting
DPC	Dirty Paper Coding
ECBA	Extended Correlation Based Algorithm
EV	Error Variance
ETSI	European Telecommunications Standards Institute
EDGE	Enhanced Data rates for GSM Evolution
FFT	Fast Fourier Transform
FEC	Forward error correction
FDMA	Frequency Division Multiple Access
FO	Frequency Offset
GSM	Global System for Mobile Communications
GPRS	General Packet Radio Service
HIPERLAN	High Performance Radio LAN
ISI	Inter Symbol Interference
IMT	International Mobile Telecommunications

ITU	International Telecommunications Union
ITU-R	ITU Radio communication Sector
iDEN	Integrated Digital Enhanced Network
IS-95	Interim Standard 95
IDFT	Inverse Discrete Fourier Transform
IFFT	Inverse Fast Fourier Transform
ICI	Inter Carrier Interference
IAI	Inter Antenna Interference
LOS	Line of Sight
LTE	Long Term Evolution
LPF	Low pass filter
MA	Margin Adaptive
MCI	Multi Channel Interference
MF	Matched Filter
MISO	Multiple Input Single Output
MIMO	Multiple Input Multiple Output
MMS	Multimedia Messaging Service
MLE	Maximum Likelihood Estimation
MUT	Multiuser Transmission Technique
MUI	Multiuser Interference
OBA	Optimal Bit Allocation
OFDM	Orthogonal Frequency Division Multiplexing
PN	Pseudo Noise
PDF	Probability Density Function
PDC	Personal Digital Cellular
PDS	Power Density Spectrum
PSD	Power Spectral Density
PCS	Personal Communication Systems
QoS	Quality of Service
QAM	Quadrature Amplitude Modulation
QPSK	Quadrature Phase-shift Keying

RA	Rate Adaptive
RMS	Root Mean Square
SVD	Singular Value Decomposition
SNR	Signal to Noise Ratio
STC	Space Time Codes
STBC	Space Time Block Codes
STTC	Space Time Trellis Codes
SDMA	Space-Division Multiple Access
TDMA	Time division multiple access
TD-CDMA	Time Division CDMA
TD-SCDMA	Time Division Synchronous CDMA
TTP	Total Transmit Power
TACS	Total Access Communication System
WCDMA	Wideband CDMA
WLAN	Wireless Local Area Network
WMAN	Wireless Metropolitan Area Network
WSS	Wide-Sense Stationarity
ZF	Zero Forcing

Notations

$\min f(.)$	the minimum value of the function $f(.)$
$\max f(.)$	the maximum value of the function $f(.)$
$\arg\min f(x)$	the value of x (argument) that minimizes f
$\arg\max f(x)$	the value of x (argument) that maximizes f
ϕ	empty set
$\subset$	subset of
$\in$	belongs to
$(.)^{T}$	transpose of a vector or matrix
$(.)^{H}$	complex conjugate transpose of a vector or matrix
$\lVert(\cdot)\rVert$	Euclidean norm of a vector or matrix
$trace(.)$	Trace operation
$\sum_{i=1}^{n} x_i$	sum over i : $i = 1,2,\ldots,n$
$[\cdot]_{2\pi}$	2π correction
$diag(.)$	Diagonal elements of a matrix
$[.]^{+}$	psedo-inverse of a matrix

Author's Declaration

At no time during the registration for the degree of Doctor of Philosophy has the author been registered for any other University award.

This study was funded by a University bursary.

Publications:

[1] Fan Wu and Mosa Ali Abu-Rgheff, "Time and Frequency Synchronization Techniques for OFDM Systems operating in Gaussian and Fading Channels: A Tutorial", Proceeding of the 8th Annual Postgraduate Network Symposium (PGNET) on The Convergence of Telecommunications, Networking and Broadcasting, Liverpool John Moores University in 28th & 29th , June, 2007, pp. 263-268

[2] Fan Wu and Mosa Ali Abu-Rgheff, "An Efficient Sub-optimal Subcarrier Allocation Algorithm for Multiuser OFDM System", Fifth International Conference on Wireless and Mobile Communications, ISBN: 978-0-7695-3750-4, Cannes/La Bocca, France, August 23-August 29, 2009

[3] Fan Wu and Mosa Ali Abu-Rgheff, "FFT-Based Frequency Offset Estimation in OFDM Systems", The 15th IEEE Mediterranean Electrotechnical Conference, 26-28 April 2010

[4] Fan Wu and Mosa Ali Abu-Rgheff, "Efficient Resource Allocation in Downlink Multiuser MIMO-OFDM Systems", The 15th International OFDM-Workshop, Hamburg, Germany, 1-2 September 2010

[5] Fan Wu and Mosa Ali Abu-Rgheff, "Efficient Subcarrier Allocation in Downlink Multiuser MIMO-OFDM Systems", the 7th IEEE International Symposium on Wireless Communication Systems, York, UK, 19-22 September 2010

Word count of the thesis: 32,539

Signature: Fan Wu.

Date: 15/11/2010

Chapter 1

Introduction

The increased demand for reliable and secure wireless communication services is reflected in the deployment of the first generation (1G) systems to the third generation (3G) systems and the fast development of fourth generation (4G) systems to provide a comprehensive and secure all-IP based solution. The evolution of wireless communication systems are reviewed in Section 1.1. This thesis concentrates on developing efficient synchronization algorithms and resource allocation techniques for the 4G systems where the Orthogonal Frequency Division Multiplexing (OFDM) technique and Multiple Input Multiple Output (MIMO) technique play important roles in. In Section 1.2, the OFDM system and the OFDM-MIMO system under single user and multiuser environment are reviewed respectively. Section 1.3 and 1.4 describe the importance of synchronization and resource allocation in OFDM systems. Section 1.5 presents the project scope and objectives, whereas the thesis organization is given in Section 1.6.

1.1. Evolution of Wireless Communication Systems

The first telegraph network was invented by Samuel Morse in 1838 and later was replaced by the telephone [1]. In 1895, Guglielmo Marconi and Alexander Popov demonstrated the first ship-to-shore radio communication with distance of 18 miles. Radio systems have increased in importance since that time for both voice and data communication over larger distances with better quality, less power, and smaller, cheaper devices.

It is predicted that by 2010 there will be over 1700 million mobile subscribers worldwide [2]. The rapid expansion in the demand for all types of wireless services, ranging from voice and low rate data services up to high rate data and multimedia applications, has fuelled the evolution of wireless communication systems from the first generation analogue system to the third generation system that support high-speed wireless communications [3].

- The first generation of cellular wireless system (1G)

  The 1G system operates on 800 MHz-900MHz band and uses Frequency Division Multiple Access (FDMA) technology to divide the total system bandwidth into specific frequency channels that are assigned to individual user to transmit analogue voice signals with the low date rate between mobile phones and near-by radio stations. For example, the Total Access Communications System (TACS) used in the UK divides the bandwidth spaced by 25 kHz and provides 8 kb/s data rate, and the Advanced Mobile Phone System (AMPS) used in USA divides the bandwidth spaced by 30 kHz and provides 10 kb/s data rate. The 1G system was first launched in late 1970s to early 1980s and has been out of our sight gradually.

- The second generation of cellular wireless system (2G)

  In 1990s, two types of 2G system were standardized and deployed. One is deployed in Europe originally under the name of cellular mobile systems (CMS) such as Global System for Mobile Communications (GSM), which is more prevalent today and with cell radius length of 3-5 kilometres. The other is called as the personal communication systems (PCS) deployed in

USA originally which has much smaller cells, typically 200-500 meters in radius. In PCS, the distance between mobile phones and the near-by base station is shorter than that in CMS, which reduces the power required to transmit signals and improves the voice quality. However, a larger number of cells is required in PCS to cover the same area, thus making it suitable to more densely populated metropolitan and urban areas.

Compared with 1G, the 2G system provides the digital data services such as short messaging in addition to voice over a radio channel. It improved voice security and quality, and increased capacity to handle calls with higher data rates which is between 9.6 kb/s to 14.4 kb/s. The standards used in Europe and Japan such as GSM and Personal Digital Cellular (PDC) are employing the Time Division Multiple Access (TDMA) technology where time is divided orthogonally and each channel occupies the entire frequency band over its assigned timeslot. In North America and part of Asia, the Interim Standard 95 (IS-95) standard exists with GSM. It uses the Code Division Multiple Access (CDMA) technique which employs spread spectrum technology and a special coding scheme to allow multiple users to be multiplexed over the same channel. Overall speaking, these standards-based systems all allow more efficient use of the radio spectrum than the previous FDMA technology [4].

But there are too many standards for 2G systems because of the great market potential such as IS-95, Integrated Digital Enhanced Network (iDEN) in USA, and GSM900, PDC in Europe and Japan. These standards are all incompatible and do not interoperate with each other. This fact makes the roaming between different countries impossible if they use different standards. Thus many cellular phones today are multi-mode. In addition, Pulse nature of TDMA transmission used in 2G interferes with some electronics, especially certain audio amplifiers.

Currently, there are some enhanced technologies for the evolved 2G system, such as General Packet Radio Service (GPRS). The data rate can reach from 56 kb/s to 144 kb/s. The GPRS extends the GSM and make more services available such as the "Always on" internet access and Multimedia messaging service (MMS). Subsequently, the Enhanced Data rates for GSM Evolution (EDGE) which is known as Enhanced GPRS, is developed to improve the data rates further. It provides the data transmission rate up to 236.8 kb/s, and requires no hardware or software changes to be made in GSM core networks. It meets the International Telecommunications Union (ITU) requirement for a 3G network. With EDGE, the service providers can offer more wireless data application including web-based email and video conferencing.

- The third generation of cellular wireless system (3G)

In late 1990s, the standardization of the 3G systems was started [2]. The main characteristics of 3G systems known collectively as International Mobile Telecommunications (IMT) –2000 is a set of requirements defined by the ITU. Many 3G standards are developed according to IMT-2000. The main standards used in 3G systems are the wideband CDMA (WCDMA) standard and Universal Mobile Telecommunication System (UMTS), which provides different data rates depending on mobility and location, from 384 kb/s for pedestrian use to 144 kb/s for vehicular use to 2 Mb/s for indoor office use. In addition, the 3G mobile services are compatible with 2G networks. Therefore, the appearance of 3G provides higher data transmitting speed, increases support for multimedia data applications, such as video and photography, and keep constantly online which means customers are charged by the quantity of data they transmitted, not the time connected to the network. However, the 3G systems still have some remaining problems shown as follow:

a. There are many 3G standards such as UMTS in Europe, CDMA2000 in USA and Time Division Synchronous CDMA (TD-SCDMA) in China. It is still difficult to achieve globe seamless roaming.
b. Transmitting speed is still not high enough to satisfy multimedia requirements.

Furthermore, the Third-Generation Partnership Project (3GPP) works on further extensions to 3G standards and tries to make a globally applicable 3G mobile phone system specification. It is named as Long Term Evolution (LTE) and developed according to the specifications already displayed for the fourth Generation (4G) systems by IMT. Its specification provides downlink peak rates of at least 100 Mb/s, and uplink of at least 50 Mb/s. It also supports both frequency division duplexing (FDD) and time division duplexing (TDD) in the same platform, and seamless passing to cell towers with older network technology such as GSM and W-CDMA. LTE is the last step towards to 4G systems and classified as Pre-4G.

- The fourth Generation (4G) Communication systems

Currently, wireless communication is moving towards the Next Generation ('beyond 3G' or '4G') featured by all-IP based networks, seamless connection, high mobility, and very high rate transmissions [2, 5, 6]. 4G system is expected to support at least 100 Mb/s peak rates in fullmobility wide area coverage and 1 Gb/s in low-mobility local area coverage, according to the requirements of the ITU-Radiocommunication Sector (ITU-R) [4]. It is projected to solve the remaining problems of 3G systems as mentioned previously.

The 4G system will operate on a global standard that provides global mobility and service portability so that service provider will no longer be limited by single-system [3]. In other words, 4G should be able to provided very smooth global roaming ubiquitously. Furthermore, the 4G standard will be broadband IP-based and entirely applying packet switching for transmission with seamlessly access convergence [2]. It means that 4G integrated all access technologies, services and applications can unlimitedly be run through wireless backbone using IP address.

In addition to high data rates, future system must support a higher Quality of Service (QoS) than current cellular systems, which are designed to achieve 90 - 95% coverage [6]. Thus, 4G systems are likely to require a QoS close to 100%. In order to achieve this goal, the communication system is required to be more flexible and adaptive. In many applications it is more important to maintain network connectivity than the actual data rate achieved [5]. If the channel is very poor, the data rate has to drop to maintain the link. Alternatively, for applications requiring a fixed data rate, the QoS can be improved by allocating additional resources to users with a poor transmission path. Currently, a large part of European research activities on 4G have been gathered into the WINNER project [7], while other parallel activities have been carried out, e.g. in the Wireless World Research Forum [8] or the Chinese FuTuRE project [9, 10].

Orthogonal Frequency Division Multiplexing (OFDM) technique has the potential to surpass the capacity of CDMA systems and to provide the wireless access method for 4G systems [5]. In addition, the Multiple Input

Multiple Output (MIMO) technique is combined with OFDM to be considered in various multiuser systems including ADSL, Digital Video Broadcast (DVB), Digital Audio Broadcast (DAB), European Telecommunication Standard Institute's (ETSI) HIPERLAN/2, high-speed wireless local area networks (WLAN) and 4G systems [11,12,13].

1.2. OFDM Architecture Background

The OFDM and MIMO-OFDM technologies are used in the project systems and are introduced in this section. The multiple access techniques are also combined with these systems to optimize the resource sharing between multiple users.

1.2.1. Review of OFDM Technique

Orthogonal Frequency Division Multiplexing (OFDM) is a high speed multi-carrier transmission technique which divides the spectrum to many sub-carriers and each subcarrier being modulated by a low data rate stream. As shown in Figure.1.1, OFDM technique makes the sub-carriers overlapping but orthogonal each other to increase the spectral efficiency by comparing with Frequency Division Multiplexing (FDM) technique.

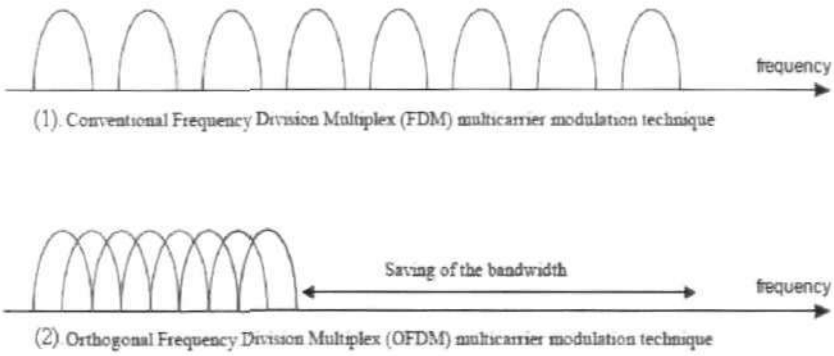

Figure.1.1. (1).FDM spectrum and (2).OFDM spectrum [112]

Signals are orthogonal if they are mutually independent of each other. Orthogonality is a property that allows multiple information signals to be transmitted perfectly over a common channel and detected, without interference [17]. In OFDM system, information is allocated to subcarriers where each one has a sinusoid. The summation of these sinusoids is the OFDM signal. There are two conditions to achieve the orthogonality between subcarriers. First, all subcarriers have an integer number of cycles per OFDM symbol. Second, the adjacent subcarriers are also chosen to be exact one cycle difference per OFDM symbol.

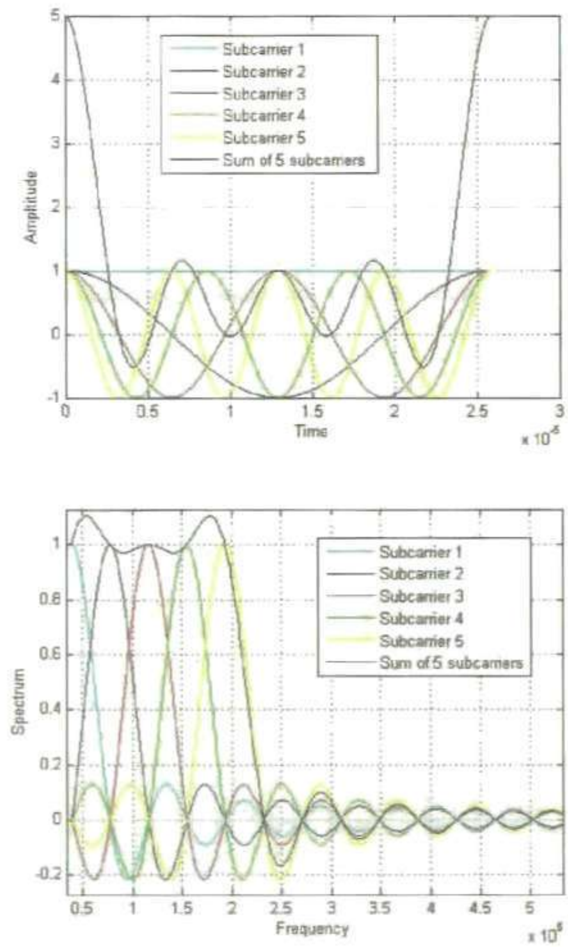

(a)

(b)

Figure.1.2. (a) Time domain construction of an OFDM signal with 5 subcarriers (b) Spectrum of OFDM signal with 5 subcarriers

Figure.1.2 shows the construction of 5 subcarriers for an OFDM signal in both time and frequency domain. In (a), 5 subcarriers are content with the two conditions of Orthogonality. In (b), each subcarrier has a peak at the centre frequency and nulls evenly spaced by a gap equal to the carrier spacing, and the peak of each subcarrier is corresponding to the nulls of all other subcarriers, which represents the Orthogonality between subcarriers.

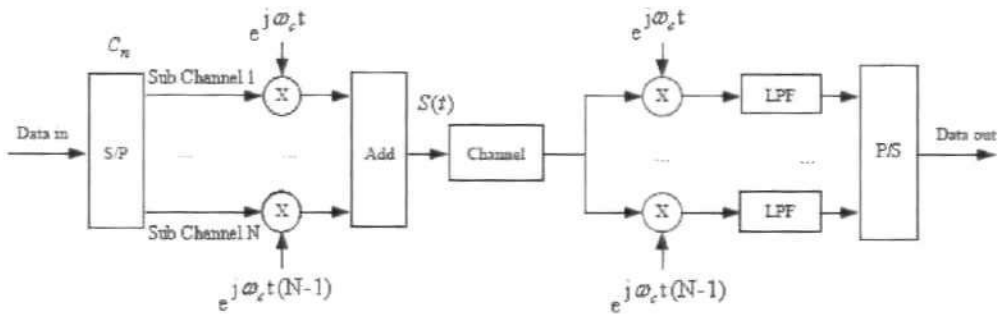

Figure.1.3. Theoretical OFDM system model [18, 21-23]

The model of theoretical OFDM systems [18, 21-23] is shown in Figure.1.3. ω_c is the angular frequency shift between subcarriers, and is equal to $(2\pi.\frac{1}{NT_s})$ where T_s is the sample interval, N is the number of subcarriers and $\frac{1}{NT_s}$ is the subcarrier spacing frequency. The OFDM transmitted signal is given by:

$$S(t) = \sum_{n=0}^{N_c-1} c_n e^{jn\omega_c t} \tag{1-1}$$

where c_n is the baseband modulated data. We can see that lots of oscillators are needed to generate the subcarriers in the transmitter and lots of Low-Pass Filters (LPF) for demodulation in receiver, which make OFDM not suitable for practical use. In 1970s, S. Weinstein proposed to apply the Discrete Fourier Transform (DFT) to reduce the difficulties of modulation and demodulation [14]. For discrete time, subcarriers are sampled by kT_s ($k = 0,1,...N$), the OFDM transmitted signal can be written as:

$$S(k) = \sum_{n=0}^{N_c-1} c_n e^{j2\pi.nk/N} \tag{1-2}$$

The Equation (1-2) is the Inverse Discrete Fourier Transform (IDFT) which can be computed efficiently using Inverse Fast Fourier Transform (IFFT) algorithm. The typical OFDM system model is shown in Figure.1.4.

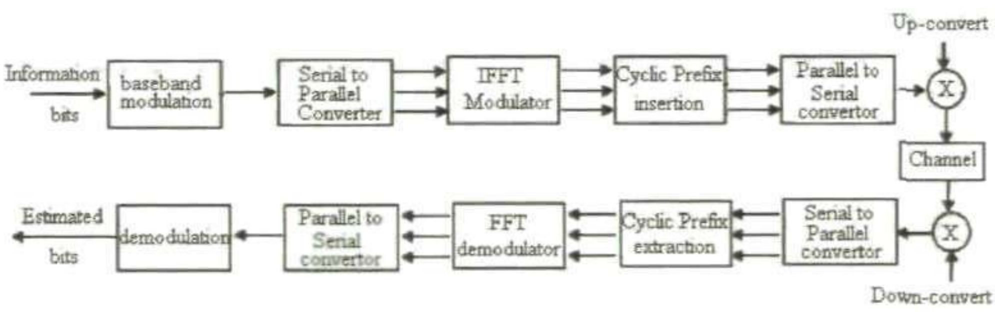

Figure.1.4. Typical OFDM system model

Furthermore, in the existing 2G and 3G systems, the Inter-symbol-interference (ISI) imposed by multipath effect which will be described in Chapter 3, can be efficiently mitigated by the use of an complex equaliser. As shown in Figure.1.4 of OFDM system, the cyclic prefix (CP) the cyclic prefix (CP) is chosen to be longer than the channel delay spread which is the time difference between first path and the last path, and inserted into the beginning of OFDM symbol S_k , and then the CP-added OFDM symbol is converted from parallel status to serial status and up-converted for transmission. And in the receiver side, the CP is discarded so that the ISI can be eliminated easily because the interfered samples caused by the ISI only exist in the CP range. This significantly simplifies the channel equalisation at the receiver in comparison with conventional single-carrier modulation. The received signal is down-converted first followed by the serial-to-parallel conversion, and then recovered by using the Fast Fourier Transform (FFT) algorithm. Finally the recovered data is demodulated to achieve the original information bits.

Although OFDM provides many advantages over traditional transmission techniques, OFDM system has some main drawbacks including its high sensitivity to frequency and timing offset.

1.2.2. Review of MIMO and MIMO-OFDM Systems

MIMO system

Currently, the principal technique combined with the future OFDM based wireless communication systems is MIMO technique [20, 21]. Due to the promising gain in channel capacity and dramatic improvement in physical-layer performance, MIMO systems attract significant attention in wireless communications recently [24-27, 32], and will play an important role in future wireless communication system. In MIMO system, multiple antennas are deployed at both the transmitter and receiver in order to exploit the spatial dimension freedom, and combat the harmful effects in mobile radio communication. For example, in complex wireless fading channel, MIMO system can significantly improve the link reliability without sacrificing the bandwidth efficiency, and increase the data throughput and link range without additional bandwidth or transmit power [28] [29].

MIMO technique constitutes a cost-effective approach to high-throughput wireless communications. The concepts of MIMOs have been under development for many years in wireless systems. The earliest MIMO applications in wireless communications date back to the mid-1980s, when Winters in [93-95] published a number of breakthrough contributions. He introduced a technique of transmitting data from multiple users using multiple antennas at both the transmitter and receiver ends. Since then, Winters and others have made further significant advances in the field of MIMOs [96-100], especially in [98], G. J. Foschini refined new approaches to MIMO technique which is called as Bell Laboratories Layered Space-Time (BLAST). The BLAST is offering spatial multiplexing by allocating data over transmit antennas so that the multiple data streams can be transmitted simultaneously within a single frequency band to improve the data capacity of the system effectively and result in a multiplexing gain. Other MIMO techniques employ the Space Time Codes (STC) to explore the space diversity and result in a diversity gain. There are two types of STC which are Space Time Trellis Codes (STTC) and Space Time Block Codes (STBC) [101, 102]. STTC uses convolutional encoders to encode the signal and then create separate streams. Each stream is transmitted over a transmit antenna. The receiver decodes the signal using a Viterbi decoder. For STBC, the data is split into blocks. Each data block is sent independently after converting from serial to parallel over different antennas, and then the data is retransmitted in different formats for t time slots and each antenna transmits a different symbol every time slot. In receiver, the signals received over t time slots are combined for decoding. By comparing STTC with STBC, STBC is straightforward design over every time slot and STTC requires more complicated Viterbi algorithm to achieve maximum likelihood decoding.

However, multi-channel interference (MCI) is the key problem in MIMO system. The channel inversion and SVD techniques are proposed to overcome this problem [87, 103]. The channel inversion is using the inversed channel matrix as the pre-processing in transmitter in order to separate the multiple channels and cancel MCI. The SVD is using the right singular matrix as pre-processing in transmitter, and left singular matrix as post-processing for signal reconstruction in receiver, so that the data is only weighted by real singular values without MCI after transmitting in the channel.

MIMO-OFDM system

In a very high data rate MIMO communication system, the radio channel introduces the ISI. In this case, MIMO systems require highly complex equalization techniques. However, OFDM simplifies the channel equalisation by inserting CP, and OFDM also converts the frequency-selective channel into a set of parallel flat-fading channels so that the MIMO-related algorithms easy to be implemented with OFDM systems [83]. Therefore OFDM can be combined with MIMO transceiver to increase the diversity gain including the spatial diversity obtained by spatially separated antennas in a multipath scattering environment and the frequency diversity obtained by the data transmission in multiple frequency components, with the aim of combating signal fading, enlarging the system capacity, and improving the transmission rate, the transmission range and the transmission reliability. The comprehensive overview of MIMO techniques in OFDM system is given in [111].

A MIMO-OFDM system transmits independent OFDM modulated data from multiple antennas simultaneously. At the receiver, after OFDM demodulation, MIMO decoding on each of the subcarriers extracts the data from all the transmitting antennas on all the subcarriers. The block diagram of a MIMO-OFDM system with N_T transmit antennas and N_R receive antennas is shown in Figure.1.5. At the transmitter side, the input data is converted in parallel and distributed over N subcarriers, so that there are M data streams $d(n)$ in the n^{th} subcarrier. The data streams are weighted by a $N_T x M$ Pre-coder matrix $F(n)$ in the n^{th} subcarrier, and the weighted data streams from all N subcarriers generate the inputs of IFFT processors of N_T transmit antennas. Consequently, the outputs of the $n_T{}^{th}$ IFFT processor are inserted by the CP to generate the signal ready to be sent in the $n_T{}^{th}$ transmit antenna. At the receiver, the data stream in the $n_R{}^{th}$ receive antenna is processed by FFT processor after removing CP. Then the outputs of all FFT processors are derived with the precoding and channel information. Finally, the original data is estimated in the Detector.

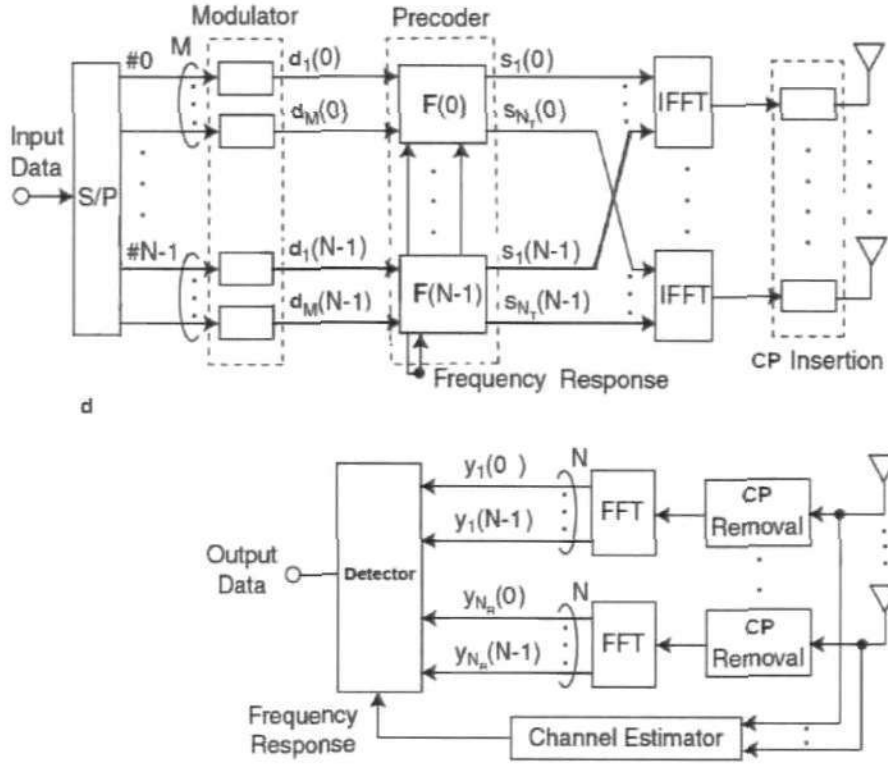

Figure.1.5. MIMO-OFDM System

The received data vector in the n^{th} subcarrier $y(n)$ can be expressed as:

$$\mathbf{y}(n) = \mathbf{H}(n)\mathbf{s}(n) + \mathbf{w}(n) \tag{1-3}$$

where

$$\mathbf{s}(n) = \mathbf{F}(n)\mathbf{d}(n) \tag{1-4a}$$

$$\mathbf{H}(n)=\begin{bmatrix} H(n,1,1) & H(n,1,2) & \cdots & H(n,1,N_T) \\ H(n,2,1) & H(n,2,2) & \cdots & H(n,2,N_T) \\ \vdots & \vdots & \cdots & \vdots \\ H(n,N_R,2) & H(n,N_R,2) & \cdots & H(n,N_R,N_T) \end{bmatrix} \tag{1-4b}$$

$$\mathbf{F}(n)=\begin{bmatrix} F(n,1,1) & F(n,1,2) & \cdots & F(n,1,M) \\ F(n,2,1) & F(n,2,2) & \cdots & F(n,2,M) \\ \vdots & \vdots & \cdots & \vdots \\ F(n,N_T,1) & F(n,N_T,2) & \cdots & F(n,N_T,M) \end{bmatrix} \tag{1-4c}$$

$$\mathbf{d}(n)=\left[d(n,1),d(n,2),\dots.\ d(n,M)\right]^T \tag{1-4d}$$

$\mathbf{H}(n)$ is the $N_R x N_T$ channel frequency response matrix in the n^{th} subcarrier, and $\mathbf{w}(n)$ is the noise vector. In addition, the number of data streams M for each subcarrier is usually chosen according to equation (1-5), so that the data in the receiver can be easily detected under this condition. Because as shown in (1-3) and (1-4), there are N_R equations with M unknown data variables in the receiver data detector if the precoder information is also known by receiver. So if system meets the condition of (1-5), these unknown data variables can be estimated, otherwise additional technique such as STC has to be applied for data recovery.

$$M \le \min(N_T, N_R) \tag{1-5}$$

1.2.3. Multiuser OFDM and MIMO-OFDM Systems

One of the main limitations for wireless communication systems is that the bandwidth must be shared by multiple users [1, 19]. Traditionally, the radio resources have been shared between users in time, frequency and/or code domains, using time-, frequency- or code division multiple access (TDMA, FDMA or CDMA), respectively [1, 19]. The multi-carrier system can also be combined with the multiple access method to provide separation of multiple users. Orthogonal frequency division multiple-access (OFDMA) combines FDMA with OFDM by assigning a unique set of subcarriers to each user, and then the receiver processes the received signal to separate the transmitted signal for users according to their assigned subcarriers. For static allocation, the subcarriers allocated to each user are fixed without considering the channel conditions, therefore dynamic resource allocation is required to provide flexibility to allocate different QoS to different users based on users' channel conditions. For OFDMA, one subcarrier can only be used by one user at given time. However, for the multiuser MIMO-OFDM system, the subcarrier is allowed to be shared between several users. Further research on dynamic resource allocation in OFDMA system and multiuser MIMO-OFDM system at the downlink is discussed in Chapter 5.

In a K users downlink MIMO-OFDM system as shown in Figure.1.6, N_T antennas are located in transmitter and N_k antennas are located at the k^{th} user. At the transmitter, the data are processed before transmission, which we refer to as transmit preprocessing, and then launched into the MIMO channel. Let $\mathbf{d}_{k,n}$ represent the $L_k \times 1$ simultaneously transmitted data symbol vector(s) for the k^{th} user at the n^{th} subcarrier. This data symbol vector is passed through a transmit precoder $\mathbf{F}_{k,n}$ which is a $N_T \times L_k$ matrix, in order to output N_T terms

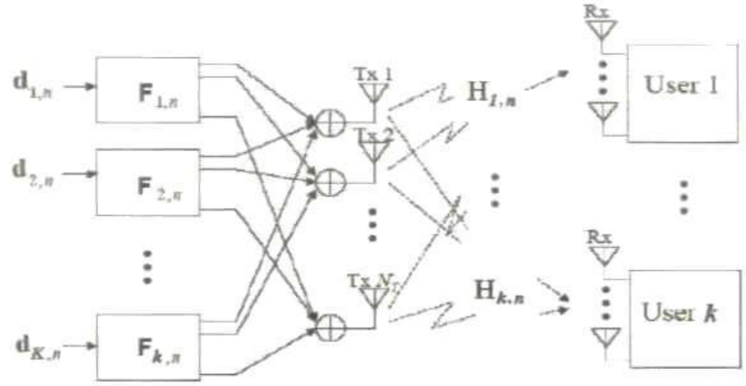

Figure.1.6. Downlink multiuser MIMO-OFDM system at the n^{th} subcarrier [83]

to be the data transmitted to the k^{th} user over N_R antenna at the n^{th} subcarrier. We also refer $\mathbf{H}_{k,n}$ as the MIMO channel for user k, which is a $N_k \times N_T$ matrix. At the receiver of user k, the receive signals can be written as:

$$\begin{aligned} \mathbf{y}_{k,n} &= \mathbf{H}_{k,n} \sum_{k=1}^{k \in S_n} \mathbf{F}_{k,n} \sqrt{\mathbf{P}_{k,n}} \mathbf{d}_{k,n} + \mathbf{w}_{k,n} \\ &= \mathbf{H}_{k,n} \mathbf{F}_{k,n} \sqrt{\mathbf{P}_{k,n}} \mathbf{d}_{k,n} + \mathbf{H}_{k,n} \sum_{i=1, i \neq k}^{i \in S_n} \mathbf{H}_{k,n} \mathbf{F}_{i,n} \sqrt{\mathbf{P}_{i,n}} \mathbf{d}_{i,n} + \mathbf{w}_{k,n} \end{aligned} \tag{1-6}$$

where S_n is the set of users who transmit data simultaneously on the n^{th} subcarrier and $S_n \in [1,2,...K]$. As shown in equation (1-6), the second term represents the multiuser interference (MUI) which affects the signal reception of user k. Several methods have been developed to cancel this interference such as Zero Forcing (ZF) and Singular value Decomposition (SVD). Further details are described in Chapter 5. The MCI which is also called as Inter-antenna Interference can be cancelled with the aid of SVD. Finally the data can be easily recovered.

1.3. Importance of Synchronization in OFDM System

As described in Section 1.2.1, Synchronization is one of the main drawbacks and has been one of the crucial research topics in OFDM system because of its sensitivity to the timing and frequency errors [33]. To guarantee the fast and accurate data transmission, ISI and Inter Carrier Interference (ICI) caused in the transmission have to be eliminated or reduced to minimum. In OFDM system, ISI can be avoided by inserting CP with length greater than the channel delay spread, and the ICI can be eliminated by maintaining the orthogonality between carriers under the condition that the transmitter and the receiver have the exact same carrier frequency. But in the real mobile transmission, frequency offset (FO) (Δf) will be arising from the frequency mismatch of the transmitter and the receiver oscillators and the existence of Doppler shift in the channel. The consequence caused by frequency offset is shown in Figure.1.7 (b). By comparing with Figure.1.7 (a), the FO results in the reduction of the amplitude of desired signal and introduces the ICI.

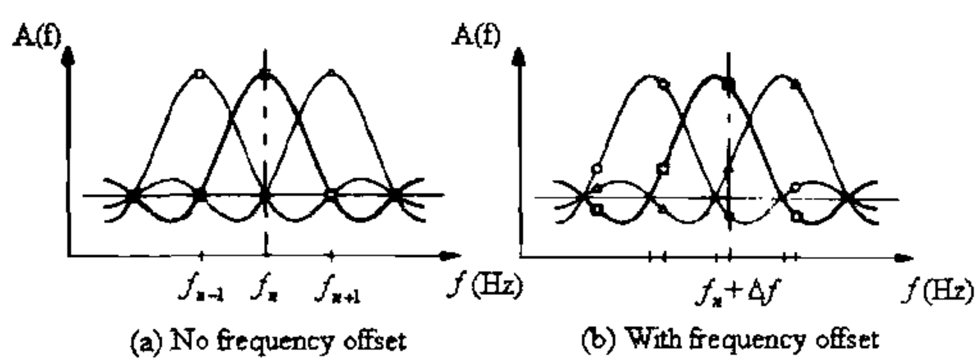

Figure.1.7. OFDM symbol spectrum [112]

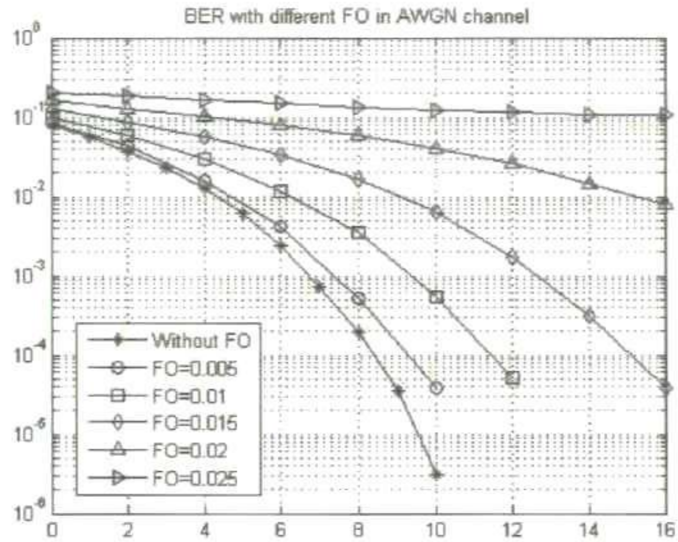

(a)

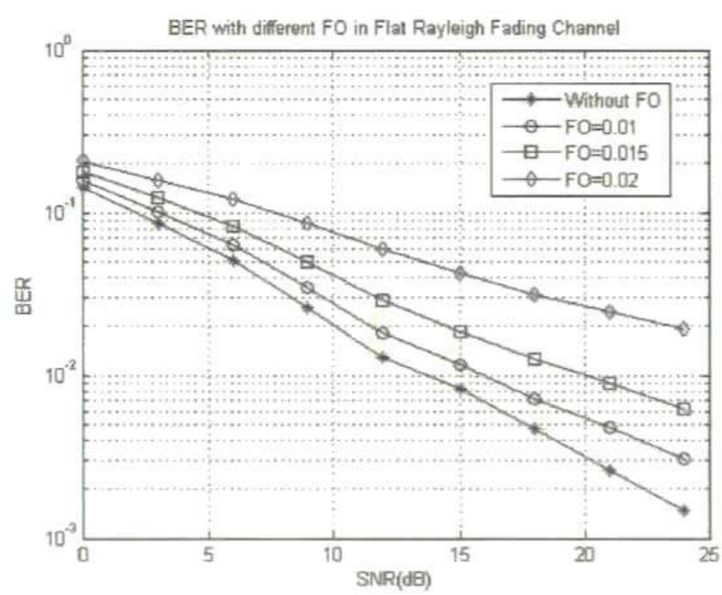

b)

Figure.1.8. BER performances with different normalized FO in (a) AWGN channel (b) Rayleigh flat fading channel

Also as shown in Figure.1.8, in both AWGN channel and Rayleigh flat fading channel which is described in Chapter 3, the higher frequency offset which is normalized to subcarrier spacing will cause the higher BER in OFDM system. The reason is the higher frequency offset leads higher phase shift that rotates the desired signal out of the correct decision region. In addition, due to the delay of signal when transmitting in the channel, the receiver in general starts sampling a new frame at the incorrect time instant. Therefore, it is important to estimate the frequency offset to minimize its impact, and to estimate the timing offset at the receiver to identify the start time of each frame and the FFT window position for each OFDM.

1.4. Importance of Resource Allocation in Multiuser OFDM System and Multiuser MIMO-OFDM System

As described in Section 1.2.3, the FDMA multiple access technique is combined with OFDM for multiple users to share the available bandwidth which are the subcarriers of OFDM system. For the static allocation method, each user is allocated a number of subcarriers which are fixed all the time. However, the subcarriers that experience deep fade with bad channel condition to one user may not be in deep fade for other users. In fact, it is quite unlikely that a subcarrier will be in deep fade in all users' channels, as the fading parameters for different users' channels are mutually independent. Therefore the dynamic resource allocation scheme where the subcarriers are assigned to the users based on users' channel state information (CSI) is required. Channel-aware adaptive resource allocation has been shown to achieve higher system performance than static resource allocation, and is becoming more critical in current and future wireless communication systems as the user data rate requirements increase [34]. Similarly, in multiuser MIMO-OFDM system, its spectral efficiency can be increased if the system effectively adapts to the radio channel and take advantage of the available resource in both frequency and space domains. By working with users' CSI, we aim to achieve the optimal subcarriers set assigned to each user in multiuser OFDM system and the optimal set of users sharing each subcarrier in multiuser MIMO-OFDM system. This dynamic resource allocation process normally has two goals. One is minimizing the total transmit power given the constraints on the users' data rate, and another is maximizing the overall data rate with a total transmit power constraint.

In this thesis, we consider the time division duplex (TDD) system, which uses the same carrier frequency alternately for transmission and reception, and thus, for the downlink transmission, the CSI can be tracked at the base station (BS) according to the previous received uplink frame. We assume the perfect channel estimation is carried out so that BS can achieve the dynamic resource allocation by using the perfect users' CSI.

1.5. Scopes and Objectives of the Project

The scope of this thesis in a broad sense is concentrating in two aspects. One is the Synchronization in OFDM system, and another one is the Downlink Resource Allocation in Multiuser OFDM system and Multiuser MIMO-OFDM system. In particular, the issues about synchronization especially the frequency offset estimation are explored in OFDM system, then the issues pertaining to adaptive resource allocation for future OFDM based wireless systems are examined while considering their special characteristics such as multiple access techniques and MIMO antenna techniques. The aims here are to study the system level performance of future wireless systems based on the above two aspects by using both theoretical analysis and modeling simulations. Towards these aims, the project takes the following lines of research:

Synchronization

- Fully study current algorithms for the timing offset and frequency offset estimation to develop the understanding of the main issues and problems of synchronization in OFDM system. Based on the review, we summarize the timing offset estimation algorithms and evaluate them by computer simulation. And then we focus to explore the novel frequency offset estimation algorithms.
- Two FFT-based frequency offset estimation algorithms in OFDM system are proposed. One is Linear Interpolation based algorithm; and the other is matched filter based algorithm. Modelling simulation is carried out under the additive white Gaussian noise (AWGN) channel, multipath static fading channel and multipath time-varying fading channel by evaluating the error variance (EV). More accurate and stable

estimation result in the lower EV. The simulation results show their improvement with lower EV than the conventional well-known algorithm.

- The integrated model for timing and frequency offset estimation in OFDM system is proposed.

Downlink Resource allocation

- Review in details the current adaptive resource allocation in the multiuser OFDM system to identify the main optimization methods. And then we focus on the total transmit power minimization and theoretically study the relevant optimal solution of subcarrier allocation which has high computation complexity.
- Propose a sub-optimal channel gain difference based subcarrier allocation algorithm which is evaluated by the total transmit power, the familiar bit error rate (BER) vs. Signal to noise ratio (SNR) and the computation complexity.
- Subsequently, special focus is put on resource allocation in multiuser MIMO-OFDM system. Because of the feature of subcarrier sharing among users, the pre-processing techniques ZF and SVD, prior to data transmission in the MIMO channel are examined.
- According to the SVD assisted pre-processing multiuser MIMO-OFDM system, a subcarrier allocation algorithm is proposed to assign the users for each subcarrier with the goal of total power minimization in the whole system.

1.6. Organization of the Thesis

The thesis is written as a monograph for the sake of clarity, but parts of the contributions in Chapters 4, 5 have been published or accepted for publication in the publications listed in Section 1.7. The rest of the thesis follows the organization given below.

Chapter 2 contains the literature review of previous work related to the contributions of the thesis. The review includes the current timing offset and frequency offset estimation algorithms in OFDM system. Furthermore, the downlink resource allocation in multiuser OFDM system, MIMO link, pre-processing techniques and resource allocation in multiuser MIMO-OFDM system are also reviewed.

Chapter 3 presents the wireless channel models including the theoretical analysis and computer simulation of Rayleigh flat fading channel, frequency selective fading channel, and the MIMO-OFDM channel model. The channel models developed here will be applied in the later research work.

Chapter 4 considers the synchronization techniques including timing and frequency offset estimation in OFDM system. Some of the popular algorithms are fully studied, and two FFT-based frequency offset estimation algorithms are proposed.

Chapter 5 focuses on the downlink resource allocation in multiuser OFDM system and multiuser MIMO-OFDM system. The optimal solution of subcarrier allocation in multiuser OFDM system is studied and a novel channel gain difference based subcarrier allocation algorithm is proposed and evaluated. Furthermore, the ZF and SVD assisted pre-processing techniques in MIMO system are studied. Then a subcarrier allocation algorithm is proposed for multiuser MIMO-OFDM system according to the SVD based pre-processing technique.

Chapter 6 concludes the thesis. The main results and conclusions are summarized. Moreover, some open questions and directions for future research are pointed out.

Chapter 2

Literature Review

In this chapter we review the challenges as well as some existing solutions of the Synchronization Techniques in OFDM system, the downlink Resource Allocation in Multiuser OFDM system, MIMO system, Multiuser MIMO system and the downlink Resource Allocation in Multiuser MIMO-OFDM system. In Section 2.1, the comprehensive study of current synchronization techniques is presented including the timing synchronization and frequency synchronization. Section 2.2.1 reviews existing downlink resource allocation algorithms in Multiuser OFDM system. Section 2.2.2 reviews the point to point MIMO system followed by the Multiuser MIMO system presented in section 2.2.3. In section 2.2.4, the downlink Resource Allocation in Multiuser MIMO-OFDM system is reviewed. Finally section 2.3 gives the summary of literature review.

2.1. Synchronization in OFDM System

In order to realize the synchronization in OFDM system, two methods are mainly used which are data-aided and non-data-aided respectively.

For the data-aided method, special signals such as training sequence and pilot symbols are transmitted, which are specially chosen to achieve rapid synchronization. These special signals can be continuously transmitted signals or periodically transmitted symbols, specified by their shape, auto-correlation function, spectrum and other specific parameters [35, 88]. The synchronism is established quickly with high accuracy and low computation, but such scheme uses part of the available bandwidth and consequently reduces the data transmission speed. It is appropriate for common access systems, systems with packet transmission, and local networks [88].

For the non-data aided method, also named as blind synchronization, the CP is often used for estimation [89-92]. This type of synchronization requires sufficiently large number of samples to get a reliable estimation. The CP length and SNR value will influence the estimation performance. If CP is containing the interference from previous symbol in ISI channel, the performance will be reduced. In addition, estimation range of blind synchronization is relatively small, not suitable for acquisition.

In this thesis, data-aided methods are focused on due to their wide use when researching modern WLAN systems. Some of the well-known timing and frequency synchronization methods are now reviewed in section 2.1.1 and section 2.1.2 respectively.

2.1.1. Timing Synchronization in OFDM System

Schmidl and Cox in [35] proposed a timing synchronization method. Two training symbols are placed at the beginning of the frame. The first symbol has identical halves in time domain, so that the correlation between these two halves can be carried out to find out the timing metric in the receiver. However, the metric suffers from a plateau which leads some uncertainty in determining the start of the frame. To alleviate this, the authors propose a 90% averaging method to finalize the start time. H. Minn et al. in [36] modified Schmidl's method in [35] and proposed two new timing synchronization methods. The first method uses two modifications: 1) all samples over one symbol period (excluding CP) are used in calculation of half symbol energy required in designing timing metric and 2) averaging of timing metrics over a window of CP length is used instead of 90% maximum points averaging. The second method uses a training symbol containing four equal length parts: the first two are identical and the last two are the negative of the first two. Both methods give smaller estimator error variance than the timing synchronization method in [35], especially second method, but still have large Mean Square Error (MSE) in ISI channel. Byungjoon Park et al. in [37] presented a novel timing offset estimation method by modifying the training symbol structure, which produces an even sharper timing metric and has significantly smaller MSE than Schmidl's in [35] and Minn's in [36]. Nanda Kishore et al. in [38] proposed a method which has same preamble structure with [35], but he assumes that the receiver knows the one half of the preamble first, and then join it to the calculation of timing metric to yield a sharp peak at the correct symbol boundary. Seung et al. in [39] proposed timing offset estimation method and designed a new time domain preamble to give smaller MSE than in [35], [36] and [37] especially in the fast varying channel. Its main advantage is found in applications operating in fast Rayleigh fading channel without assuming the dominant path by using the window search method.

2.1.2. Frequency Synchronization in OFDM System

Moose et al. in [40] analyzed the effects of the frequency offset on the OFDM system, and found that the main problem is the ICI between the subcarriers. He also described a technique to estimate the frequency offset using two repeated OFDM symbols. The maximum likelihood estimation (MLE) algorithm and variance of estimation are also derived, but the estimation range is limited inside half sub carrier interval. Classen et al. in [41] use the pilot symbols distributed over the subcarriers of two OFDM symbols to carry out the frequency acquisition and tracking. This technique is very computationally complex because it uses a trial and error method where the carrier frequency is incremented in small steps over the entire acquisition range until the correct carrier frequency is found, and consequently it is impractical. By considering a preamble consisting of two OFDM symbols, Schmidl et al. in [35] proposed a method for frequency synchronization. Two training symbols are placed at the beginning of the frame. The first symbol has identical halves in time domain, which is used to generate timing metric for timing synchronization as explained in section 2.1.1. At the optimum symbol time, the phase of the numerator term of the timing metric is examined for frequency fractional estimation, and if the absolute value of phase is greater than π, the correlation between compensated first and second training symbol is carried out for integral estimation after FFT in frequency domain. We know the training symbol's structure is related to synchronization capability. Lambrette et al. in [42] proposed a method using CAZAC (Constant Amplitude Zero Autocorrelation) sequence. He inserted repeated CAZAC sequence every few OFDM symbols to get the accurate frequency offset estimation. Yun Hee Kim et al. in [43] proposed a method using one differentially coded training symbol to find out the integral part of the frequency offset. Therefore there is only one OFDM training symbol needed. Morelli et al. in [44] proposed best linear Unbiased Estimation (BLUE) method. Its training symbol is made by many repeated parts. It improved the frequency offset estimation range and accuracy but increased the computation. Kan shi et al. in [46] proposed scheme exploiting the repetitive structure of a training symbol and extended the range of the carrier estimate which is up two subcarrier spacing. In WLAN system, training sequences are also widely used for synchronization. According to the IEEE 802.11 standardization group and the corresponding preamble design specified by the IEEE standard, Jian Li et al. in [45] presented an efficient carrier frequency offset estimation algorithm for the OFDM based WLANs. Short training symbols results in better accuracy than long training symbols.

2.2. Resource Allocation in Multiuser OFDM System and Multiuser MIMO-OFDM System

One of the main limitations for wireless communication systems is that the bandwidth must be shared by multiple users [1, 19], which also exists in OFDM system and MIMO-OFDM system. The users observe multipath fading but have independent fading parameters due to their different locations. The probability that a subcarrier has been in deep fade for one user may also be in deep fade for other users is quite low. Therefore efficient resource allocation algorithms allocating the subcarrier, power and bit adaptively according to the user's CSI are required in Multiuser wireless communication system in order to increase the system efficiency.

2.2.1. Adaptive Resource Allocation in Multiuser OFDM System

In the single-user OFDM system, the user utilizes all good and stable available subcarriers, and then the adaptive loading algorithms are applied to allocate the bits over subcarriers. Many algorithms have been developed to achieve this goal [47-50].

In the multi-user OFDM systems, Mattias et al. in [51] carried out the conceptual Study of OFDM with traditional multiple access techniques, including OFDM-FDMA, OFDM-TDMA and OFDM-CDMA, their performance for downlink of OFDM systems are studied in [52]. The OFDM-FDMA allocates each user a particular band of subcarrriers, the OFDM-TDMA allocates each user a particular time slot with all subcarrriers, and OFDM-CDMA allocates each use a subset of orthogonal codes for spreading over subcarriers. We focus the work on downlink OFDM -FDMA system.

For the traditional OFDM-FDMA system, the resource allocation does not consider the users' CSI, and the subcarriers allocated to user are fixed in all channel environments. In real world, different users will experience peaks in their channel quality at different times. This effect has been called multi-user diversity. When the number of users is large, the system performance can be improved if the base station (BS) schedules its transmission to those users with favorable channel fading conditions. Because of the various channel conditions among different users, it is possible that the user with higher average channel gains will use most of the system resources. To optimize the system in a fair way for downlink transmission system, the CSI of each user needs to be gained in the BS. In our work, we assume that (a) the transmitted signals experience quasi static frequency selective fading which can be modelled as a collection of M parallel flat fading channels. As a result, the channel remains unchanged from the time that measurements are made until the data packet is transmitted to receivers, (b) users' CSI are perfectly known by the BS and users' receivers. Generally speaking, there are two classes of optimization techniques that have been proposed in the literature: margin adaptive (MA) [53], [54], [55] and rate adaptive (RA) [56], [57], [58].

Margin adaptive (MA) Resource Allocation in Multiuser OFDM system

The objective of the margin adaptive resource allocation is to achieve the minimum overall transmit-power given the constraints on the users' data rate or bit error rate (BER). Wong et al. in [53] proposed an optimization algorithm based on Lagrange relaxation in order to minimize the total transmission power with satisfying all users' rate requirement in downlink transmission system. The algorithm is applied in BS to allocate subcarriers first by achieving the minimum total transmission power and satisfying all users' rate requirement, then the single user optimal bit allocation (OBA) is applied on the assigned subcarriers for each user. The algorithm significantly outperforms the fix allocation schemes (e.g. OFDM-FDMA), but it is very complex and has heavy computation. To cope with this problem, the authors in [54] proposed a simplified sub-optimal algorithm with performance close to optimal solution. However the modified scheme fixes the number of assigned subcarriers of each user which is not a good strategy in practical systems. Didem Kivanc and Hui Liu in [55] proposed the craving greedy subcarrier and power allocation algorithm for downlink transmission system. The algorithm was separated into two stages: the first stage determines the number of subcarriers based on SNR and users' rate requirement, the second stage allocates appropriate subcarriers to each user by using amplitude craving greedy (ACG) subcarrier assignment algorithm in order to minimize the total transmit power. To reduce the computational complexity, Kim et al in [59] converted the nonlinear optimization problem into a linear integer-programming problem. However, the complexity still grows exponentially with the number of subcarriers and users. Li Zhen et al. in [60] modified the algorithm in [55] and proposed the improved ACG algorithm to further improve the system performance. Guodong Zhang et al. in [61] proposed a novel dynamic subcarrier and bit allocation algorithm for real-time services in multiuser OFDM systems, which takes advantage of the instantaneous channel gain in subcarrier and bit allocation properly without relying on the nonlinear optimization technique like algorithm in [53], in order to reduce the computational complexity.

Mathematically, the original problem of margin adaptive resource allocation in Multiuser OFDM system can be formulated as:

$$P = \min_{C_{k,n} \in D} \sum_{n=1}^{N} \sum_{k=1}^{K} \frac{1}{\alpha_{k,n}^{2}} \cdot f_k(c_{k,n}) \tag{2-1}$$

Where P is the total transmit power, $c_{k,n}$ is the bit rate for the k^{th} user on the n^{th} subcarrier in one OFDM symbol, $\alpha_{k,n}^{2}$ is the channel power gain for the k^{th} user on the n^{th} subcarrier, and $D \in [0, M]$ is the set of all possible constellation values for $c_{k,n}$ with maximum allowed value M.

In addition, $f(c)$ is the required received power for reception of c bits/symbol when channel gain equals to unity, here we consider the system employing MQAM, therefore $f(c)$ is given as [53]:

$$f(c) = \frac{N_0}{3}[Q^{-1}(\frac{P_e}{4})]^2(2^c - 1) \tag{2-2}$$

where N_0 is the noise power spectral density (PSD), P_e is the given BER, and Q represents Q-function. And the minimization is subject to the following constraints.

$$R_k = \sum_{n=1}^{N} c_{k,n} \tag{2-3}$$

$$c_{k',n} \neq 0 \text{, then } c_{k,n} = 0 \text{ for } k \neq k' \tag{2-4}$$

where R_k is the required data rate for user k. And as shown in equation (2-4), one subcarrier can only be assigned to one user.

<u>Rate adaptive (RA) Resource Allocation in Multiuser OFDM system</u>

The objective of rate adaptive resource allocation is to adapt the transmit power by allocating bits using with water-filling scheme for each user in each subcarrier and maximize the overall data rate with a total transmit power constraint. W. Rhee et al. in [56] described an optimal subcarrier allocation algorithm and proposed a sub-optimal adaptive subchannel allocation algorithm in order to maximize the total data rate. But the frequency selective nature of users' channel is ignored by allocating equal power across all subcarriers. H.Yin et al. in [57] proposed a two-step algorithm that maximizes the total rate subject to users' rates and the total power constraints. The algorithm first estimates the resource required to satisfy the rate requirement of each user according to their average channel gain; and then pick the subcarriers with good channel gains so that the total rate is maximized. Gerhard Münz et al. in [62] proposed a computationally efficient water-filling algorithm to determine the subcarrier allocation for a multiple access OFDM system. It maximizes the target rate under the constraints of individual user power budgets. After that, the bit and power allocation for each user is determined by one of single-user loading algorithms. J. Jang et al. in [58] proposed algorithm to maximize the total capacity under constant total power and proved that the sum capacity is maximized when each subchannel is assigned to the user with the best subchannel gain and power is then distributed by the water-filling algorithm. Z. Shen et al. in [63] discussed the solution for Quality of Service (QoS) which is neglected in [58]. The proportional fairness is introduced in order to control the capacity ratios among users, and ensure that each user is able to meet his target data rate. It also takes into account the frequency selective nature of a user's channel through the use of water-filling during power allocation to each user. Chandrashekar Mohanram et al. proposed an algorithm that performs joint subcarrier and power allocation in multiuser OFDM [64]. The aim is to maximize the overall rate while achieving proportional fairness amongst users under a total power constraint.

Mathematically, the original problem can be formulated as:

$$\max_{P_{k,n},A_k} \sum_{k=1}^{K} R_k \tag{2-5}$$

$$R_k = \sum_{n \in A_k} \log_2 (1 + P_{k,n} \gamma_{k,n})$$

$$\gamma_{k,n} = \frac{|\alpha_{k,n}|^2}{N_0 (B / N)}$$

$$\text{Subject to } \sum_{n=1}^{N} \sum_{k=1}^{K} P_{k,n} \leq P_{total} \tag{2-6}$$

$$P_{k,n} \geq 0 \text{ for all } k, n$$

$$A_1, A_2, \ldots, A_k \text{ are all disjoint}$$

$$A_1 \cup A_2 \cup \ldots \cup A_k = \{1, 2, \ldots, N\}$$

Where K is the total number of users, N is the total number of subcarriers, P_{total} is the overall power constraint, $P_{k,n}$ is the power allocated to the k^{th} user in the n^{th} subcarrier, $\gamma_{k,n}$ is the channel gain to noise power ratio for the k^{th} user in the n^{th} subcarrier, $\alpha_{k,n}$ is the channel gain for the k^{th} user in the n^{th} subcarrier, N_0 is the noise power spectral density (PSD) of AWGN, B is the overall available bandwidth, A_k is the set of all subcarriers allocated to the k^{th} user, and R_k is the k^{th} user's rate.

Different classes of algorithms for MA and RA resource allocation

Some outstanding research in the MA and RA based resource allocation in multiuser OFDM systems are classified as follow:

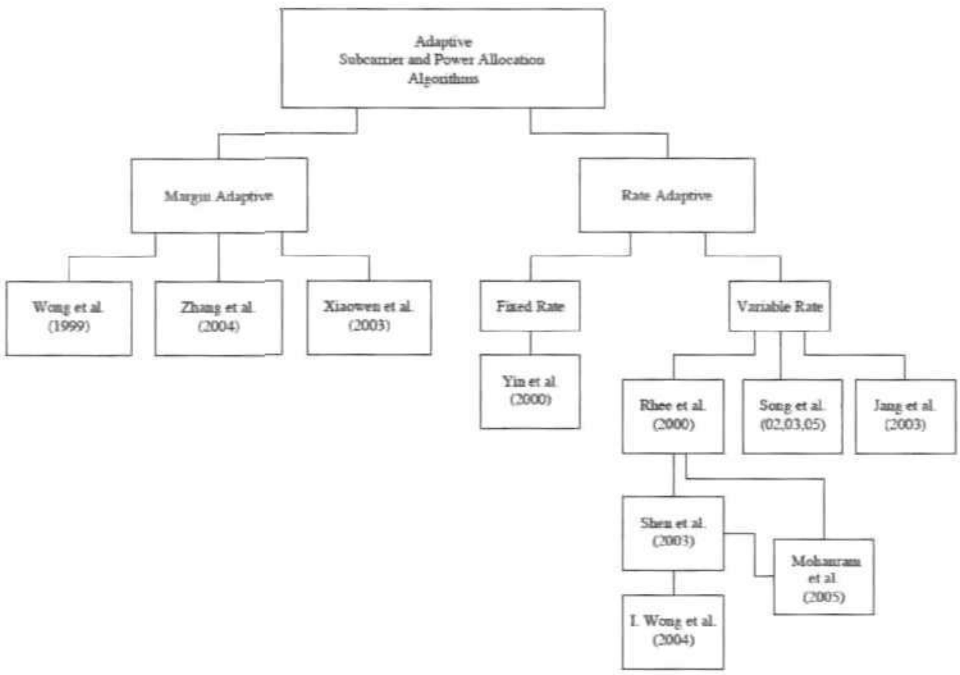

Figure.2.1. Different classes of alogorithms for MA and RA resource allocation [110]

Our work will focus on the margin adaptive optimization technique, because the multimedia service plays an important role in the future wireless communication system, of which the delay-critical real-time interactive applications such as the voice or video transmission may require a fixed data rate [65]. Thus the total power minimization is necessary to achieve the high system performance. We will review the optimal solution and propose a simple but efficient sub-optimal method in Chapter 5.

2.2.2. Multiuser MIMO System

For a multiuser MIMO system, the optimal sum capacity based on the resource allocation over different dimensions (users, space, frequency) is given by the actual sum rate capacity of the frequency-selective MIMO downlink broadcast channel which are discussed in [66, 67, 68]. However, heavy computation is required to achieve the optimal sum capacity by solving the convex optimisation problem. Therefore, sub-optimal with less complex techniques have been proposed. Multiuser diversity for the dirty paper coding (DPC) with ZF approach was studied by Tu et al. in [69], where they proposed a greedy algorithm for the selection of users and their encoding order for maximising the sum rate. This algorithm combined with ZF-DPC was shown to have a sum rate very close to the capacity. Tejera et al. [70] investigated different spatial sub-channel allocation algorithms aiming to maximize the sum rate of the multiuser MIMO BC. However, these papers aimed to maximize the system capacity through joint power control, but the instantaneous QoS provisioning is not guaranteed. In other words, although the data rate-sum is maximized, some user's data rate might be very low for certain time intervals due to poor channel conditions. Therefore, other transmitter design criteria should be considered in order to guarantee the QoS for all users. Lee et al. [71] studied the symmetric capacity of MIMO downlink channel which is defined to be the maximum rate that can be allocated to every user in the system, of which the fairness between users is guaranteed.

The algorithms generally require very complex nonlinear computation based on the DPC [67]. The sub-optimal with less complex transmission techniques are necessary. Linear beamforming, which is also known as Spatial Division Multiple Access (SDMA), is a sub-optimal transmission strategy that enables the spatial separation of concurrent users. The data stream of each user is multiplied by the beamforming weight vector independently and spread over the multiple antennas. The multiuser interference (MUI) between multiple data streams can be eliminated by the proper selection of weight vectors among users. Unlike the DPC applied in MIMO broadcast channel, the optimal beamforming cannot be written as a convex optimization problem [71]. In addition, beamforming can combine with a proper selection of users to have the same asymptotic sum-rate as the DPC, when there are a large number of users existing in the system [71, 72]. Because the probability of finding a set of close-to-orthogonal users with large channel gains is increased along with the growing of the number of users. Lai et al. in [73] proposed a ZF-based precoding approach to decompose the multiuser MIMO downlink channel into multiple parallel independent single-user MIMO downlink channels. Each equivalent single-user MIMO channel has the same properties as a conventional single-user MIMO channel. Furthermore, Liu et al. in [74] proposed a novel Singular Value Decomposition (SVD) based precoding approach in downlink multiuser MIMO system, which takes into account the specific characteristics of the individual users channel matrix, instead of treating all the users' channels jointly as in the traditional ZF-based multiuser transmission (MUT) technique, and then the maximum rate scenario is considered under the user' power constraints. Both algorithms in [73] and [74] assumed all users to transmit data simultaneously and the number of transmit antennas in BS is related with the number of users and the number of users' receive antennas. For a downlink MIMO system with large number of users, it requires large number of the transmit antennas in BS which is impractical. Therefore, in real resource optimized system with large number of users, a set of users is selected to transmit data simultaneously over multiple antennas, and then the relevant precoding technique is applied for the selected set of users. Dimic et al. in [75] utilized the sub-optimal greedy user selection algorithm in the ZF beamforming based downlink MIMO system where users' receivers all have single antenna. Yoo et al. in [72] also used the greedy user selection algorithm in ZF beamforming based MIMO system, but with an additional semi-orthogonality test between users. The performance shows its asymptotical optimality. In Chapter 5, we will discuss performance of downlink Multiuser MIMO systems that applied the precoding techniques in [73] and [74] respectively, and then extend the Liu's precoding technique in [74] to the downlink Multiuser MIMO-OFDM system.

2.2.3. Adaptive Resource Allocation in Multiuser MIMO-OFDM System

In previous sections, the MA and RA resource allocation algorithms proposed in Multiuser OFDM system has been fully studied. Subsequently, we introduce the Multiuser MIMO system applying various precoding techniques such as ZF and SVD. In this section, the OFDM is combined with Multiuser MIMO system with precoding techniques, and then the resource allocation in Multiuser MIMO-OFDM system is reviewed.

There are some challenging issues raised in the Multiuser MIMO-OFDM system. First of all, with the similarity in Multiuser MIMO system, the multiple users are allowed to transmit data simultaneously on each subcarrier, which is called as subcarrier sharing between users and generates the MUI between users. This fact makes the optimization problem combinatorial and nonconvex. Furthermore, adapting the transmission of one user affects the interference to other co-channel users, which, in turn, changes the optimal transmission schemes of all users. The proper precoding techniques in Multiuser MIMO system can be extended to Multiuser MIMO-OFDM system to solve this problem. Second, the inter-antenna interference (IAI) caused by the signals from multiple transmit antennas of a given user being received on the same receive antenna, makes the signals more difficult to be separated and decoded from multiple antennas. Third, MIMO-OFDM systems are occupying both the space and frequency domains, so that we have to decide which dimension should be used by which set of users. Finally, QoS requirements require additional constraints on the optimization problem.

For each subcarrier of Multiuser MIMO-OFDM system, the maximum number of data streams that can be allocated is limited by the number of transmit antennas at the BS, while the number of streams per user is limited by the number of receive antennas at the terminal. If the total number of allocated streams exceeds the number of BS antennas, the system becomes interference limited [78]. In real system serving a large number of users by fixed number of BS antennas, it is impossible to assign all users in each subcarrier which may cause the total number of allocated streams exceeds the number of BS antennas. Therefore, the efficient user selection algorithm is required to allocate the best users for each subcarrier. The user selection algorithm can also be known as subcarrier allocation which represents to assign best users on each subcarrier. The adaptive subcarrier allocation algorithm for Multiuser MIMO-OFDM system has attracted increasing research interest recently.

With consideration of combining MIMO with OFDM, Tsang et al. in [76, 77] extended the rate maximization problem to the Multiple-Input-Single-Out (MISO)-OFDM system. The authors found that the optimal and sub-optimal solution to maximize the total date rate by considering best assignment of users on each subcarrier subject to total power constraints and each user's QoS requirements. Obviously, the number of users in a subcarrier has two conflicting effects on the system throughput. One is that adding more users on a subcarrier increases the number of spatial channels; however, another effect is that more users introduce more interference among the users which reduces the throughput in each spatial channel. The authors take into consideration these two conflicting effects when solving the maximization problem. Subsequently, Zhang et al. in [79, 80] extended the resource allocation to Multiuser MIMO-OFDM system, and the dynamic subcarrier allocation algorithm is simplified to group users according to the spatial signatures or comparability of the user channels, with the aim of minimizing the total transmit power in uplink transmission subject to the fulfillment of each user's QoS requirements including bit-error rate (BER) and data rate. In order to maximize the capacity of each user, several subcarrier allocation algorithms have been obtained in [52, 53]. However, these subcarrier allocation algorithms only outperform two scenarios. One is the static allocation; another one is that one subcarrier is only assigned to one user. In [83, 84], Chan et al. considered the optimal power allocation for a multiuser MIMO-OFDM system using ZF precoder based multiplexing with the objective to maximize the system capacity. The authors also extend the user selection to antenna selection and dimension selection. In [85], Maw et al. proposed another method to maximize the total throughput under the constraints of total power and proportional data rate fairness among users instead of equal power allocation. In [86], the multiuser MIMO-OFDM system with ZF beamformer was proposed to remove the multiuser interference among the simultaneously transmitting users. The aim is to minimize the total transmit power under the constraints of users' data rates. In [87], Karaa et al. developed linear precoding schemes for downlink in MIMO-OFDM systems, and then endeavours to optimize the power allocation across OFDM subcarriers. So far, significant research work has been carried out for power allocation in order to maximize the system capacity. Not much work is considered for the total power minimization under users' data rate constraints, especially in downlink Multiuser MIMO-OFDM system. In addition, fixed data rate may be required for the delay-critical real-time interactive applications such as the voice or video transmission in future multimedia based wireless communication system [65]. Therefore the total power minimization under users' data rate constraints in the downlink MIMO-OFDM systems is focused on our work.

In the Chapter 5, we propose a novel and efficient user selection algorithm with the aim of total transmit power minimization based on the extended downlink Multiuser MIMO-OFDM system from [74].

Chapter 3

Wireless Channel Modelling

Wireless channel is the medium of data transmission between transmitter and receiver. It is an important factor that influences the performance of wireless communication systems. In this chapter we comprehensively study the wireless channel characterization through theoretical analysis, channel modelling, and computer simulations. We will use the multipath fading channel model in the analysis and simulation in our research. In Section 3.1, the wireless channel characterization is presented. Section 3.2 theoretically analyzes the multipath fading channel, and the corresponding computer simulation is carried out to measure the channel models. Section 3.3 evaluates the performance of MIMO/MIMO-OFDM systems operating in the multipath channel model. Finally section 3.4 summarizes conclusions from this chapter.

3.1. Wireless Channel Characterization

After signal is sent out from the transmitter and before signal arrives the receiver, all the paths the signal passes through are called communication channel. The wireless channel can be the simple Line of Sight (LOS) transmission, or distorted by various factors such as Path loss which describes the power loss in space, shadowing over large areas, and the multipath effects caused by the signal reflection from buildings, mountains and tree leaves and results in the signal fading or enlargement. In addition, the signal will also be affected by the Doppler Effect if there is relative movement between transmitter and receiver. The Doppler Effect makes the channel varies with time and spread the signal energy in frequency domain, which increases the uncertainty of the signal quality. Because of the diversity and time variation of channel, the channel characterization plays the key role in the receiver design. And because of increased uncertainty, wireless channels are normally analysed and simulated by the statistics methods. The wireless channel is not only susceptible to noise, interference, but also channel impediments where the received signal is affected by Path loss, Large-scale propagation and small-scale propagation. These impediments are discussed in details below.

3.1. 1. Path Loss

The Path loss describes the loss in power as the radio signal propagates in space, the signal power will be decreased by the increased distance, and path loss is a function of distance and will be increased with distance. Variation due to path loss occurs over very large distances (100-1000 meters) [1]. There are two popular channel models to describe the path loss propagation.

One is called free space propagation model. It treats the region between the transmitter and receiver as being free of all objects that might absorb or reflect radio frequency (RF) energy, and within this region, the atmosphere behaves as a perfectly uniform medium [1]. This model is widely used in the satellite communication. Another one is called Log-Distance path loss model. In the indoor or outdoor environment, the receive signal power will have exponential decay along with the increase of distance.

3.1. 2. Large-scale Propagation

The Large-scale propagation represents the average signal power attenuation or path loss due to motion over large areas. This phenomenon is affected by prominent terrain contours (hills, forests, billboards, clumps of buildings, etc.) between the transmitter and receiver, and is often represented as being "shadowed" [1]. In another word, if two receivers have same distance with one transmitter, they will receive the signal with different power because their signals are shadowed by different terrain and objects. The most common model for this attenuation is log-normal shadowing. This model has been confirmed empirically to accurately model the variation in received power in both outdoor and indoor radio propagation environments [1].

3.1. 3. Small-scale Propagation

This small-scale propagation is used to describe the variation of signal power in short distance or time, which is also called as fading. The variation includes amplitude, phase, and frequency. There are mainly two factors to consider for small-scale fading, which are the Multipath Effect and the Doppler Effect. The Multipath Effect represents the signal arrives at the receiver from multiple paths with different phase, amplitude and time delay, therefore results in the Time Dispersion and Frequency selective fading. And yet the Doppler Effect results in the Frequency Dispersion and Time selective fading. These four factors exist together in the channel, however the signal bandwidth (BW) and symbol period will determine which effect is more obvious.

Time Dispersion

The signal arrives at the receiver from multiple paths with different fading and time delay. Figure.3.1 shows the Multipath Effect on the received signal.

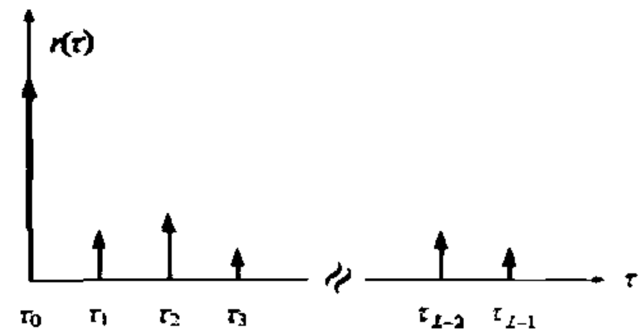

Figure.3.1. Multipath Effect on the received signal

In Figure.3.1. we use $\tau_0, \tau_1, ..., \tau_{L-1}$ to represent the time delay of the signal arriving at the receiver from L paths. The received signal which is the addition of signal from all L paths is dispersed on time and having longer time duration then the transmitted signal. In addition, if the interval between different path delays is more than the one symbol period, these paths are called as Resolvable because receiver can distinguish them. Otherwise if two or more paths arrive at the receiver almost at the same time with time difference less than one symbol period, they are seen as one path and called as Un-resolvable. In real wireless channel, for one resolvable path, its signal is actually consisting of the signals from many un-resolvable paths. The signals from these un-resolvable paths are presenting the Rayleigh Distribution, which will be described in later section.

Subsequently, the time difference between first path and the last path is called as delay spread τ_{max} . Due to delay spread, one symbol in the received signal will be interfered by τ_{max} / T_s previous symbols where T_s is symbol period, causing ISI (Inter-symbol interference). To avoid ISI, T_s should be greater than τ_{max} . Relative to delay spread, the coherence bandwidth can be defined according to the Root mean square (RMS) delay spread. If the signal bandwidth is less than the coherence bandwidth, the signal will have same fading in all signal frequencies; otherwise the signal variation in its constituent frequencies will be different.

Flat fading and Frequency selective fading

Based on coherence bandwidth, we define the system as Narrowband if the signal bandwidth is smaller than the coherence bandwidth or the delay spread is less than symbol period. In Narrowband system, the signal has same fading in frequencies which is known as Flat fading. In flat fading channel, although the signal arrive at the receiver from different paths with certain delays, all the delays are less than symbol period, therefore, the multipath signals are all un-resolvable, and are recognized as one path.

Inversely, if the signal bandwidth is greater than the coherence bandwidth or the delay spread is greater than symbol period, the system is defined as Wideband, and the signal has different fading in frequencies which is known as Frequency selective fading. In frequency selective fading channel, the delays of several paths are greater than symbol period, which will results in the ISI. In fact, frequency selective fading channel is merging several flat fading channels together, each one having own average power and path delay.

Frequency Dispersion

If there is relative motion between transmitter and receiver, the Doppler Effect will affect the signal so that the signal frequency is shifted by Doppler shift f_d within the range of maximum Doppler shift f_m. f_d and f_m are given as:

$$f_d = f_m \cos\theta$$

$$f_m = \frac{vf_c}{c} \tag{3-1}$$

where v is mobile station speed, f_c is carrier frequency, c is light speed and θ is the angle of signal wave and mobile station direction. If the mobile station is moving toward the transmitter, Doppler shift is positive, so the signal frequency will increase, inversely, it will decrease. The signal transmitted from mobile station centred at f_c is distributed in ($f_c - f_m$, $f_c + f_m$). In the Power density Spectrum (PDS) point of view, if there is no Doppler shift existing, the signal power is converging around the central frequency f_c . Otherwise, the PDS is converging to maximum Doppler shift f_m as U sharp shown in Figure.3.2, and results in the low PDS around the central frequency f_c .

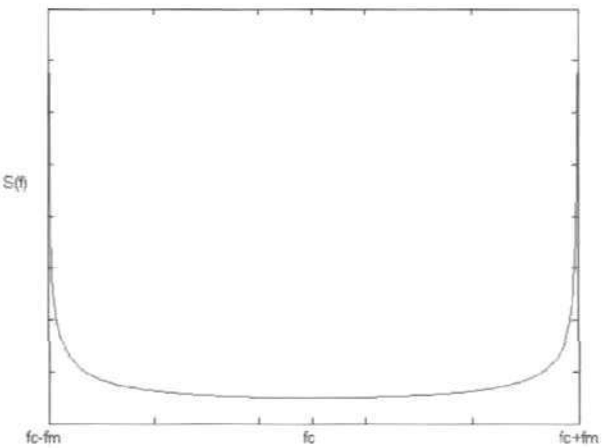

Figure3.2. U sharp of PDS caused by Doppler Effect

Relative to Doppler shift, the coherence time which is defined according to the maximum Doppler shift, measures the time duration that the channel impulse response is invariant and highly correlated. If the symbol period is greater than coherence time, the channel varies before completely transmitting one symbol.

Slow fading and fast fading

Based on the coherence time, if symbol period is greater than the coherence time, the channel is called as fast fading which means the channel variation speed is faster than signal transmission speed. The channel is varied before one symbol finishing transmission. We also call it as time selective fading.

Inversely, if symbol period is less than the coherence time, the channel is called as slow fading which means the channel variation speed is slower than signal transmission speed. We can assume the channel doesn't vary over couple of symbols in this case. We also call it as time flat fading.

3.1.4. Summary

Path loss, Large-scale propagation and small-scale propagation exist together in the real wireless channel. But in the theory based research, we normally don't use them together because of the high complexity. If we analyse the system capacity, signal covering area or Handoff algorithms, the channel model with path loss propagation and large-scale propagation is widely used. However if we focus on the baseband signal processing between transmitter and receiver, channel model with small-scale propagation is used because baseband signal processing operates on samples with short period time, the signal variation over short time becomes an important and key factor.

We have overviewed the wireless channel characterization. Because we work on the baseband signal processing, we focus on the small-scale propagation. In the followed sections, we will analyse the multipath fading channel model and MIMO channel model, and then utilize the computer simulation to show the variation of signal affected by the small-scale propagation and the system performance.

3.2. Fading Channel Modelling

We will carry out the mathematical analysis on Rayleigh distribution. It is used to model the flat fading channel which is consisting of the frequency selective fading channel. Subsequently, we will study the well-known Improved Jake's model which is widely applied to build up the Rayleigh fading channel.

3.2.1. Basic Analysis

We consider a baseband waveform $g(t)$, so the transmitted signal $s(t)$ can be represented as:

$$s(t) = \mathrm{Re}\{ g(t)e^{j.2\pi.fc.t} \} \tag{3-2}$$

where f_c is carrier frequency. Then in the receiver, the received signal $r(t)$ added from N path can be represented as:

$$\begin{aligned} r(t) &= \mathrm{Re}\{[\sum_{n}^{N} \alpha_n.g(t).e^{j.[2\pi(fc+f_m.\cos\theta_n).t+\phi_n]}]\} \\ &= \mathrm{Re}\{[\sum_{n}^{N} \alpha_n.g(t).e^{j(2\pi.f_m.\cos\theta_n.t+\phi_n)}].e^{j.2\pi.fc.t} \} \end{aligned} \tag{3-3}$$

where α_n is the path attenuation, f_m is the maximum Doppler frequency Doppler shift, θ_n is the path arrive angle, and ϕ_n is the carrier initial phase in path. According to equation (3-3), the received baseband signal $r'(t)$ is:

$$r'(t) = g(t).\sum_{n}^{N} \alpha_n.e^{j(2\pi.f_m.\cos\theta_n.t+\phi_n)} \tag{3-4}$$

According to equation (3-4), fading process $f(t)$ is given by:

$$\begin{aligned} f(t) &= \sum_{n}^{N} \alpha_n . e^{j(2\pi . f_m . \cos\theta_n . t + \phi_n)} \\ &= \sum_{n}^{N} \alpha_n . \cos(2.\pi . f_m . \cos\theta_n . t + \phi_n) + j . \sum_{n}^{N} \alpha_n . \sin(2.\pi . f_m . \cos\theta_n . t + \phi_n) \end{aligned} \tag{3-5}$$

Now we introduce two random process $Xc(t)$ and $Xs(t)$ where

$$Xc(t) = \sum_{n}^{N} \alpha_n . \cos(2.\pi . f_m . \cos\theta_n . t + \phi_n) \tag{3-6}$$

$$Xs(t) = \sum_{n}^{N} \alpha_n . \sin(2.\pi . fm . \cos\theta_n . t + \phi_n) \tag{3-7}$$

Then $f(t)$ can be replaced as:

$$f(t) = Xc(t) + j.Xs(t) \tag{3-8}$$

As shown in above analysis, the received signal is made of N paths, and the $Xc(t)$ and $Xs(t)$ are both Gaussian random processes for large N by Central Limit Theorem [104]. We denote the fading envelop of $f(t)$ as r, and r has a Rayleigh Probability Density Function (PDF) shown as:

$$P_{Rayleigh}(r) = \begin{cases} \dfrac{r}{\sigma^2} \exp\left(-\dfrac{r^2}{2\sigma^2}\right) & 0 \le r \le \infty \\ 0 & r < 0, \end{cases} \tag{3-9}$$

$$\sigma^2 = \frac{E\left[r^2\right]}{2} \tag{3-10}$$

3.2.2. Review of Jake's Model

Jakes derived his well-known simulation model for Rayleigh fading channel [105]. N low-frequency oscillators are needed to generate N Doppler shift. In order to reduce the number of low-frequency oscillators and the complexity, Jakes makes the assumptions for path attenuation α_n and path arrive angle θ_n shown as:

$$\alpha_n = \frac{1}{\sqrt{N}} \tag{3-11}$$

$$\theta_n = \frac{2.\pi.n}{N}, n = 1,2,..., N \tag{3-12}$$

$$N = 4M + 2 \tag{3-13}$$

Now the number of distinct Doppler frequency shifts is reduced from N to $M+1$, only $M+1$ low-frequency oscillators are needed to generate Rayleigh fading channel. Subsequently, the normalized fading process of this model can be represented as:

$$u(t) = uc(t) + j.us(t) \tag{3-14}$$

$$uc(t) = \frac{2}{\sqrt{N}} \sum_{n=0}^{M} a_n \cos(2.\pi.fd_n.t) \tag{3-15}$$

$$us(t) = \frac{2}{\sqrt{N}} \sum_{n=0}^{M} b_n \cos(2.\pi.fd_n.t) \tag{3-16}$$

where

$$a_n = \begin{cases} \sqrt{2}\cos\beta_0, n = 0 \\ 2\cos\beta_n, n = 1,2...M \end{cases} \tag{3-17}$$

$$b_n = \begin{cases} \sqrt{2}\sin\beta_0, n = 0 \\ 2\sin\beta_n, n = 1,2...M \end{cases} \tag{3-18}$$

$$\beta_n = \begin{cases} \frac{\pi}{4}, n = 0 \\ \frac{\pi . n}{M}, n = 1,2...M \end{cases} \tag{3-19}$$

$$fd_n = \begin{cases} fm, n = 0 \\ fm.\cos\theta_n, n = 1,2...M \end{cases} \tag{3-20}$$

There are various modifications of Jakes' model proposed. We call them the family of Jakes' simulators. Among the Jakes' simulator family, the improved Jakes' model proposed by Pop and Beaulieu [106] is widely used due to its wide-sense stationarity (WSS) [104]. Compared with original Jakes' model, the improved Jake's model lies in the random initial phases ϕ_n which is uniformly distributed on $[-\pi, \pi)$; however, the original Jakes' model assumes that $\phi_n = 0$ for all n. The introduction of these random phases ϕ_n eliminates the stationarity problem occurring in original Jake's model [104]. The normalized fading function of the improved Jake's model is modified from (3-14), (3-15) and (3-16), and given by:

$$u(t) = uc(t) + j.us(t) \tag{3-21}$$

$$uc(t) = \frac{2}{\sqrt{N}} \sum_{n=0}^{M} a_n \cos(2.\pi.fd_n.t + \phi_n) \tag{3-22}$$

$$us(t) = \frac{2}{\sqrt{N}} \sum_{n=0}^{M} b_n \cos(2.\pi.fd_n.t + \phi_n) \tag{3-23}$$

where a_n, b_n, β_n and fd_n are the same as those in original Jake's model. The improved Jakes' model is used in our research.

3.2.3. Simulation and Performance Evaluation

In this section, we will evaluate the performance of wireless systems operating in Rayleigh flat fading channel and frequency selective fading channel by computer simulations.

3.2.3.1. Rayleigh Flat Fading Channel

The model for Rayleigh flat fading channel is built up according to the analysis of improved Jakes' model in Section 3.2.2. The required parameters are listed in Table.3.1.

Data symbol length	2000
Minimum time resolution (Symbol period) (s)	0.5×10^{-4}
Number of Oscillator	16
Carrier Frequency (GHz)	2.0
Mobile unit speed (km/h)	100/300

Table.3.1. Flat fading channel model parameters I

According to Table.3.1, 100 ms is needed to transmit 2000 data symbol when the symbol period is 0.5×10^{-4} s. We evaluate the power and phase variations over this 100ms in the flat fading channel with the vehicle speed of 100 km/h and 300 km/h. The results are shown in Figure.3.3 (a) and (b) respectively.

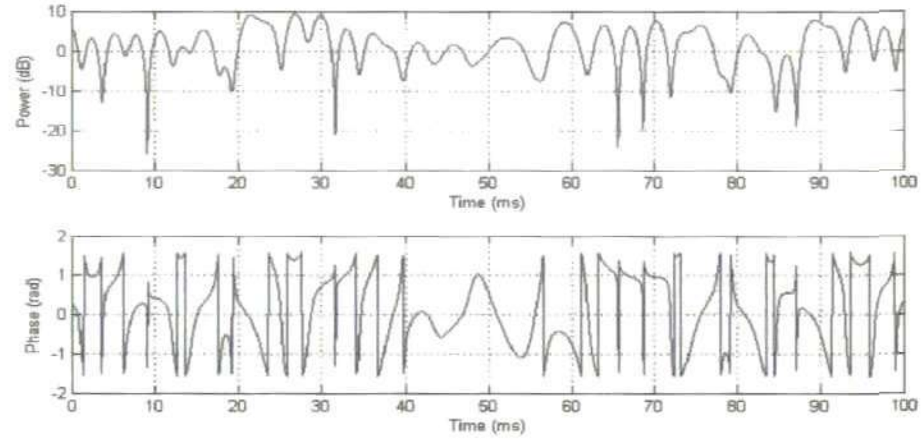

(a) Speed of mobile unit 100 km/h

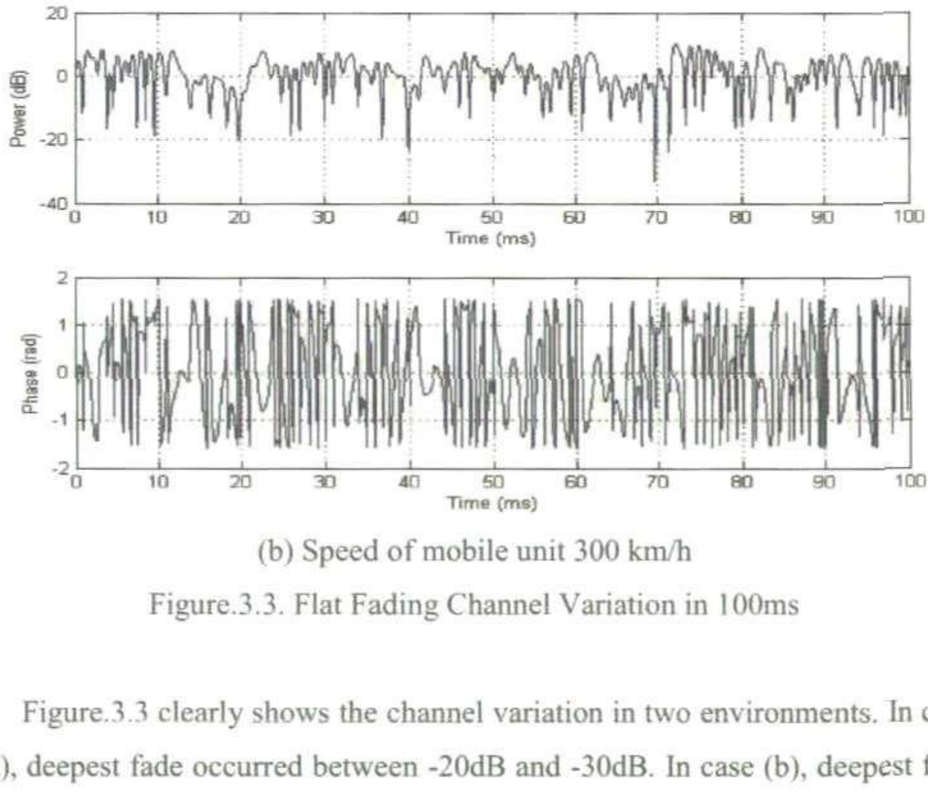

(b) Speed of mobile unit 300 km/h

Figure.3.3. Flat Fading Channel Variation in 100ms

Figure.3.3 clearly shows the channel variation in two environments. In case (a), deepest fade occurred between -20dB and -30dB. In case (b), deepest fade occurred between -30dB and -40dB. The channel in case (b) varies more frequently than case (a). Therefore, the faster mobile unit, the frequent the channel changes (Power and Phase) which will results in more distortion to the transmitted signal.

In addition, we also evaluate the signal envelop in the flat fading channel, which should have the Rayleigh distribution. Figure.3.4 shows the envelop distribution PDF achieved by simulation and the corresponding theoretical Rayleigh PDF calculated from equation (3-14).

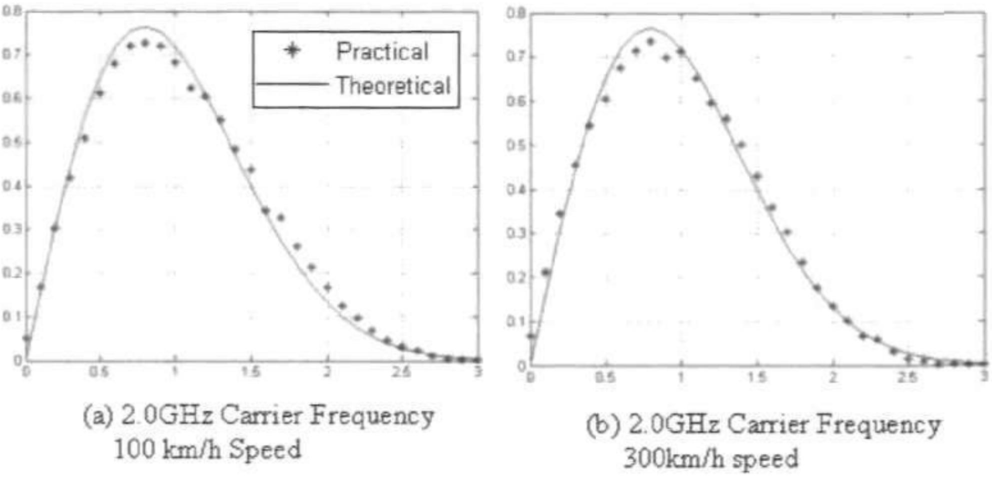

Figure.3.4. Rayleigh distribution of signal envelop

As shown in Figure.3.4, the received signal envelop distribution is mostly satisfied with the theoretical Rayleigh Distribution in both two environments.

3.2.3.2. Frequency Selective Fading Channel

Section 3.1.3 shows the frequency selective fading channel is consisting of several independent flat fading channels. The amplitude of signal in each flat fading channel is Rayleigh Distributed, and each flat fading channel also has its own average power and the time delay. The diagram in Figure.3.5 shows block diagram model of frequency selective fading channel.

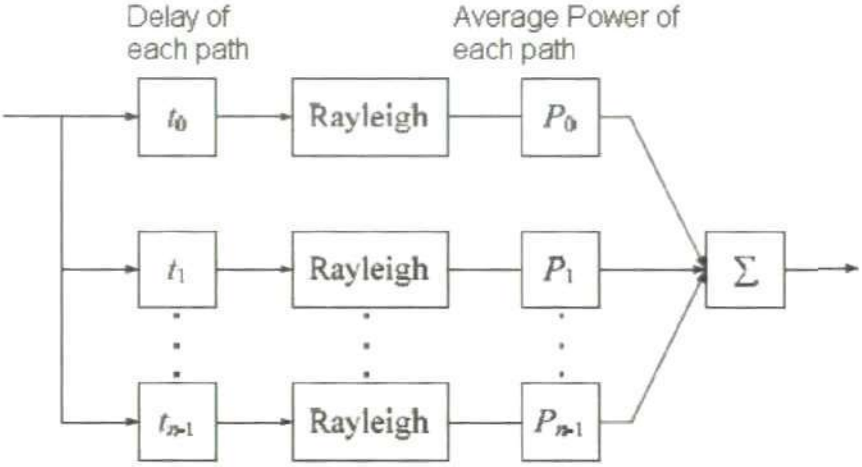

Figure.3.5. Frequency Selective Fading Channel model

Based on the model shown in Figure.3.5, the required parameters to evaluate frequency selective fading channel are listed in Table.3.2. We assumes there are 38400 data symbols, the symbol interval is 260ns. Therefore there are totally 99.84ms (approximately 100ms) needed to transmit 38400 data symbols. The power and phase variations over 100ms in frequency selective fading channel with vehicle speed of 125 km/h and 250 km/h are shown in Figure.3.6 (a) and (b) respectively.

Data symbol length	384000
Symbol period (sec)	260×10^{-9}
Number of Paths	4
Path delay (sec)	$[0, 260 \times 10^{-9}, 521 \times 10^{-9}, 781 \times 10^{-9}]$
Average power (dB)	[0,-3,-6,-9]
Carrier Frequency (GHz)	2.0
Vehicle speed (km/h)	125 /250

Table.3.2. Frequency selective fading channel model parameters II

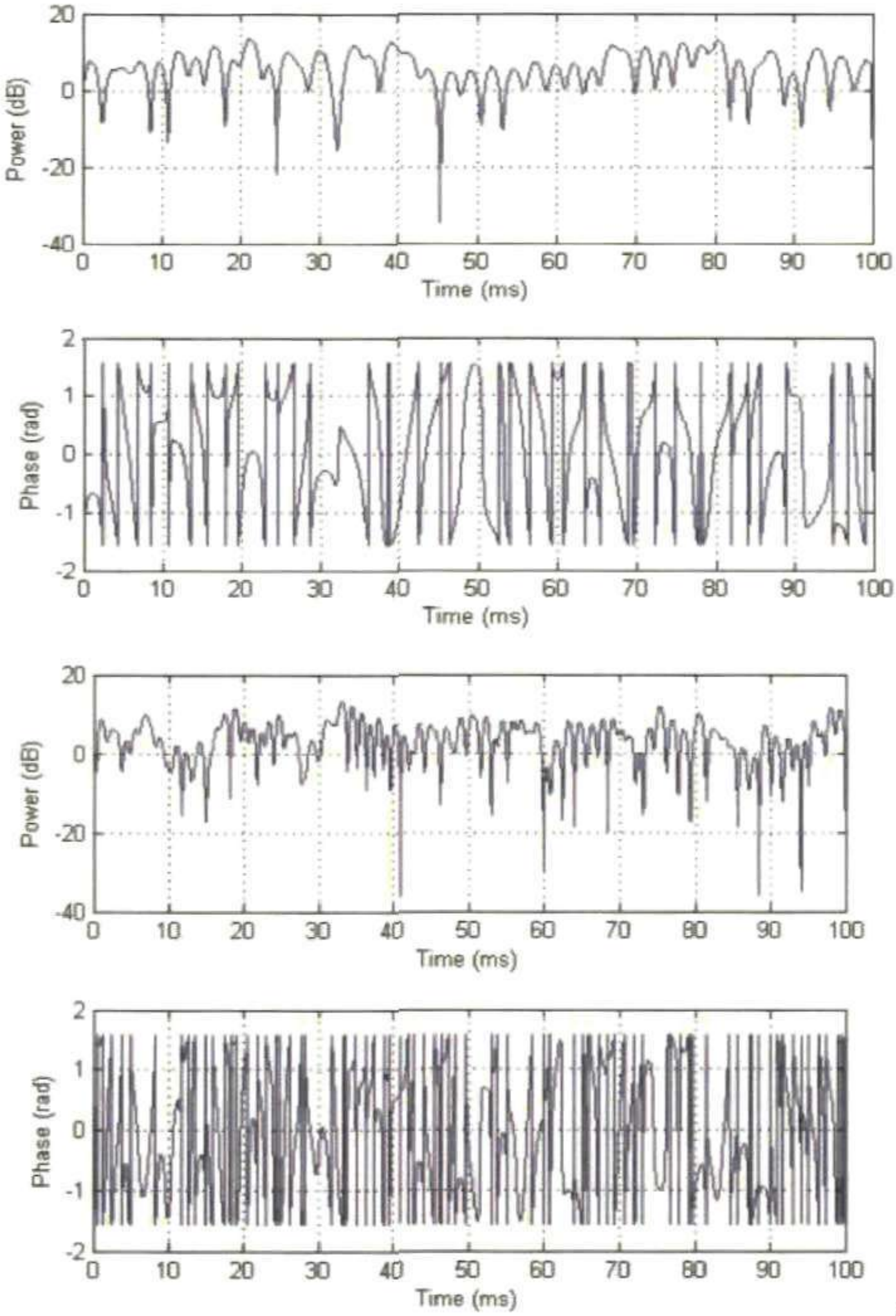

(a)

(b)

Figrue.3.6. Frequency Selective Fading Channel Variation in 100ms

(a). 125 km/h speed (b). 250 km/h speed

As with flat fading channel, the frequency selective channel shown in Figure.3.6, the faster vehicle results in the rapid channel variation in both power and phase, thereby results in more distortion in the signal. These facts further explain the fast fading and slow fading described in section 3.1.3.

In addition, the use of an OFDM scheme is optimum for dealing with the frequency-selective fading channel because OFDM converts frequency selective fading channel into a number of parallel flat-fading channels. Therefore, we are able to continuously evaluate the performance of OFDM system operating in the frequency selective fading channel. The required OFDM system and frequency selective fading channel parameters are listed in Table.3.3, and the results are shown in Figure.3.7 and Figure.3.8 respectively.

Number of subcarriers	64
Symbol period (sec)	100×10^{-9}
Modulation scheme	QPSK
Number of Paths	5
Path delay (sec)	$[0,\ 200 \times 10^{-9}, 400 \times 10^{-9}, 600 \times 10^{-9}, 800 \times 10^{-9}]$
Average power (dB)	[0,-4,-8,-13,-18]
Carrier Frequency (GHz)	2.0
Vehicle speed (km/h)	60
Average SNR (dB)	3

Table.3.3. OFDM system and frequency selective fading channel parameters

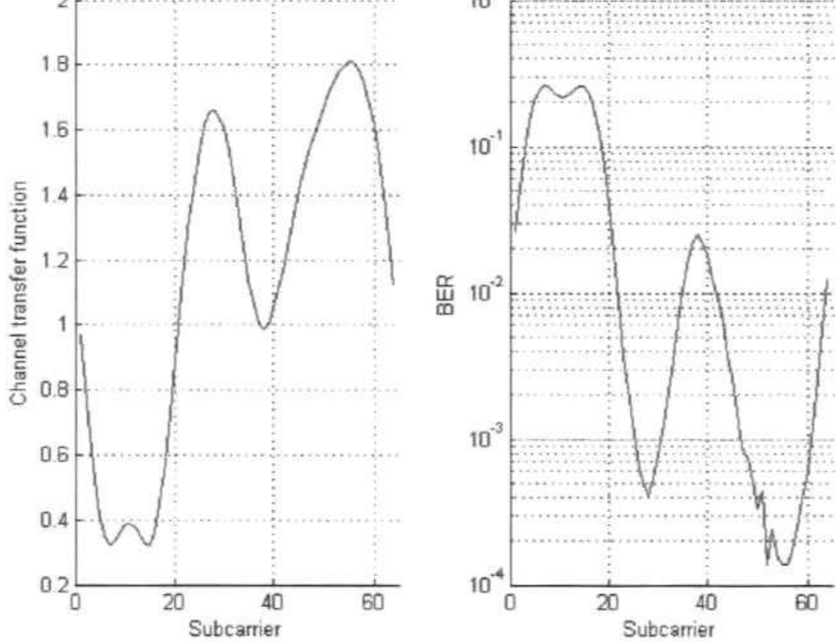

Figure.3.7. Transfer function and BER of QPSK-OFDM system in frequency selective fading channel

The Figure.3.7 shows the subcarriers' transfer function and the BER of a QPSK-OFDM system for specific realization of this frequency selective fading channel. Obviously, the BER is highest in the subcarrier with the deepest fading. The BER on "good" subcarriers can be as low as 10^{-4}, and the BER on subcarriers that are in deep fading are up to 0.3. This also has a significant impact on the average BER: higher channel transfer function leads lower BER, and the BER on "bad" subcarriers dominates the behavior.

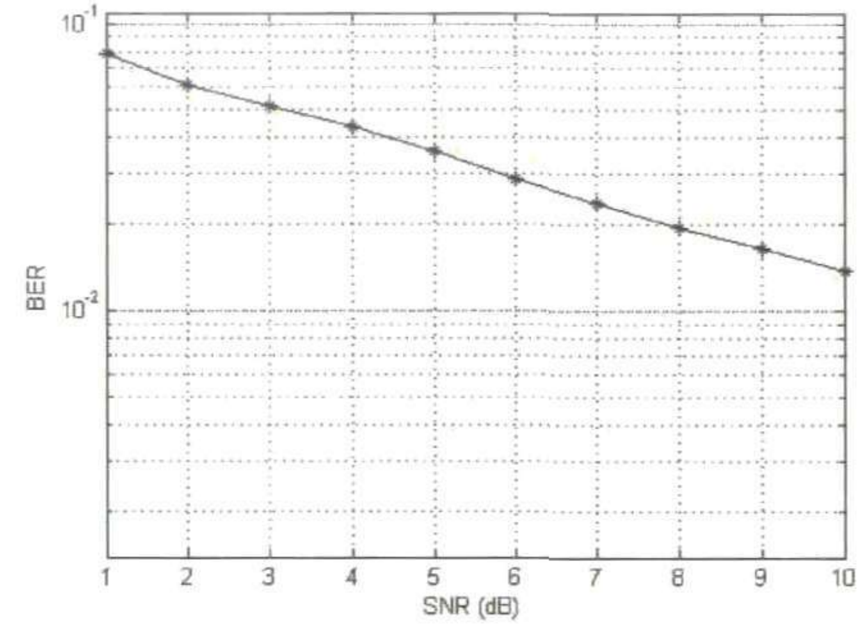

Figure.3.8. BER of QPSK-OFDM system for various of SNR

Subsequently, the Figure.3.8 shows the BER performance of the QPSK based OFDM system in a frequency selective channel specified in Table.3.3. The BER decreases almost linearly as the SNR increases.

3.3. MIMO Channel Model

The multiple antennas are used for three purposes which are beamforming, diversity and spatial multiplexing. Here, we consider a MIMO channel with N_T transmit and N_R receive antennas. When the transmitter knows the channel, we can form N_T different orthogonal beams and transmit parallel datastreams generated by spatial multiplexing over these beams. The increase in spectral efficiency and channel capacity offered by MIMO systems is based on the utilization of space diversity at both the transmitter and the receiver. We will analyze the capacity of MIMO Rayleigh flat fading channel and MIMO frequency selective fading channel in this section. The channel gain matrix is assumed to be perfectly known by transmitter and receiver.

3.3.1. Capacity of MIMO Rayleigh Flat Fading channel

3.3.1.1 Review of SISO Channel

Before exploring the MIMO channel capacity, we firstly study the SISO channel capacity for comparison with MIMO channel capacity later on. In Rayleigh flat fading channel, the channel gain H is time varying and Rayleigh distributed. At the i^{th} time slot over total transmit period T, the instantaneous received SNR is $\gamma[i] = P[i]H[i]^2 / N_0 B$ where B is the bandwidth, $P[i]$ is the transmit power at time i, and N_0 as noise power spectral density. The capacity C is computed using Shannon capacity formula for an AWGN channel with SNR γ, averaged over the distribution of γ.

$$\begin{aligned} C &= \frac{1}{L}\sum_{i=1}^{L} B\log_2(1+\gamma[i]) \\ &= \frac{1}{L}\sum_{i=1}^{L} B\log_2\left(1+\frac{P[i]H[i]^2}{N_0 B}\right) \end{aligned} \tag{3-24}$$

where L is the number of time period in T. The channel gain matrix g is perfectly known by transmitter, and we let the transmit power $P(i)$ vary with time subject to an average power constraint $\overline{P}$:

$$\frac{1}{L}\sum_{i=1}^{L} P[i] = \overline{P} \tag{3-25}$$

The water-filling scheme can be applied for optimum power allocation over time T for $P(i)$.

3.3.1.2 Review of MIMO Channel

In MIMO channel whose channel gain matrix experiences Rayleigh flat fading, we denote the $N_R \times N_T$ matrix of the MIMO channel gain as:

$$H = \begin{pmatrix} h_{11} & h_{12} & \cdots & h_{1N_T} \\ h_{21} & h_{22} & \cdots & h_{2N_T} \\ \vdots & \vdots & \cdots & \vdots \\ h_{N_R 1} & h_{N_R 2} & \cdots & h_{N_R N_T} \end{pmatrix} \tag{3-26}$$

where $h_{i,j}$ is time varying transfer function from the j^{th} transmit to the i^{th} receive antenna and Rayleigh distributed over transmit time T. There are M channel matrix realizations during time T. The channel's capacity is measured by the expected value of the capacity taken over all M channel realizations. For each channel realization, SVD is applied to covert MIMO channel as

$D = \min(N_T, N_R)$ independent parallel subchannels. The total capacity is given by:

$$C = \frac{1}{M}\sum_{m=1}^{M}\sum_{d=1}^{D} B\log_2(1+\frac{P[d]\sigma[d]^2}{N_0 B}) \quad (3\text{-}27)$$

where B is the bandwidth, $P[d]$ is the transmit power at the d^{th} parallel subchannel of the m^{th} channel realization, $\sigma[d]$ is the d^{th} nonzero singular value of the channel gain H at the m^{th} channel realization, and N_0 as noise power spectral density. Here we use the short-term power constraint which assumes the total power associated with each channel realization is equal the average power constraint $\overline{P}$, and the transmit power $P(i)$ in each channel realization vary between parallel channels subject to $\overline{P}$.

$$\frac{1}{D}\sum_{d=1}^{D} P[d] = \overline{P} \quad (3\text{-}28)$$

Then for each channel realization, the channel gain matrix H is perfectly known by transmitter so that the water-filling scheme is applied for optimum power allocation over parallel channels for $P(i)$.

3.3.1.3. Simulation and Performance Evaluation

We evaluate the capacity of MIMO flat fading channel through comparing with that in SISO flat fading channel. The parameters of the flat fading channel between each transmit antenna and receive antenna are listed in Table.3.4, and simulation results are shown in Figure.3.9.

Bandwidth	20kHz
Noise power spectral density (N_0)	10^{-9}
Number of Oscillator	16
Carrier Frequency (GHz)	2.0
Vehicle speed (km/h)	125

Table.3.4. Flat fading channel model parameters II

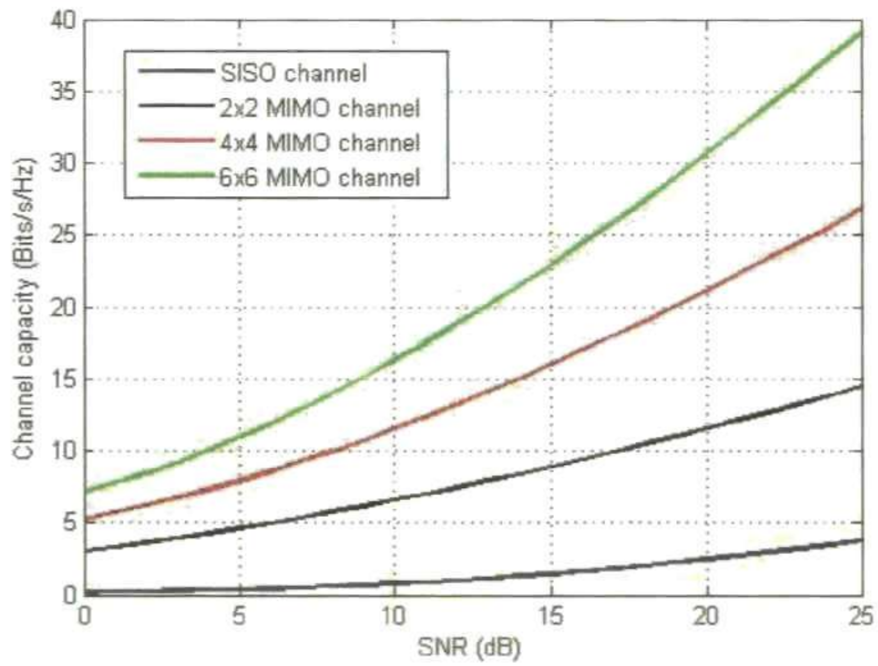

Figure.3.9. Capacity of SISO and MIMO flat fading channels

As shown in Figure.3.9, the channel capacity increases as the increase of number of antennas in flat fading environment. Thus the experiment proves that the MIMO technique results in the increase of flat fading channel capacity compared with SISO system by exploring the space diversity between multiple antennas.

3.3.2. Capacity of MIMO Frequency Selective Fading Channel

Again, the use of an OFDM scheme is optimum for dealing with the frequency selective fading channel because OFDM converts frequency selective fading channel into a number of parallel flat-fading channels. Thus we analyze the capacity of MIMO frequency selective fading channel by using OFDM technique. We denote N as the number of subcarriers of OFDM system, and the transmit time as T .

3.3.2.1. Review of SISO Channel

Firstly, we study the SISO frequency selective fading channel capacity using OFDM technique. At the i^{th} time slot over total transmit period T , each subcarrier experiences independent flat fading, and the power $P[n]$ is allocated to each subcarrier subject to a total power constraint P_i. We also assume P_i is equal to the average power $\overline{P}$ over transmit time T . Then the capacity at time i is the sum of capacities on the flat fading channels of all subcarriers averaged over N subcarriers. The total capacity is the sum of capacities of all time periods averaged over time T and given by:

$$C = \frac{1}{L}\sum_{i=1}^{L}\frac{1}{N}\sum_{n=1}^{N} B_c \log_2(1+\frac{P[n]H[n]^2}{N_0 B_c}) \qquad (3\text{-}29)$$

where L is the number of time period in T , $H[n]$ is the channel gain in subcarrier n at the time i , N_0 as noise power spectral density, B is the total bandwidth, $B_c = B / N$ is the bandwidth of each subcarrier, and

$$P_i = \sum_{n=1}^{N} P[n] \tag{3-30}$$

At time i, the channel gain $H[n]$ for each subcarrier n is perfectly known by transmitter, so that the water-filling scheme is applied to allocate optimum power to $P[n]$ subject to (3-30).

3.3.2.2. Review of MIMO Channel

There are L time periods over the transmit time T. At time i, we assume that the total power P_i is equal the average power $\overline{P}$ over T, and is equally distributed to N subcarriers so that the total power of each subcarrier at time i is $P_{n,i} = P_i / N$. Applying OFDM results in that each subcarrier has an independent flat fading MIMO channel realization H at time i, which is converted to $D = \min(N_T, N_R)$ parallel subchannels by using SVD. Therefore, the capacity of each subcarrier at time i is the sum of capacities over D parallel subchannels. Subsequently, the capacity at time i is the expected value of capacities over N subcarriers, which represents the total capacity over T is the expected value of capacities over L time periods, which is given by:

$$C = \frac{1}{L}\sum_{i=1}^{L}\frac{1}{N}\sum_{n=1}^{N}\sum_{d=1}^{D} B_c \log_2\left(1 + \frac{P[d]\sigma[d]^2}{N_0 B_c}\right) \tag{3-31}$$

where B is the total bandwidth, $B_c = B/N$ is the bandwidth of each subcarrier. $P[d]$ is the transmit power at the d^{th} parallel subchannel of the n^{th} subcarrier at the time i, $\sigma[d]$ is the d^{th} nonzero singular value of the channel gain H of the n^{th} subcarrier at the time i, and N_0 as noise power spectral density.

The MIMO channel gain matrix H of the n^{th} subcarrier at time i is perfectly known by transmitter so that the water-filling theory is applied for optimum power allocation over the D parallel subchannels for the n^{th} subcarrier at time i, subject to $P_{n,i}$ shown as:

$$\sum_{d=1}^{D} P[d] = P_{n,i} \tag{3-32}$$

3.3.2.3. Simulation and Performance Evaluation

We evaluate the capacity of MIMO frequency selective fading channel through comparing with that in SISO frequency selective fading channel in OFDM system. The parameters of OFDM system and the frequency selective fading channel between each transmit antenna and receive antenna are listed in Table.3.5, and simulation results are shown in Figure.3.10.

Number of Subcarrier	64
Bandwidth (Hz)	10MHz
Noise Power spectral density	$10^{\text{[illegible]}}$
Sample period (sec)	100×10^{-9}
Number of Paths	5
Path delay (sec)	$[0,\ 200 \times 10^{-9}, 400 \times 10^{-9}, 600 \times 10^{-9}, 800 \times 10^{-9}]$
Average power (dB)	[0,-4,-8,-13,-18]
Carrier Frequency (GHz)	2.0
Vehicle speed (km/h)	60

Table.3.5. Frequency selective fading channel model parameters II

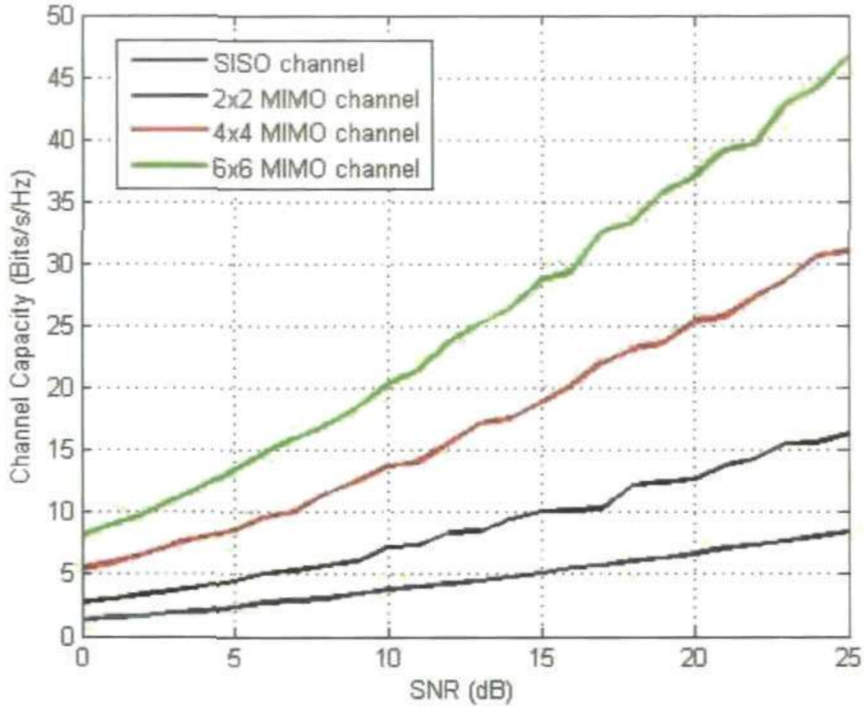

Figure.3.10. Capacity of SISO and MIMO frequency selective fading channels

As shown in Figure.3.10, the channel capacity increases with the increase of number of antennas in frequency selective fading environment. Thus the experiment also proves that the MIMO technique results in the increase of frequency selective fading channel capacity compared with SISO system by exploring the space diversity between multiple antennas.

3.4. Summary

In this chapter, we present an introduction to the characterization of wireless channel including Path loss, Large-scale propagation and small-scale propagation. Then because we focus on the baseband signal processing between transmitter and receiver, the channel model with small-scale propagation is described in detail due to its sensitive variation over short time. In small-scale propagation, the Multipath Effect and Doppler Effect results in the time dispersion and frequency dispersion so that the wireless channel can be classified as flat fading, frequency selective fading, slow fading and fast fading. Subsequently, the improved Jakes' model is designed based on the mathematical analysis of Rayleigh fading property to generate the Rayleigh flat fading channel. The frequency selective fading channel is consisting of several independent Rayleigh flat fading channels, each one having its own average power and time delay. Furthermore, the signal's power and phase variation are evaluated in two situations. One when data transmitted in the Rayleigh flat fading channel from vehicles with different speeds. Another when data transmitted in the frequency selective fading channel from vehicles with different speeds. The results prove that the faster vehicles results in rapid channel variations in both power and phase, thereby more distortion in the signal. Finally, the MIMO flat fading channel and MIMO frequency selective fading channel are introduced by focusing on the channel capacity analysis. By exploring the space diversity between multiple antennas in both flat fading and frequency selective fading environments, the simulation results prove that MIMO technique results in an increase of channel capacity as number of antennas increases.

Chapter 4

Synchronization Techniques in Downlink OFDM System

In this chapter, we focus on the synchronization techniques in single user OFDM System. Synchronization has been one of the crucial research topics in OFDM system because of its sensitivity to the timing and frequency errors [33]. Only by achieving the accurate synchronization, the data can be received in correct timing and compensated by frequency offset, so that the resource allocation which will be described in Chapter 5 can perform its advantages in the OFDM systems. In Section 4.1, an introduction to the synchronization problems in the OFDM system is given. Then the theory of several well-known timing offset estimators is reviewed in theory and their performances are evaluated by computer simulation in Section 4.2. Furthermore, we proposed two novel FFT-based frequency offset estimators in Section 4.3, which provide lower error variances than previous algorithm in different channel environments. In Section 4.4, the integrated model for timing and frequency synchronization is proposed based on our novel FFT-based frequency offset estimators, and followed by the chapter summary in Section 4.5.

4.1. Introduction

Frequency offset (FO) will be arising from the frequency mismatch of the transmitter and the receiver oscillators and the existence of Doppler shift in the channel. The frequency offset will reduce the amplitude of desired signal and introduces the ICI. In addition, due to the delay of signal when transmitting in the channel, the receiver in general starts sampling a new frame at the incorrect time instant. Therefore, it is important to estimate and compensate for the frequency offset to minimize its impact, and to estimate the timing offset at the receiver to identify the start time of each frame and the FFT window position for each OFDM.

As we know, the OFDM signal S_k is generated at baseband by taking the N points IFFT of modulated (QAM) symbols distributed in $N_d(\leq N)$ data subcarriers. Then the signal will be up-converted to a carrier with high frequency f_c for transmission in the channel. It can be express as:

$$S(t) = S_k e^{j2\pi . f_c . t} \tag{4-1}$$

In the receiver, the signal will be down-converted by $f_c^{'}$. The sampled received signal r_n can be expressed as:

$$r_n = e^{j2\pi . \Delta f_c nT_s} \sum_{m=0}^{v-1} S_{k-te} h_m + \varphi_n \tag{4-2}$$

where h_m is the channel impulse response with length v, Δf_c is the frequency offset which is normally normalized with subcarrier spacing $1/NT_s$ where T_s is the sample interval, te is the symbol delay, and φ_n is the white Gaussian noise. Therefore, as shown in equation (4-2), timing offset is modelled as a delay in the received signal, and frequency offset is modelled as a phase distortion of the received data in time domain.

In OFDM system, there are two types of methods for the timing and frequency synchronization which are data-aided and non-data-aided as described in chapter 2. In this thesis, we focus on the data-aided method. We will find out how the different preamble design and patterns improve the estimation performance.

4.2. Timing Synchronization

We will briefly overview several Timing estimators of OFDM system in this section. Different design and pattern of training symbols are sent through the channel and in receiver the timing metric is generated to indicate the start point and the FFT window position for OFDM symbol.

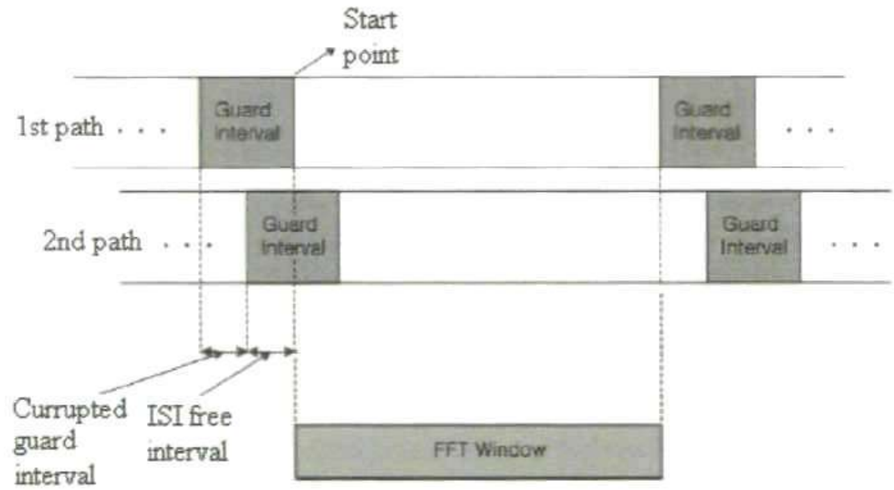

Figure.4.0. OFDM timing estimation

As shown in Figure.4.0, the job of timing estimation is to find out the start point of each frame, and make this start point as the FFT window position for OFDM symbol. Ideally, the start point is shown in the Figure.4.0, which is the boundary of useful part of training symbol. However in practical, the start point will be shifted right or left by couple of samples especially in fast varying channel. The number of shifted samples is called timing offset. Therefore the algorithms are explored in order to minimize the timing offset. Here we use a sliding window with length N. This window is slid until the peak point is generated at the boundary of training symbol which is seen as the correct timing point.

4.2.1. Schmidl's Timing offset Estimator

Schmidl et.al proposed the classical methods for both timing and frequency offset estimation in OFDM systems [35]. Two training symbols are placed at the beginning of each frame as preamble. The m-sequence is used to generate the training sequences. The first training symbol has two identical halves in the time domain. It has the following pattern:

$$S_S = [A, A] \tag{4-3}$$

We use first training symbol to detect the frame. The conjugate of a sample from the first half is multiplied by the corresponding sample from the second half, and the products of each of these pairs of samples are summed. At the start of the frame, the magnitude of the sum will be peaked. The timing metric of this estimator is given by [37]:

$$M\ (d) = \frac{|P(d)|^2}{(R(d))^2} \tag{4-4}$$

where

$$P(d) = \sum_{m=0}^{L-1} r^*_{d+m} . r_{d+m+L} \tag{4-5}$$

$$R(d) = \sum_{m=0}^{L-1} |r_{d+m+L}|^2 \tag{4-6}$$

$L = N/2$ is the length of complex samples in one half of first training symbol excluding CP, and d is a time index corresponding to the first sample in a sliding window of 2L samples.

The second training sequence will be used for frequency offset estimation, which will be described in Section 4.3.1.

4.2.2. Minn's Timing offset Estimator

Because the timing metric of Schmidl's method reaches a plateau which leads to some uncertainty as to the start of the frame, Minn et al [36] modified the training sequence's pattern and timing metric's definition, and then designed the first training symbol having four parts with following patterns:

$$S_M = [A, A, -A, -A] \tag{4-7}$$

where A represents samples of length $L = N/4$ generated by $N/4$ point IFFT of $N_c/4$ length modulated data of a PN sequence. The timing metric applied is same as (4-4), but

$$P(d) = \sum_{k=0}^{1}\sum_{m=0}^{L-1} r^{*}_{d+2Lk+m} \cdot r_{d+2Lk+m+L} \tag{4-8}$$

$$R(d) = \sum_{k=0}^{1}\sum_{m=0}^{L-1} | r_{d+2Lk+m+L} |^2 \tag{4-9}$$

where d is a time index corresponding to the first sample in a sliding window of 4L samples.

4.2.3. Park's Timing offset Estimator

Minn's method [36] reduces the timing metric plateau found in Schmidl's method [35] but the MSE is still large particularly in ISI channels. This is resulted from the timing metric values around the correct timing point in Minn's method are almost the same. Park et al [37] proposed to increase the difference between the peak timing metric with respect to other metric values. The proposed method entails modifying the training sequence's pattern and timing metric's definition to maximize the different pairs of product between them. The training symbol having four parts with the following patterns:

$$S_P = [A, B, A^*, B^*] \quad (4\text{-}10)$$

where A represents samples of length $L = N/4$ generated by IFFT of a PN sequence. B is designed to be symmetric with A which means B is the reversed sequence of A. A^* and B^* are conjugate of A and B respectively. The timing metric applied is same as (4-4), but

$$P(d) = \sum_{k=0}^{N/2} r_{d-k} \cdot r_{d+k} \quad (4\text{-}11)$$

$$R(d) = \sum_{k=0}^{N/2} | r_{d+k} |^2 \quad (4\text{-}12)$$

where d is a time index corresponding to the first sample in a sliding window of 4L samples.

4.2.4. Seung's Timing offset Estimator

In fast varying channel where the first channel path is not always dominant, the performance of Park's method [37] is degraded since it assumed the first arrived channel path is dominant. Seung et al proposed a modified method to define the time domain preamble pattern as follow [39]:

$$S_C = [A, B^*] \quad (4\text{-}13)$$

where A represents the sequence with length of $L = N/2$ generated by IFFT of the constant amplitude zero auto-correction (CAZAC) sequence modulated by QPSK. B^* represents the complex conjugate of B, which is time reversed version of A.

This method then uses zero padding for the guard interval of the preamble instead of the conventional cyclic prefix. The timing metric applied is same as (4-4), but

$$P(d) = \sum_{k=0}^{N/2-1} r_{d-k} \cdot r_{d+k+1} \tag{4-14}$$

$$R(d) = \frac{1}{2} \sum_{k=0}^{N/2} | r_{d+k-N/2} |^2 \tag{4-15}$$

where d is a time index corresponding to the first sample in a sliding window of 2L samples. The Seung's timing metric has impulse peak at the correct symbol timing point. In fast varying channel, the impulses from timing metric are thresholded by a pre-defined value and combined in the moving summation block. The point with maximum value in the moving summation block is defined as estimated correct time point. By using this threshold-based window method, the interval between the peak point and the estimated correct time point is estimated, and then the peak point is compensated by this interval to produce more accurate estimation

4.2.5. Evaluation of Timing offset Estimators

In this section, the performance of these Timing estimators is investigated by computer simulation in single user OFDM system. The system and multipath channel parameters are listed in Table.4.1.

System Parameters:	
Number of data subcarriers (N_d)	1000
IFFT points (N)	1024
Data modulation	QPSK
Date rate (Mbits/s)	18
CP length	10% of OFDM symbol
Frequency offset	12.4 subcarrier spacing
Multipath channel parameters:	
Number of Paths	16
Path delays τ_i (samples)	[0,4,8,…60]
Path gains h_i	$h_i = \frac{\exp(-\tau_i / 60)}{\sqrt{\sum_{k=1}^{16} \exp(-\tau_k / 30)}}$
Max Doppler shift f_d (Hz)	60

Table.4.1. OFDM system and multipath channel parameters

The OFDM symbols are generated by 1000 frequencies, and then slightly oversampled at a rate of 1024 samples for the useful part of each symbol.

4.2.5.1. Timing Metrics

First of all, under the no noise and distortion condition, the timing metrics of Schmidl's, Minn's, Park's and Seung's are evaluated. In order to show clearly the sharp timing metrics of Park's and Seung's methods, Seung's method is individually shown in Figure.4.1 (b), and the Schmidl's, Minn's and Park's methods are shown in Figure.4.1 (a) respectively. In the figures, the correct start time point (index 0 in the figure) is taken as the start of the useful part of training symbol (after cyclic prefix).

As shown in Figure.4.1, the timing metric of Schmidl method will reach a plateau that causes the ambiguity when estimating precise start time point. The Minn's method reduced the timing metric plateau, but adjacent samples to metric peak value have almost the same values as the metric at the preamble boundary (peak metric value) when data is transmitted in the channel with noise and fading distortion. This occurrence causes some incorrect estimation. The Park's and Seung's method gives impulse-shaped timing metrics which make them outperform the Schmidl's and Minns' methods. But Park's method has lots of small subpeaks at the other positions of correct timing which will cause incorrect estimation in fast varying channel. In Seung's method, the shape of timing metric is the ideal impulse and the small subpeaks in Park's method are suppressed.

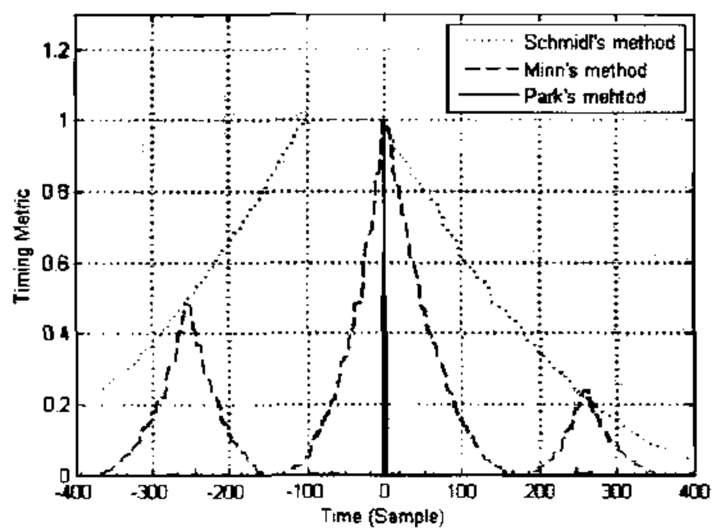

(a) Schmidl's, Minn's and Park's Timing metrics

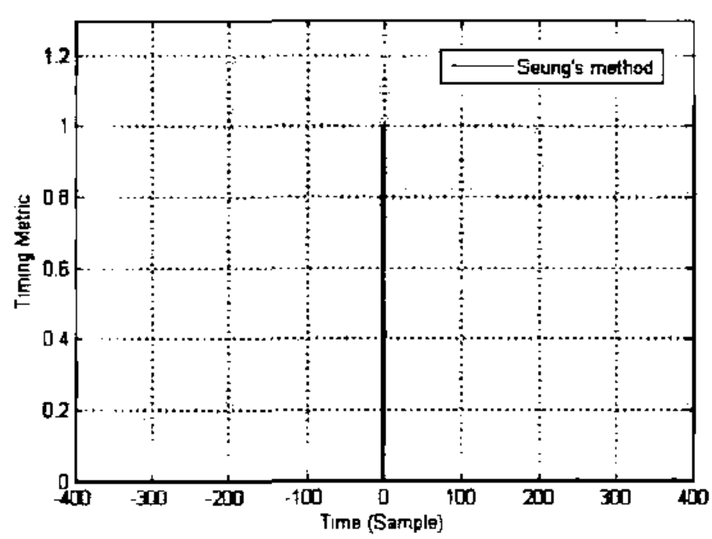

(b) Seung's Timing metric

Figure.4.1. Timing metrics of Timing offset estimators under no noise and distortion condition

So far, we have investigated the timing metrics of all timing offset estimators under the condition of no noise and distortion. Subsequently, we investigate the timing metrics of these timing offset estimators under both ISI static channel and multipath time-varying fading channel. The Schmidl's and Minn's methods are shown in Figure.4.2 (a) and Figure.4.2 (b), the Park's method is shown in Figure.4.2 (c) and Figure.4.2 (d), and the Seung's method is shown in Figure.4.2 (e) and Figure.4.2 (f). The parameters of multipath time-varying channel are listed in Table.4.1, and the path gains of the static ISI channel are fixed and assumed to be same as the path gains of the multipath time-varying channel.

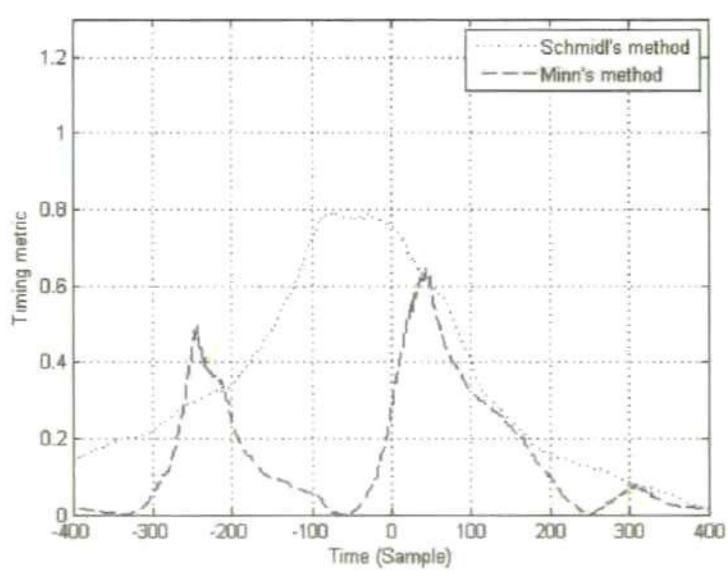

(a). Timing metric of Schmidl's and Minn's method in ISI static channel

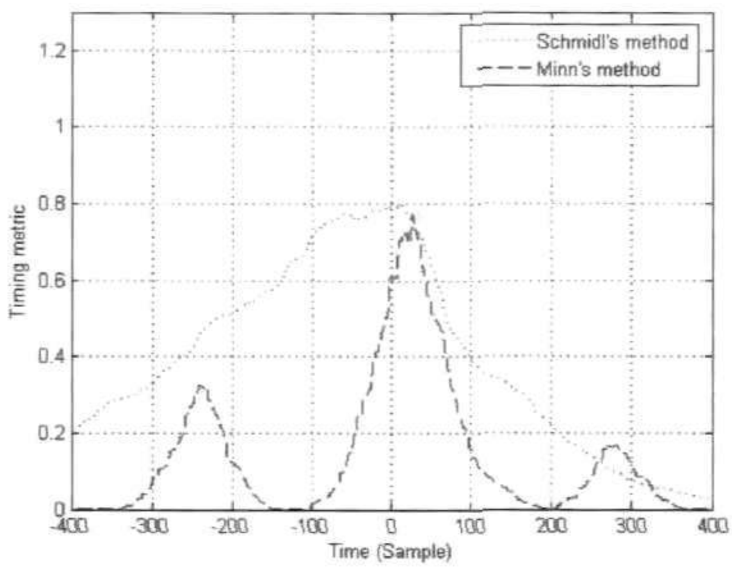

(b). Timing metric of Schmidl's and Minn's method in multipath time-varying channel

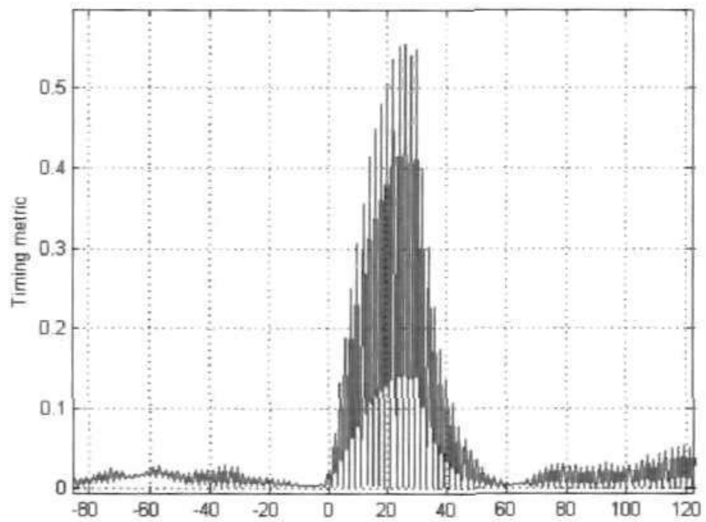

(c). Timing metric of Park's method in ISI static channel

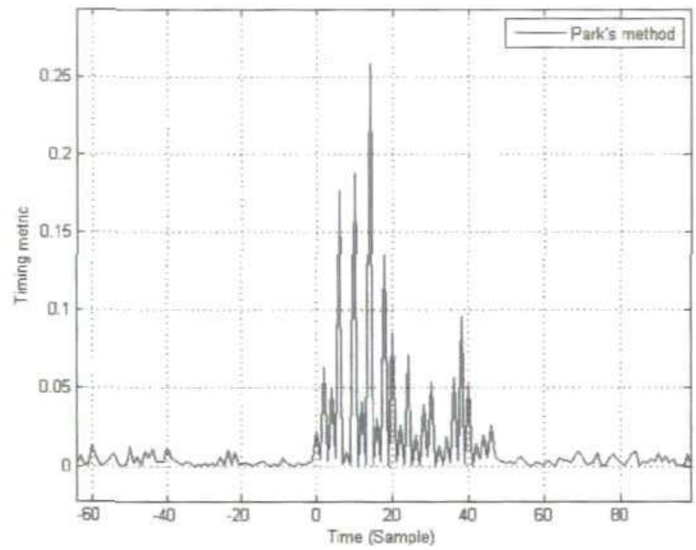

(d). Timing metric of Park's method in multipath time-varying channel

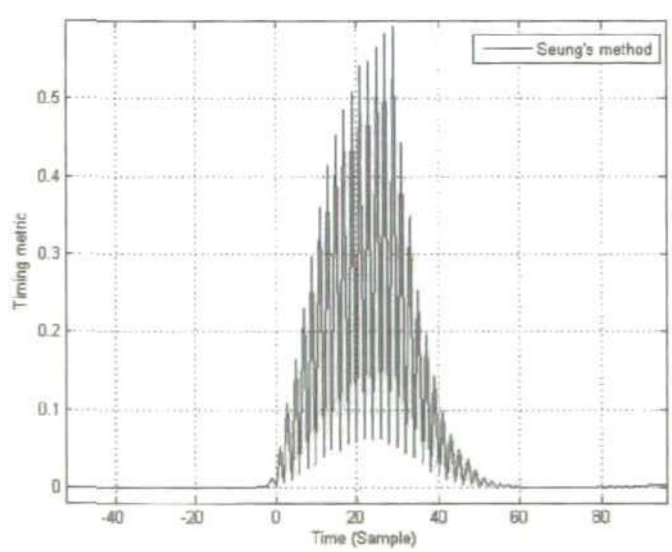

(e). Timing metric of Seung's method in ISI static channel

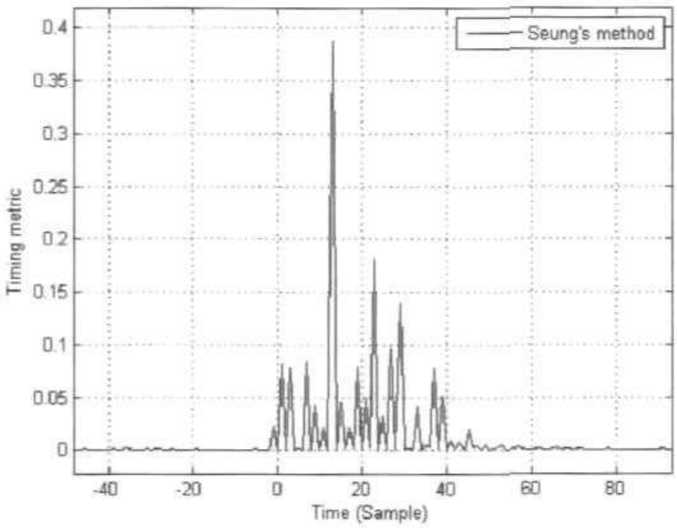

(f). Timing metric of Seung's method in multipath time-varying channel

Figure.4.2. Timing metrics of Timing offset estimators under ISI static channel and multipath time-varying channel

As shown in Figure.4.2, in both ISI static channel and multipath time-varying channel, these timing metrics are not generating the peak in the correct start time point. The signal in receiver is the summation of signals from multiple paths, and the path with strongest signal is random in the channel, so multiple peaks are generated instead of one peak at the correct start point. For Schmidl's, Minn's and Park's methods, they all assume the first path is dominant so that the highest peak point is determined as the time start point. But the Seung's method proposed a simple threshold-based windowing method to find out the interval between the highest peak point and the correct time point, and then the highest peak point is compensated by this interval to produce more accurate estimation. In the Section 4.2.5.2, the mean and error variance of these timing offset estimators are evaluated.

4.2.5.2. Mean and Error Variance of Timing offset in Static ISI Channel and multipath Time-varying Channel

In this section, we evaluate the timing offset estimators by their mean and error variance in both ISI static channel and Multipath time-varying channel under different SNR conditions (0-20dB). The channel parameters are the same as that listed in Table.4.1. For each SNR, we estimate the timing offsets in 1000 different channel environments for all these methods, and then the mean and error variance for each method on each SNR are calculated. Finally the results are shown in Figure.4.3 (a) and Figure.4.3 (b) respectively.

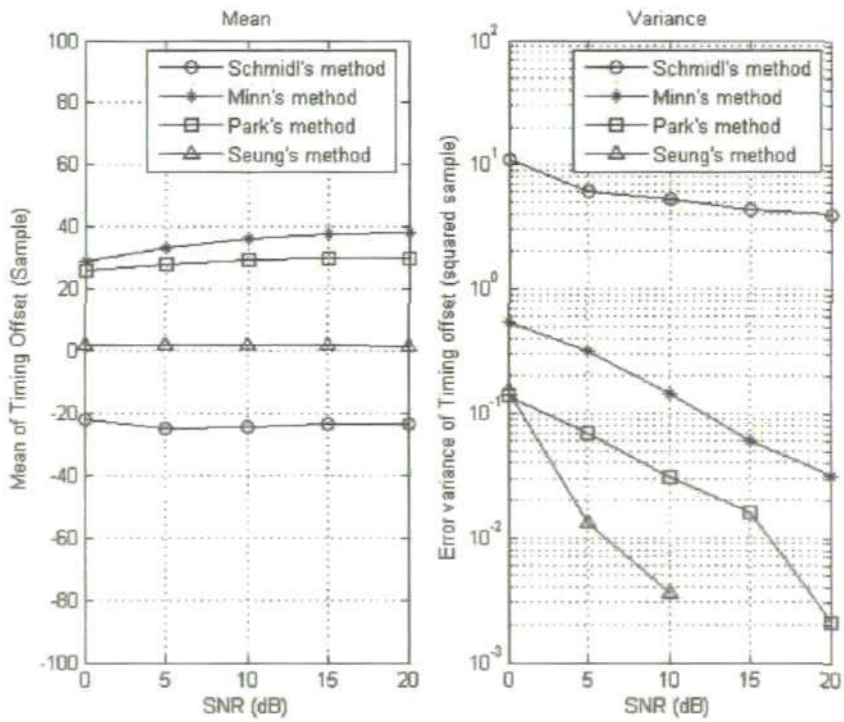

(a). Mean and Error variance of Timing offsets in ISI static channel

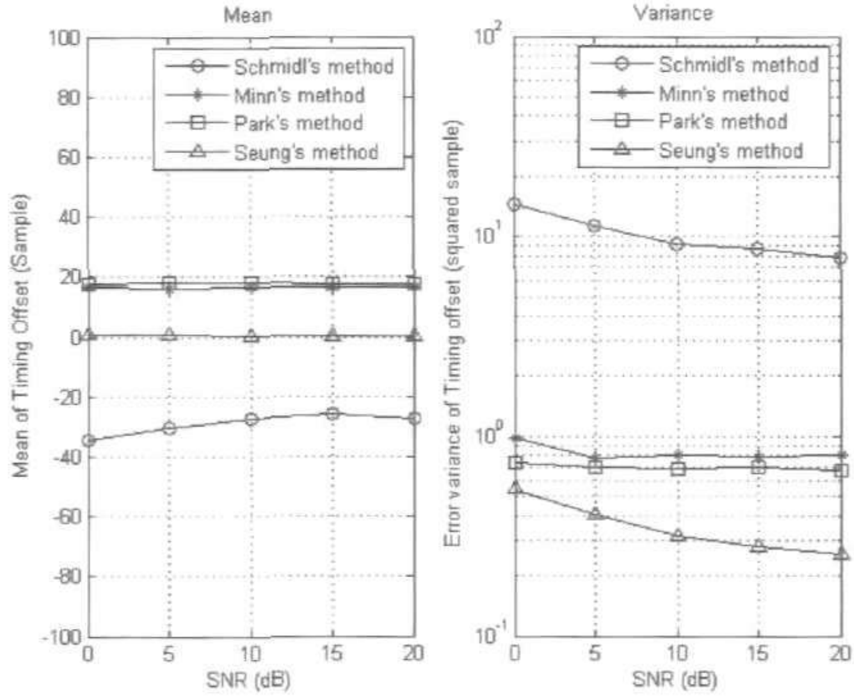

(b). Mean and Error variance of Timing offsets in Multipath time-varying channel

Figure.4.3. Mean and Error variance of Timing offsets in both ISI static channel and Multipath time-varying channel

As shown in Figure.4.3 (a) and Figure.4.3 (b), the followings are observed in both ISI static and multipath time-varying channel:

1. The means of peak points for each SNR in the Schmidl's, Minn's and Park's methods have significant gap with zero point which is marked as correct timing point. As shown in the Figure.4.3, the minus mean points for Schmidl's method over the SNR values mean that the peak points generated by Schmidl's method are mostly located at the left hand side of correct timing point. Subsequently, we can also find out the Seung's

method generates near zero point estimation by applying threshold-based windowing method, which means the more accurate estimation is achieved compared with Schmidl's, Minn's and Park's methods.

2. Schmidl's method generates the highest error variance in the estimates for the SNR range considered. And Seung's method has smaller error variance than all other three methods. This fact gives same conclusion with the evaluation done by Timing metrics. The Seung's method applying the threshold-based windowing method produces the best performance and Park's method having ideal impulse timing metric but with sub-peaks produces the second good performance, and the Minn's method reducing the timing metric plateau of Schmidl's method therefore outperforms Schmidl's method.

4.3. Frequency Synchronization

After reviewing the Timing synchronization techniques, we will briefly overview the Schmidl's Frequency offset estimator proposed in [35] because it is classic and popular used. Subsequently, we propose two simple but efficient FFT-based Frequency offset estimators.

4.3.1. Schmidl's Frequency offset Estimator

As mentioned in Section 4.2.1, Schmidl et al designed two training symbols as preamble. The first one has two identical parts $s_{1,n}$ and $s_{1,n+L}$ with $N/2$ samples each and $L\ (=N/2)$ delay between identical samples. They will remain identical after passing through the channel, except the phase difference ϕ between them due to the frequency offset (Δf_c). The received two parts of first training symbol $r_{1,n}$ and $r_{1,n+L}$ are given as:

$$r_{1,n} = s_{1,n} e^{j2\pi.\Delta f_c nT_s} + \varphi(nT_s) \tag{4-16}$$

$$\begin{aligned} r_{1,n+L} &= s_{1,n+L}.e^{j2\pi.\Delta f_c (n+L)T_s} + \varphi(nT_s) \\ &= r_{1,n} e^{j2\pi.\Delta f_c .LT_s} + \varphi(nT_s) \end{aligned} \tag{4-17}$$

Consequently, without noise, the two parts will have the following relation:

$$r_{1,n+L} = r_{1,n}.e^{j2\pi.\Delta f_c LT_s} \tag{4-18}$$

The phase of their correlation is:

$$\phi = 2\pi.\Delta f_c LT_s = \pi.\Delta f_c NT_s \tag{4-19}$$

which can be estimated at the best timing point.

$$\phi = angle(P(d)) \tag{4-20}$$

Then if $|\phi|$ is less then π, the frequency offset will be:

$$\Delta f_c = \frac{\phi}{\pi NT_s} \tag{4-21}$$

Otherwise

$$\Delta f_c = \frac{\phi}{\pi NT_s} + \frac{2\hat{l}}{NT_s} \tag{4-22}$$

where $\hat{\ell}$ is an integer. To find the unknown second term in (4-22), the two training symbols are partially corrected with the known frequency offset by multiplying the samples with

$$\exp(-j2\pi\frac{\phi}{\pi NT_s}t) = \exp(-j2\frac{\phi}{NT_s}t) \tag{4-23}$$

Let the FFT's of received first and second offset frequency corrected training symbols ($F_{1,k}$, $F_{2,k}$) and the differentially modulated even frequencies of the second training symbol be (u_k). The sliding correlation between the FFTs and (u_k) is given by

$$B(\ell) = \frac{|\sum_{k \in X} F^*_{1,k+2\ell} . u^*_k . F_{2,k+2\ell}|^2}{2(\sum_{k \in X} |F_{2,k}|^2)^2} \tag{4-24}$$

where X is the set of indices for even frequency components of the second training symbol. Finally, the l corresponding to the maximum value of $B(l)$ is marked as $\hat{\ell}$, and used to calculate integral frequency offset in (4-22).

4.3.2. Proposed FFT-based Frequency offset Estimators

We propose two FFT-based frequency offset estimators in this section by using the first training symbol of Schmidl's method. This training symbol is inserted in the beginning of data frame. In the receiver, we synchronize the data frame in time first to find out the boundary of the useful part of received training symbol, which is denoted as r_n.

$$r_n = A_n e^{j2\pi.\Delta f_c (n+N_g)T_s} \qquad (4\text{-}25)$$

where A_n is the training symbol which is assumed to be known to the receiver, N_g is the length of cyclic prefix of training symbol, Δf_c is the frequency offset, and T_s is sample interval. r_n is multiplied with the conjugate of the known training symbol A_n^* to get the modified received training symbol d_n, and then d_n is processed by N-points FFT to get the frequency domain spectrum F_k.

$$\begin{aligned} d_n &= r_n.A_n^* \\ &= |A_n|^2 e^{j2\pi.\Delta f_c (n+N_g)T_s} \end{aligned} \qquad (4\text{-}26)$$

$$F_k = \sum_{n=0}^{N-1} d_n.e^{-j2\pi.nk/N} \, (0 \le k \le N-1) \qquad (4\text{-}27)$$

The coarse frequency is yielded by searching for the largest magnitude given by (4-27). Let bin number of the largest magnitude be k_{max}, then the coarse frequency f_{coarse} is given by:

$$f_{coarse} = \frac{k_{max}}{NT_s} \tag{4-28}$$

When the signal d_n is highly correlated with one certain waveform within the set of $e^{-j2\pi nk/N}$, it will be represented by a large magnitude on certain frequency in the $k_{max} - th$ bin. If Δf_c is exactly same as the maximum FFT bin's frequency, this large magnitude will fall in the centre of the $|F_k(k_{max})|$, otherwise the large magnitude will be placed in one bin whose frequency is the closest to the actual Δf_c. Especially in the later case, the large magnitude is laid between two adjacent bins. Figure.4.4 shows the spectrum of d_n with various frequency offsets.

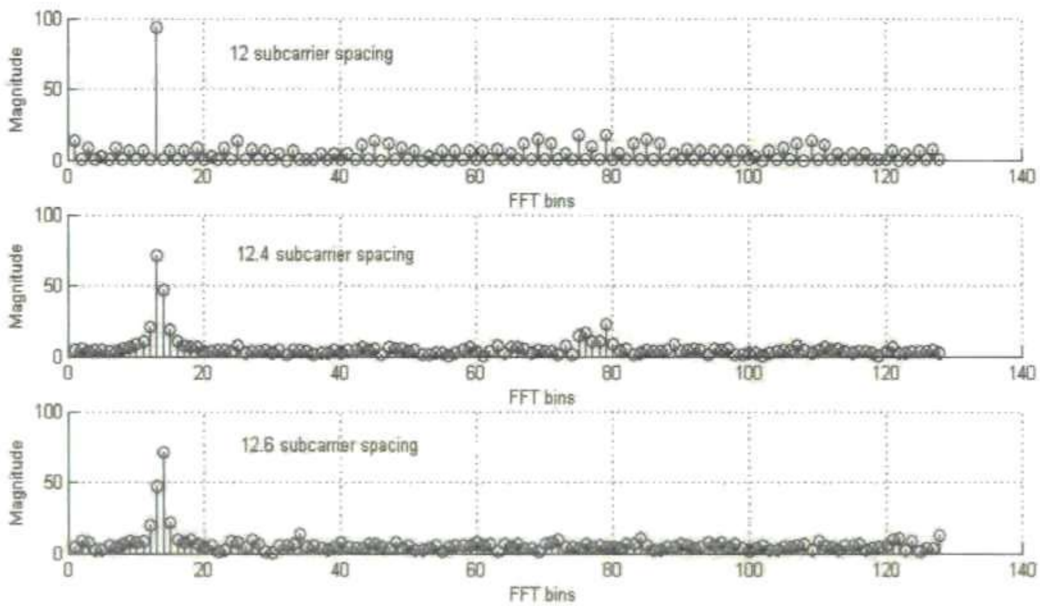

Figure.4.4. 128-FFT spectrum of d_n with various frequency offset

Figure.4.4 (a) is obtained when the Δf_c exactly equals to the 12[th] bin's frequency. Figure.4.4 (b) and Figure.4.4 (c) illustrate the spectrums when their

Δf_c is not the same as the FFT bin frequency. As shown in the Figure.4.4 (b) and Figure.4.4 (c), Δf_c of 12.4 subcarrier spacing and 12.6 subcarrier spacing are represented by the 12^{th} bin and 13^{th} bin respectively since the 12^{th} bin and 13^{th} bin are laid on the closest place of their actual Δf_c.

The coarse frequency offset estimator above can achieve precise estimation when the Δf_c equals to the FFT bin frequency. However the d_n is not always same as the FFT bin frequency due to the oscillator mismatch, Doppler shift and noise in the channel, therefore further process is necessary to estimate the fine frequency offset. To alleviate this problem, we propose two methods for the estimation of the fine frequency offset.

4.3.2.1. FFT method-I: Linear Interpolation based Estimator

This method is based on the algorithm proposed in [109] which is extended to OFDM system. It utilises the magnitude value of the largest magnitude $|F(k_{\max})|$, and magnitude of components on both sides of the largest spectrum $|F(k_{\max}-1)|$ and $|F(k_{\max}+1)|$. These three values are interpolated by using the equation (4-28), and the fine frequency offset is given as:

$$f_{fine} = \frac{1}{NT_s} \cdot \frac{\alpha}{F(k_{\max})/F(k_{\max}+\alpha)+1} \tag{4-29}$$

where the α is a switching function, and can be defined as:

$$\begin{aligned} \alpha &= 1 \quad if \quad |F(k_{\max}-1)| \le |F(k_{\max}+1)| \\ \alpha &= -1 \quad if \quad |F(k_{\max}-1)| > |F(k_{\max}+1)| \end{aligned} \tag{4-30}$$

Therefore the overall frequency offset Δf_c is expressed as:

$$
\begin{aligned}
\Delta f_c &= f_{corse} + f_{fine} \\
&= \frac{1}{NT_s}\left(k_{\max} + \frac{\alpha}{F(k_{\max})/F(k_{\max}+\alpha)+1}\right)
\end{aligned}
\tag{4-31}
$$

4.3.2.2. FFT method-II: Matched filter based Estimator

Briefly, the matched filter based estimator consists of a spectrum shifting of F_k, transformation of the shifted signal from frequency domain to the time domain, and then estimation of fine frequency offset by matched filter approach.

The first step is the spectrum shifting which is shifting the FFT's bin depending on the estimated value of the coarse frequency. Mathematically, the spectrum shifting is expressed as:

$$
\begin{aligned}
d_n^{'} &= d_n e^{-j2\pi . f_{coarse}(n+N_g)T_s} \\
&= |A_n|^2 e^{j2\pi .(f_c - f_{coarse}).(n+N_g)T_s} \\
&= |A_n|^2 e^{j2\pi . f_{fine} .(n+N_g)T_s}
\end{aligned}
\tag{4-32}
$$

This requires a high computational complexity, because we have to generate N -complex sinusoid signals and then perform N-complex multiplications. Thus our shifting algorithm is shifting the maximum bin $k_{\max}$ to zero frequency position to compensate d_n by f_{coarse} in frequency domain to get $d_n^{'}$, so that $d_n^{'}$ has the spectrum which is distorted by fine frequency f_{fine} only. Figure.4.5 illustrates the shifting process of d_n with frequency offset of 12.4 subcarrier spacing. The shifted spectrum represents the spectrum of signal $d_n^{'}$ with fine frequency offset 0.4 subcarrier spacing only in frequency domain.

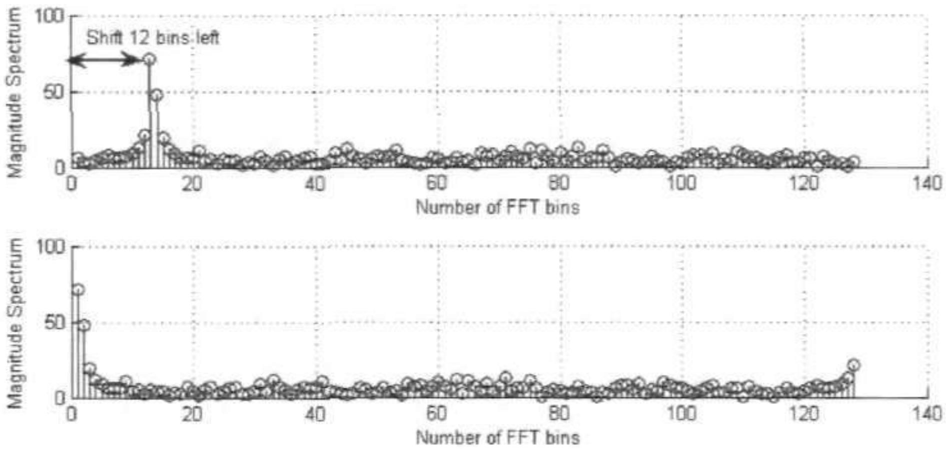

Figure.4.5. 128-points FFT spectrum of d_n and shifted signal $d_n^{'}$

Furthermore, in order to satisfy the equation (4-32) and N-points Inverse Fast Fourier Transform (IFFT) is applied to the shifted signal to transform from frequency domain to time domain, as given by:

$$d_n^{''} = \sum_{k=0}^{N-1} F_k^{'}.e^{j2\pi.k.n/N} \tag{4-33}$$

where $F_k^{'}$ is shifted F_k. For simplicity, the equation (4-33) can be expressed as:

$$d_n^{''} = M_n.e^{j\phi_n} \tag{4-34}$$

where M_u and ϕ_n are magnitude and phase of $d_n^{''}$ respectively. As we know, $d_n^{'}$ represents the expected modified received training symbol distorted by fine frequency offset only. $d_n^{''}$ is supposed to be same with $d_n^{'}$, so that the fine frequency estimator is derived under matched filter concept by matching $d_n^{''}$

with $d_n^{'}$. However, the coarse frequency offset operated over the cyclic prefix of training symbol will lead the phase change for ϕ_n, and also when ϕ_n reaches its maximum value π, immediately it will go down to the minimum value $-\pi$, and vice versa. Therefore before approaching next step analysis, we need to correct these two problems to make sure $d_n^{''}$ is exactly same with $d_n^{'}$ in both magnitude and phase. Subsequently, we use the figures to clearly explain these two problems. Figure.4.6 shows the magnitude and phase of shifted signal $d_n^{''}$ and expected signal $d_n^{'}$.

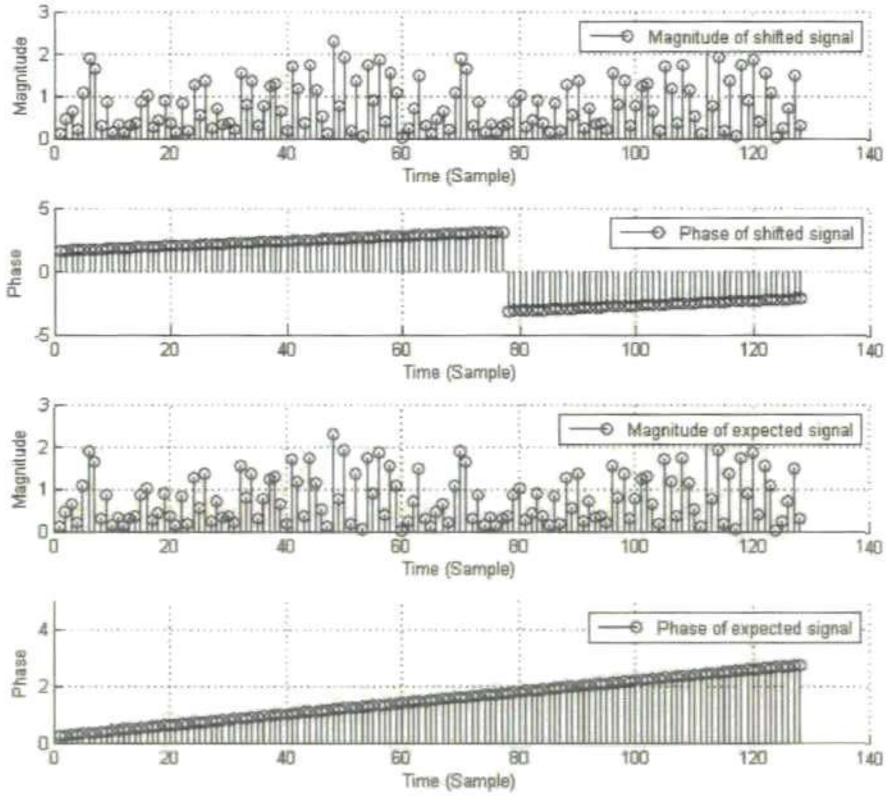

Figure.4.6. Magnitude and Phase comparison of the shifted signal $d_n^{''}$ and the expected signal $d_n^{'}$

As shown in Figure.4.6, the magnitudes of $d_n^{''}$ and $d_n^{'}$ are exactly same, but there are phase difference between $d_n^{''}$ and $d_n^{'}$. Additionally, the phase reaches maximum value π in 77th sample of $d_n^{''}$, and then from 78th sample, the phase jumps 2π to be the negative value so that the phase linear spreading is destroyed. All of these facts lead the incorrect fine frequency offset estimation. Through experiment, we find out the phase difference θ_0 is caused by the coarse frequency offset operating on the cyclic prefix of training symbol and is equal to $angle(e^{j2\pi \cdot f_{coarse} N_g T_s})$. In addition, the 2π jump can be resolved by changing the jumped phases to their 2π complement, which is called 2π correction. Figure.4.7 shows the results after the phase compensation and 2π correction.

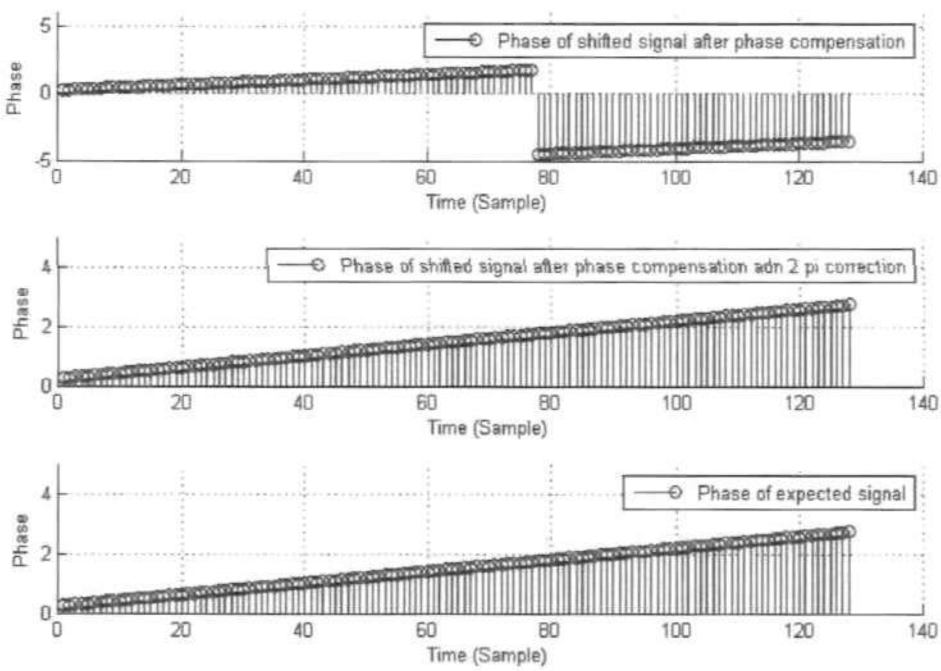

Figure.4.7. Phase of the shifted signal $d_n^{''}$ after phase compensation and 2π correction

As shown in Figure.4.7, after the phase compensation and 2π correction, $d_n^{"}$ has exactly same phase and magnitude as $d_n^{'}$, ϕ_n is modified as $[\phi_n - \theta_0]_{2\pi}$, where $[.]_{2\pi}$ means 2π correction. Then the matched filter output is given by the auto-correction of $d_n^{"}$ with $d_n^{'}$ with zero shift, and its real part can be expressed as:

$$MF(0) = \sum_{n=0}^{N-1} M_n |A_n|^2 \cos([\phi_n - \theta_0]_{2\pi} - 2\pi f_{fine}(n + N_g)T_s) \qquad (4\text{-}35)$$

$MF(0)$ can be maximized by appropriate choice of f_{fine}. Differentiate with respect to f_{fine}, and set result to zero gives:

$$\frac{dx}{df_{fine}} = -\sum_{n=0}^{N-1} M_n |A_n|^2 2\pi.(n + N_g).T_s.\sin([\phi_n - \theta_0]_{2\pi} - 2\pi f_{fine}(n + N_g)T_s) = 0 \quad (4\text{-}36)$$

If $([\phi_u - \theta_0]_{2\pi} - 2\pi f_{fine}.(n + L).T_s)$ is small then

$$-\sum_{n=0}^{N-1} M_n |A_n|^2 2\pi.(n + N_g).T_s.([\phi_n - \theta_0]_{2\pi} - 2\pi f_{fine}(n + N_g)T_s) = 0$$

$$-\sum_{n=0}^{N-1} M_n |A_n|^2 (n + N_g)([\phi_n - \theta_0]_{2\pi} - 2\pi f_{fine}(n + N_g)T_s) = 0 \qquad (4\text{-}37)$$

$$\sum_{n=0}^{N-1} M_n |A_n|^2 (n + N_g)[\phi_n - \theta_0]_{2\pi} = \sum_{n=0}^{N-1} M_n |A_n|^2 .2\pi f_{fine}(n + N_g)^2 T_s$$

Therefore the fine frequency offset f_{fine} is:

$$f_{fine} = \frac{\sum_{n=0}^{N-1} M_n |A_n|^2 .(n+N_g).[\alpha_n - \theta_0]_{2\pi}}{2\pi T_s \sum_{n=0}^{N-1} (n+N_g)^2 .M_n |A_n|^2} \tag{4-38}$$

Finally, the total frequency offset Δf_c is given by:

$$\Delta f_c = f_{coarse} + f_{fine} = \frac{k_{\max}}{NT_s} + \frac{\sum_{n=0}^{N-1} M_n |A_n|^2 .(n+N_g).[\alpha_n - \theta_0]_{2\pi}}{2\pi T_s \sum_{n=0}^{N-1} (n+N_g)^2 .M_n |A_n|^2} \tag{4-39}$$

4.3.3. Simulation and Performance Evaluation

In this section, the performance of Schmidl's and proposed frequency offset estimators is investigated by computer simulation. The system and multipath time-varying channel parameters are listed in Table.4.2. Because we also evaluate the performance in multipath static fading channel, then we assume the path gains of the multipath static fading channel to be fixed and same as the path gains in the multipath time-varying fading channel.

System Parameters:	
Number of data subcarriers (N_d)	1000
IFFT points (N)	1024
Data modulation	QPSK
Date rate (Mbits/s)	18
CP length	10% of OFDM symbol
Frequency offset	2.4 subcarrier spacing
Multipath time-varying channel parameters:	
Number of Paths	3
Path delays τ_i (samples)	[0,6,11]
Path gains h_i	[0.9,0.36,0.29]
Max Doppler shift f_d (Hz)	60

Table.4.2. OFDM system and multipath channel parameters

The OFDM symbols are generated by 1000 frequencies, and then slightly oversampled at a rate of 1024 samples for the useful part of each symbol.

4.3.3.1. Comparison of Pre-defined and Estimated Frequency offset

First of all, a series of frequency offsets are defined with values from 0 to 4.8 subcarrier spacing with interval of 0.4 subcarrier spacing. For each pre-defined frequency offset, the Δf_c estimated by the proposed methods and normalized by subcarrier spacing is compared with pre-defined value in both AWGN channel and multipath time-varying fading channel with SNR=10dB respectively. Results are shown in Figure.4.8.

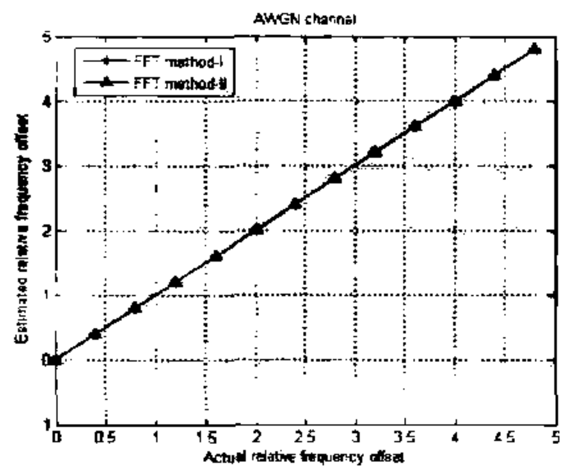

(a)

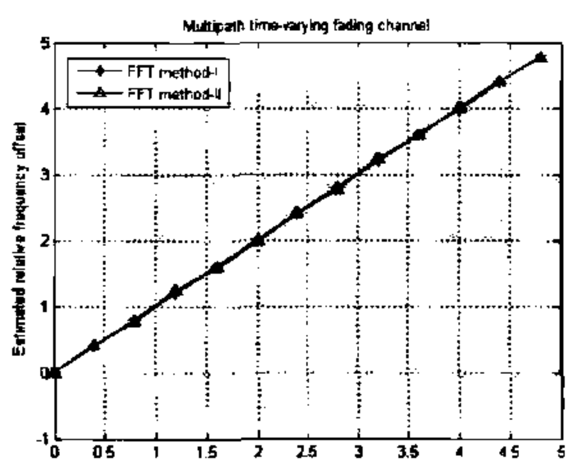

(b)

Figure.4.8. Actual and estimated frequency offset comparison in
(a) AWGN channel (b) Multipath time-varying fading channel

As shown in Figure.4.8, in both AWGN channel and Multipath time-varying fading channel, the two proposed FFT-based methods can achieve accurate estimation for all the pre-defined frequency offsets. Furthermore, in Section 4.3.3.2, we will evaluate the proposed methods by their error variances.

4.3.3.2. Error Variance of Estimated Frequency offset

Secondly, the Error Variance (EV) of the estimated frequency offset is evaluated and compared between the Schmidl's method proposed in [35] and two proposed methods. As shown in Table.4.3, the frequency offset is assumed as 2.4 subcarrier spacing. The SNR is set from 0 to 24dB with interval of 3dB. Finally the EVs of different SNR for these estimators are evaluated in AWGN channel, multipath static fading channel and multipath time-varying fading channel respectively. Results are shown in Figure.4.9.

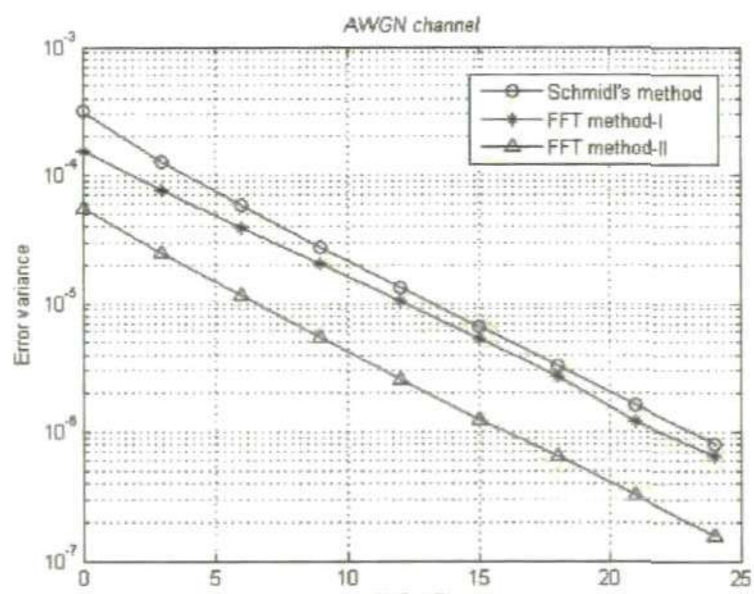

(a)

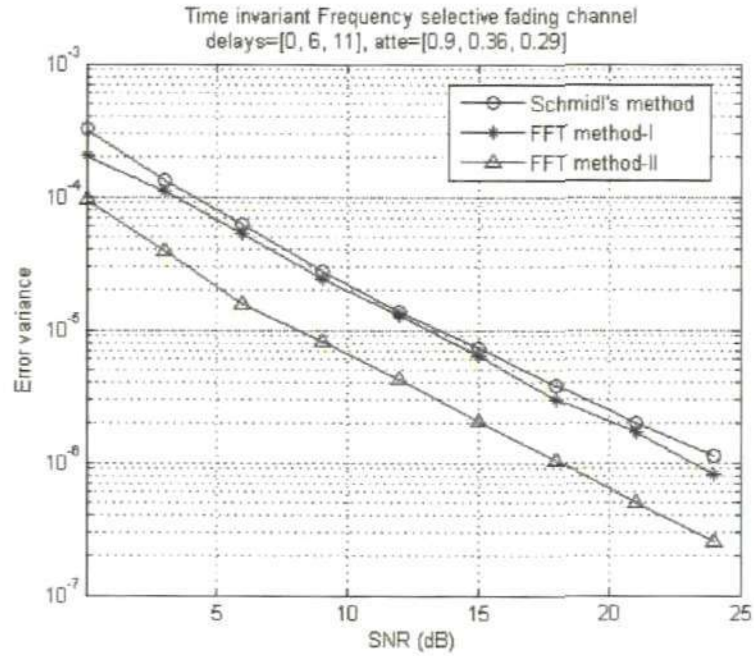

(b)

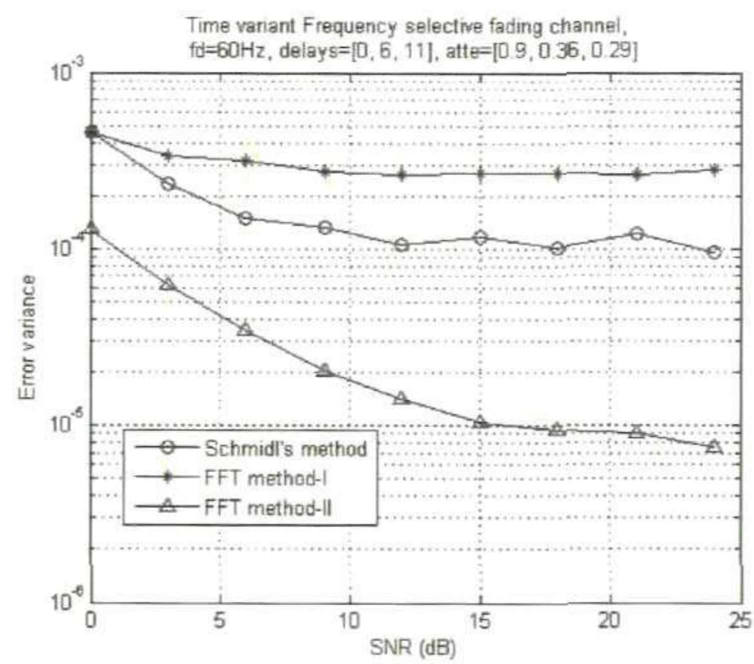

(c)

Figure.4.9. Error variances of frequency offset estimators in channels of (a) AWGN (b) Multipath static fading (c) Multipath time-varying fading

As shown in Figure.4.9, the proposed FFT-based methods produce lower error variances than Schmidl's method in both AWGN channel and multipath static fading channel. However due to the variability of random phase effected in the multipath time-varying fading channel, FFT method I-Linear Interpolation based estimator cannot provide the stable accurate estimation and give higher error variance than Schmidl's method in the multipath time-varying fading channel. The reason is that FFT method-I only considers the magnitudes of FFT outputs. Simultaneously, in the same multipath time-varying fading channel, the FFT method II-matched filter based estimator still outperforms Schmidl's method since it fully utilizes and corrects the signal phases.

The proposed algorithms can also be easily extended to multiuser downlink OFDM systems. The training sequence transmitted from base station is perfectly known by each mobile user so that the accurate frequency offset estimation can be achieved by proposed methods for each mobile user.

4.3.3.3. Computation Complexity

This section presents the comparison of the computation complexity between the two proposed methods with Schmidl method. We assume the training symbol used for estimation has 1024 samples, and Radix-2 FFT is applied when needed. The results are shown in Table.4.3.

	Addition	Product	Exponential Evaluation	Magnitude Evaluation
Schmidl's method	23445	48131	4524	5868
FFT method- I	13	1099	10	1024
FFT method- II	5142	15507	1044	4096

Table.4.3. Computational Complexity

As shown in Table.4.4, the proposed FFT-based frequency offset estimators have smaller computation complexity than Schmidl' method, which makes them useful in real practice.

4.4. Integrated Model for Timing and Frequency Synchronization

In this section, we propose the integrated synchronization model for both timing and frequency synchronization based on our proposed FFT-based frequency offset estimators in OFDM systems. The model is shown in Figure.4.10. Generally speaking, when one data frame containing training symbol and several data symbols is received, the timing synchronization is performed first to find out the boundary of training symbol, and then this training symbol will be processed by N-FFT in order to apply the proposed FFT- based methods to find out the frequency offset. Finally the frequency offset will be compensated to the OFDM data symbols to improve the quality of data demodulation.

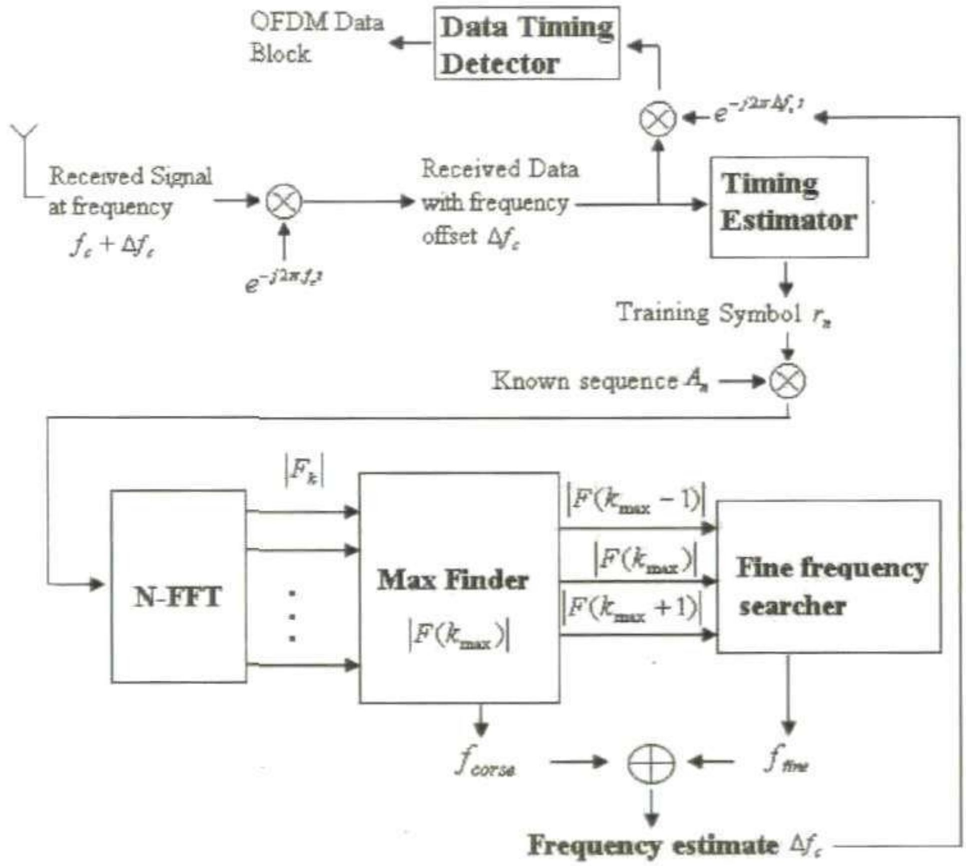

Figure.4.10. Integrated Model for timing and frequency synchronization

4.5. Summary

In this chapter, the comprehensive study of the synchronization in OFDM system is carried out including the time and frequency offset estimation. Schmidl's, Minn's, Park's and Seung's timing offset estimators reviewed and their performance is evaluated by computer simulation in MATLAB with own written codes. Under the environment of no noise and distortion, the Schmidl's method generates plateau before the correct training symbol boundary with length of cyclic prefix, Minn's method reduces the plateau but has many similar values around the correct training symbol boundary, Park's method generates timing metric with impulse sharp peak at the correct training symbol boundary but also with many small sub-peaks, and only Seung's estimator generates timing metric with impulse sharp peak at the correct training symbol boundary and without nearby sub-peaks. Then in the multipath fading environment, all these methods offset the peak point away from the correct training symbol boundary because of the random strongest path signal in the channel. However, Seung's method applied the threshold-based windowing method to estimate and compensate the offset. Therefore based on the simulation results of the timing offset error variance, it clearly shows Seung's method has the smallest error variance in both Multipath static fading channel and Multipath time-varying fading channel.

After reviewing the timing synchronization, we focus on the frequency synchronization in OFDM systems. First of all, we review the Schmidl's frequency offset estimator, and then propose two FFT-based frequency offset estimators. In the proposed algorithms, the training symbol is assumed to be known in receiver, and is multiplying with received training symbol to cancel the phase effects from the complex training symbol. Then this modified training symbol is processed by FFT. The first method is applying Linear

Interpolation technique over the magnitudes of the FFT outputs. And the second method is applying matched filter concept by considering both magnitudes and phases. Through computer simulation in MATLAB with own written codes, we find out the two proposed algorithms have lower error variance than Schmidl's algorithm and the second proposed algorithm has lower error variance than the first proposed algorithm in both AWGN channel and multipath static fading channel. In the multipath time-varying fading channel, the second algorithm still outperforms Schmidl's algorithm, but the first algorithm has slightly higher error variance than Schmidl's algorithm because of the lack of consideration on phase. Overall speaking, the two proposed algorithms can produce accurate and stable frequency offset estimation performance in the AWGN channel and multipath static fading channel such as the warehouse indoor environment. And the second matched filter-based algorithm can also produce accurate and stable frequency offset estimation performance in the multipath time-varying fading channel such as outdoor high speed movement environment.

Chapter 5

Resource Allocation in the OFDM System

In this chapter, we focus on the margin adaptive (MA) optimization technique applied for resource allocation in the multiuser SISO/MIMO-OFDM systems operating in the downlink of cellular network, with the aim of minimizing total transmit power under the users' data rate constraints, in order to meet the fixed data rate requirement of the delay-critical real-time interactive applications in future wireless communication systems. The subcarrier allocation algorithms are explored in this chapter. We review the previous published subcarrier allocation algorithms, and propose simple but efficient subcarrier allocation algorithms with better performance in both multiuser SISO and MIMO-OFDM systems.

5.1. Introduction

Resource allocation in OFDM system includes the subcarrier, bit and power allocation. As mentioned in Chapter 2, the MA optimization is to achieve the minimum overall transmit power given the constraints on the users' data rate or bit error rate (BER). In Single-user SISO-OFDM system, all subcarriers are allocated to one user, so only bit and power allocation is required to be optimized. We review the optimal greedy bit and power allocation algorithm for Single-user SISO-OFDM system in Section 5.2. In Section 5.3, we analyze the optimal solution of MA optimization in Multi-user SISO-OFDM system, review two sub-optimal algorithms, and then propose the channel gain difference based sub-optimal subcarrier allocation algorithm. Subsequently, we discuss the resource allocation in Multi-user MIMO-OFDM system in Section 5.4. Two types of transceiver design methodologies based on different precoding techniques in multiuser MIMO systems are reviewed and evaluated by computer simulation. The one with better performance is extended as our multiuser MIMO-OFDM system model. Subsequently, we review the Zhang's and Extend correlation based (ECBA) subcarrier allocation algorithms, and then propose our efficient subcarrier allocation algorithm with significant improvement compared with Zhang's and ECBA subcarrier algorithms. Finally, Section 5.5 summaries the chapter.

5.2. Bit and Power Allocation in Single-user SISO-OFDM System

In single user OFDM systems, all N subcarriers are used by the user. If number of bits allocated to the subcarrier with low channel gain is same with that allocated to the subcarrier with high channel gain, it will lead the transmit power to be wasted because it requires more power to transmit same number of bits on the subcarrier with high channel gain. Therefore there are many loading algorithms [47-50] developed to solve this problem, assigning different bits to subcarriers according to the channel gains of each subcarrier, which is transmitting more bits in subcarrier with high channel gain and less bits even zero bit in subcarrier with low channel gain.

Before solving the multi-user allocation problem, we first derive the bit allocation algorithm which minimizes the total transmit power, for single-user system. The single-user allocation problem provides an easy understanding of resource allocation problem, and will also be used in our multi-user solution.

5.2.1. Optimal Bit and Power Allocation Algorithm

For Single user OFDM system optimization, the total transmit power can be minimized by adaptively allocating c_n bits on the n^{th} subcarrier over all N subcarriers under the constraint of total date rate R. Then the optimization problem can be rewritten from equation (2-1) as:

$$P = \min_{c_n \in D} \sum_{n=1}^{N} \frac{1}{\alpha_n^2} \cdot f_k(c_n) \tag{5-1}$$

subject to

$$R = \sum_{n=1}^{N} c_n \tag{5-2}$$

As the power needed to transmit a certain number of bits in a subcarrier is independent of the numbers of bits allocated to other subcarriers, it turns out that a greedy approach is optimal [53]. The greedy algorithm assigns one bit at a time to the subcarrier that requires the least additional power. We make some modification by assigning m bits at a time. The allocation process will be completed once all R bits are assigned. The algorithm is named as Optimal Bit Allocation (OBA), and briefly described in Appendix I.

5.2.2. Simulation and Performance Evaluation

In order to see the performance of this Single user OBA algorithm, we assume 32 subcarriers for the OFDM system and channel gains are perfectly known by transmitter. Then Figure.5.1.1 shows the channel response and the bits allocation over subcarriers according to channel gains. As clearly shown in Figure.5.1.1, when the channel gain of a subcarrier is large, more bits are allocated on that subcarrier. When the channel gain of a subcarrier is small, less or even no bits are allocated on that subcarrier.

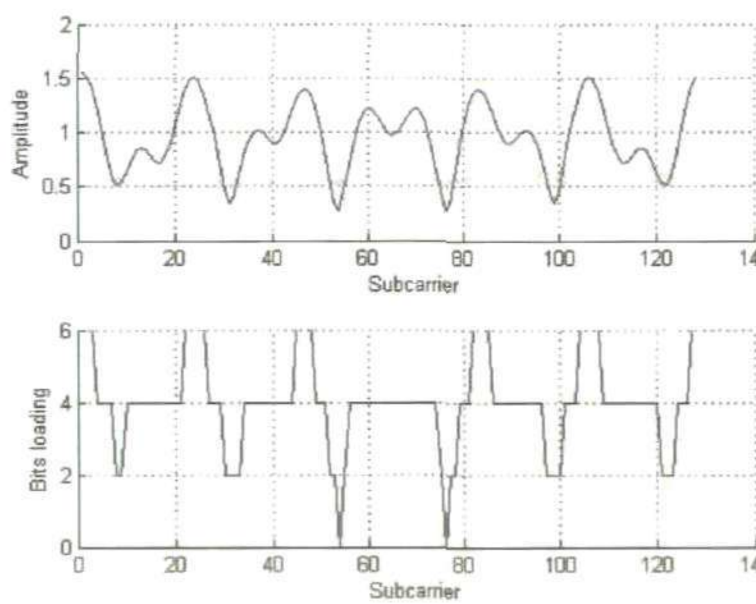

Figure.5.1.1. Frequency domain channel response and bit allocation

In addition, in order to show the further improvement of the Single user OBA algorithm, we compare the BER of the single user OFDM system with/without applying OBA in the 5-path frequency selective fading channel. The amplitude of each path varies independently of the others, according to a Rayleigh distribution with an exponential power-delay profile. The result is shown in Figure.5.1.2.

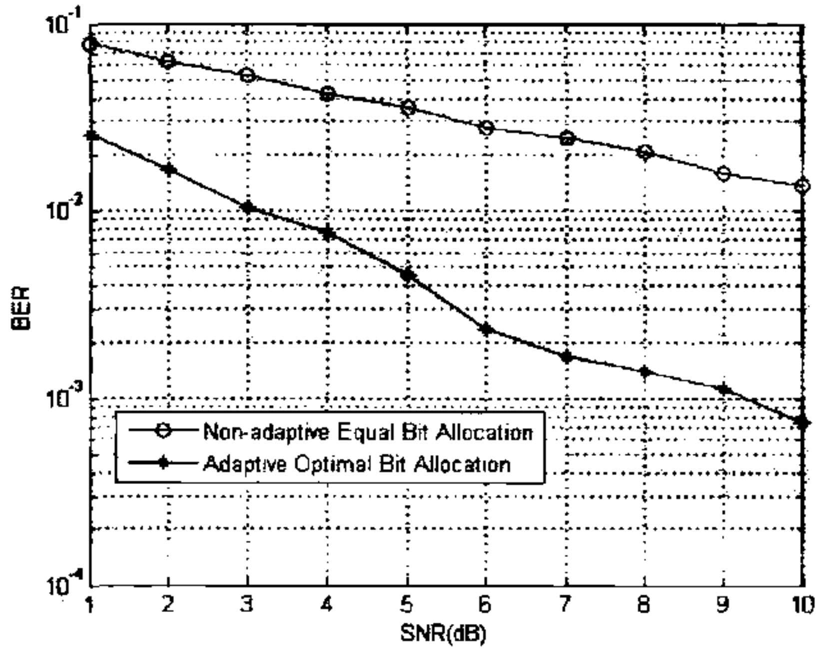

Figure.5.1.2. BER v.s. SNR in Single user OFDM system with/without applying OBA

As shown in the Figure.5.1.2, under the condition that same number of bits is transmitted in one OFDM symbol, the system performance is improved by applying OBA instead of allocating equal bits over all subcarriers.

5.3. Resource Allocation in Multiuser SISO-OFDM System

This section considers a downlink OFDM system with N subcarriers as shown in Figure.5.2, and base station serves K users. We focus on the margin adaptive optimization which is minimizing the overall transmit power under given constant data rate R_k of the k^{th} user. In the base station transmitter, the data from the K users are fed into a subcarrier mapping block which allocates subcarriers and bits to different users, and then based on the bits allocated in each subcarrier, adaptive modulation is carried out to generate one OFDM symbol containing N samples. Here, we assume the instantaneous channel conditions of all users are perfectly known at the base station for the adaptive subcarrier-bit-and-power allocation.

In the process of subcarrier, bit and power allocation, we define $\rho_{k,n}$ as the binary indicator for the k^{th} user and the n^{th} subcarrier. That is, $\rho_{k,n} = 1$ if the n^{th} subcarrier is assigned to the k^{th} user, while $\rho_{k,n} = 0$, otherwise. In addition, no more than one user is allowed to transmit on the same subcarrier. That is, for subcarrier n, if $\rho_{k',n} = 1$ then $\rho_{k,n} = 0$ for all $k \neq k'$. Moreover, let $c_{k,n}$ denote the number of bits of the k^{th} user that are assigned on the n^{th} subcarrier, which is the integer within the set of all possible QAM constellation values $[0, M]$ where M is the maximum number of bits transmitted in one subcarrier.

After the IFFT process and adding cyclic prefix, the signals are transmitted via downlink channels. When the length of the cyclic prefix is longer than the maximum time dispersion, the ISI (Inter-symbol interference) is mitigated and the channel appears flat on every subcarrier. Assume that the subcarrier-bit-and-power allocation information is sent to the users via a dedicated control channel. After removing the cyclic prefix and the FFT process, the user is able to extract its data symbols from the assigned subcarriers according to the subcarrier allocation information and map the modulated symbols to bits according to the bit and power loading information.

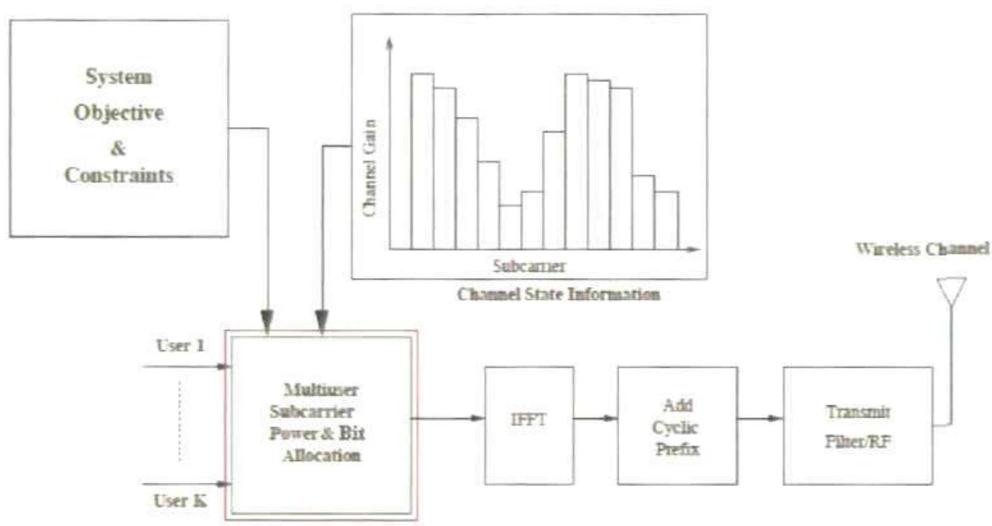

Figure.5.2. Block diagram of an Adaptive Multiuser SISO-OFDM system [110]

5.3.1. Optimal Solution

Based on this original formulation shown in equation (2-1), Wong et al. [53] proposed a combinational Lagrangian optimization solution. They relaxed the constraints of integer bits per subcarrier and no subcarrier sharing to allow the indicator $\rho_{k,n}$ as the sharing factor to be a real number within the interval [0, 1]. Also, the number of bits for the k^{th} user in the n^{th} subcarrier $c_{k,n}$ is now a real number within the interval [0, M]. We define $r_{k,n} = c_{k,n}\rho_{k,n}$ with constraint [0, $\rho_{k,n}M$]. Then the new optimization problem is formulated as a convex minimization problem over a convex set.

$$P = \min_{\substack{r_{k,n}\in[0,\rho_{k,n}M]\\ \rho_{k,n}\in[0,1]}} \sum_{n=1}^{N}\sum_{k=1}^{K}\frac{\rho_{k,n}}{\alpha_{k,n}^{2}}.f_k\left(\frac{r_{k,n}}{\rho_{k,n}}\right) \tag{5-3}$$

with constraints:

$$R_k = \sum_{n=1}^{N} r_{k,n} \tag{5-4}$$

$$1 = \sum_{k=1}^{K} \rho_{k,n} \tag{5-5}$$

Then using optimization technique, the Lagrangian L with Lagrange multipliers λ_k and β_n is obtained.

$$\begin{aligned} L = & \sum_{n=1}^{N}\sum_{k=1}^{K}\frac{\rho_{k,n}}{\alpha_{k,n}^{2}}.f_k\left(\frac{r_{k,n}}{\rho_{k,n}}\right) - \sum_{k=1}^{K}\lambda_k.\left(\sum_{n=1}^{N} r_{k,n} - R_k\right) \\ & - \sum_{n=1}^{N}\beta_n.\left(\sum_{k=1}^{K}\rho_{k,n} - 1\right) \end{aligned} \tag{5-6}$$

And L is differentiated with respect to $r_{k,n}$ and $\rho_{k,n}$ respectively, we obtain the necessary conditions for the optimal solution, $r_{k,n}^{*}$ and $\rho_{k,n}^{*}$.

$$r_{k,n}^{*} = \rho_{k,n}^{*} f_k^{'-1}(\lambda_{q,k}\alpha_{k,n}^{2}) \tag{5-7}$$

$$\rho_{k,n}^{*} = \begin{cases} 0 & \beta_n < H_{k,n}(\lambda_{q,k}) \\ 1 & \beta_n > H_{k,n}(\lambda_{q,k}) \end{cases} \tag{5-8}$$

where

$$\lambda_{q,k} = \begin{cases} f_k^{'}(0)/\alpha_{k,n}^{2}, & f_k^{'-1}(\lambda_k \alpha_{k,n}^{2}) < 0 \\ \lambda_k, & 0 \le f_k^{'-1}(\lambda_k \alpha_{k,n}^{2}) \le M \\ f_k^{'}(M)/\alpha_{k,n}^{2}, & f_k^{'-1}(\lambda_k \alpha_{k,n}^{2}) > M \end{cases} \tag{5-9}$$

$$H_{k,n}(\lambda) = \frac{1}{\alpha_{k,n}^{2}}[f_k(f_k^{'-1}(\lambda\alpha_{k,n}^{2})) - \lambda\alpha_{k,n}^{2} f_k^{'-1}(\lambda\alpha_{k,n}^{2})] \tag{5-10}$$

Since constraint (5-5) must be satisfied, we find from (5-8) that for the n^{th} subcarrier, if $H_{k,n}(\lambda_{q,k}), k = 1,...K$ are all different, only the user with the smallest $H_{k,n}(\lambda_{q,k})$ can use this subcarrier.

$$\rho_{k',n}^{*} = 1, \rho_{k,n}^{*} = 0, \text{ for all } k \neq k' \tag{5-11}$$

where

$$k' = \arg\min_{k} H_{k,n}(\lambda_{q,k}) \tag{5-12}$$

In order to get the optimal solution, we choose a fixed set of Lagrange multipliers λ_k, then use them to determine user k' assigned for the n^{th} subcarrier by (5-9), (5-10), (5-11) and (5-12), thereby $\rho_{k',n}^{*}$ and $r_{k',n}^{*}$ can be calculated for the n^{th} subcarrier. Although this leads to the optimal solution, the individual rate constraint R_k may not be satisfied. To solve this problem, starting with some small values for all λ_k, the iterative method increases one of the λ_k so that more $\rho^*_{k,n}$ becomes one while $r^*_{k,n}$ in (5-7) increases for those n, thus $\sum_{n=1}^{N} r^*_{k,n}$ increases and finally satisfy R_k for user k. Then, the process is repeated for the rest of the users.

In the process of adjusting $\lambda_k, (k = 1,\dots K)$, if for the n^{th} subcarrier, more than one $H_{k,n}(\lambda_{q,k}), k = 1,\dots K$ has the same values, $\rho^*_{k,n}$ has to take values within the interval (0, 1). This solution represents that multiple users are sharing the n^{th} subcarrier, the ratio of the symbols used by different users are proportional to $\rho^*_{k,n}$. Now, the optimal values of $\rho^*_{k,n}$ is obtained, so that the optimum number of bits for the k^{th} user in the n^{th} subcarrier $c^*_{k,n}$ is represented as:

$$c^*_{k,n} = \begin{cases} r^*_{k,n} / \rho^*_{k,n}, & \rho^*_{k,n} \neq 0 \\ 0 & otherwise \end{cases} \tag{5-13}$$

5.3.2. Wong's Sub-optimal Subcarrier Allocation Algorithm

The results obtained from the optimal solution described in Section 5.3.1 cannot be used immediately in our original problem (2-1). This is because the resulting $c^*_{k,n}$ may not be integer and within [0, M]. Another mismatch may be a resulting $\rho^*_{k,n}$ within (0, 1), indicating a subcarrier sharing solution. To solve these problems, Wong et al. proposed a sub-optimal method where the subcarrier allocation follows essentially to the above optimal solution, and $\rho^*_{k,n}$ is modified by letting for the n^{th} subcarrier,

$$\rho^{*}_{k^{*},n} = 1 \text{, where } k^{*} = \arg\max_{k} \rho^{*}_{k,n} \qquad (5\text{-}14)$$

$$\rho^{*}_{k,n} = 0 \text{, for all } k \neq k' \qquad (5\text{-}15)$$

$\rho^{*}_{k,n} = 1$ means the n^{th} subcarrier is assigned to the k^{th} user, while $\rho^{*}_{k,n} = 0$, otherwise. Finally, the single user OBA algorithm described in Section 5.2 is applied to each user on the allocated subcarriers.

5.3.3. Combined Sub-optimal Subcarrier Allocation Algorithm

In [58], Jang et al proposed a subcarrier allocation algorithm which is allocating the subcarrier to the user with the best channel condition. For each subcarrier, by comparing the channel gains of all the users, the subcarrier is allocated to the user with the highest channel gain. This process is repeated until all the subcarriers are distributed. But this method doesn't take into account the fairness between users. Because a user may have high channel gains on all subcarriers, thereby dominating the subcarriers. Then in [63], the fairness among the users is considered. The following constraint is added to determine the number of subcarriers n_k required for user k by the proportion to the required data rate R_k. The proportion of left hand side is equal to the proportion of right hand side in equation (5-16).

$$\begin{aligned} & n_1 : n_2 : \ldots : n_k = R_1 : R_2 : \ldots R_k \\ & \sum_{k=1}^{K} n_k = N \end{aligned} \qquad (5\text{-}16)$$

Here, we combined the maximum bit-rate method proposed in [58] and the constraint in [63]. Finally the bit and power allocation is done by single user OBA algorithm described in Section 5.2. The combined sub-optimal method is briefly described in the Appendix II.

5.3.4. Proposed Channel Gain Difference based Subcarrier Allocation Algorithm

In this thesis, we propose a simple but efficient sub-optimal subcarrier allocation method. A new factor D_n which is the gain difference between the maximum and the next maximum users' channel gains for each subcarrier n, is introduced. The subcarriers are allocated to different users according to this factor. Finally the single user OBA is applied for the bit and power allocation. The proposed method makes some modification on the Step II of combined sub-optimal method for the subcarrier allocation based on the new factor. The modification is briefly described in Appendix III.

5.3.5. Simulation and Performance Evaluation

In this section, we compare the performance of the proposed method with currently available schemes such as the Static subcarrier allocation method (Fixed OFDM-FDMA), the Wong' method and the combined sub-optimal method. We assume the channel of each user experiences frequency selective fading with an exponential power-delay profile.

5.3.5.1. Subcarrier Allocation Comparison

In this section, we compare the subcarrier allocation solution between combined sub-optimal method and proposed method. We first consider the 2-User OFDM system and use the figures of users' channel gains to show the improvement of proposed method. Subsequently, we consider the 3-User, 4-User, 5-User, 6-User and 7-User OFDM system. With the number of users increase, it would not be clear to show all users' channel gains in one figure. Therefore we use tables to show the total transmit power for each user on the allocated subcarriers.

2-User OFDM system

Figure.5.3 shows the comparison of subcarrier allocation between combined sub-optimal method and proposed method applied in a 2-User OFDM system. We assume a 2-User OFDM system with 128 subcarriers, and data rate ratio between user 1 and user 2 is $R_1 : R_2 = 1:3$, therefore user 1 requires 32 subcarriers and user 2 requires 96 subcarriers. The channel gains of these two users are shown in Figure.5.3 (a), and the subcarrier allocation in combined sub-optimal method and proposed method are shown in Figure.5.3

(b) and Figure.5.3 (c) respectively. The blue stars represent the subcarriers allocated to user 1, and the red circles represent the subcarriers allocated to user 2.

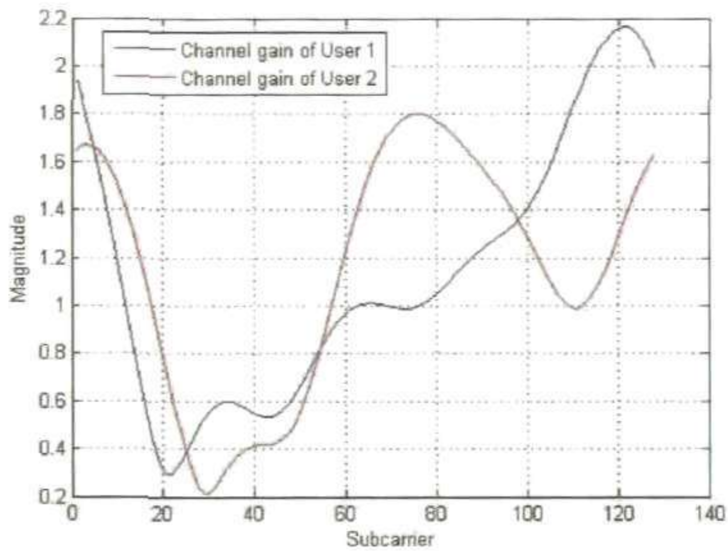

(a). The channel gains of two users in a 2-User OFDM System

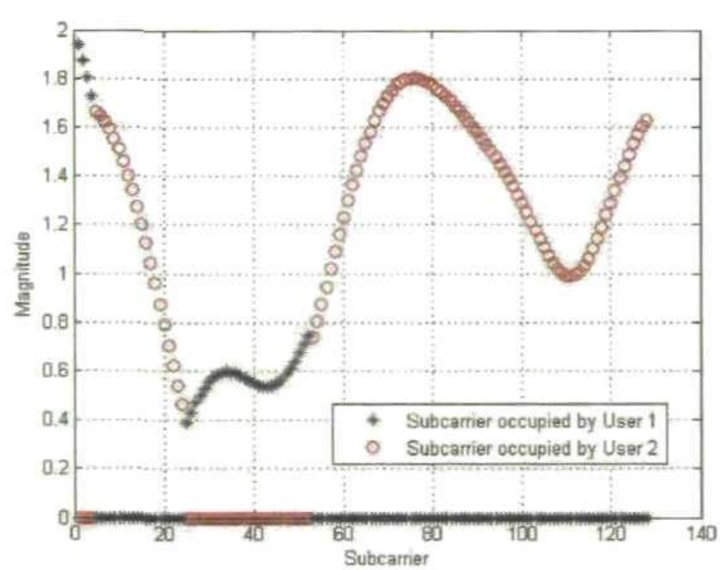

(b). The subcarrier allocation in combined sub-optimal method

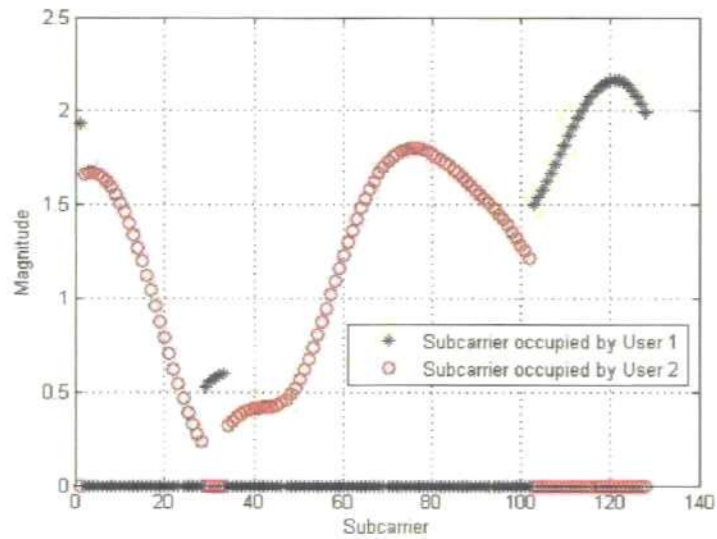

(c). The subcarrier allocation in proposed method

Figure.5.3. Subcarrier allocation in 2-User OFDM system

As shown in Figure.5.3 (a), the maximum channel gain for user 1 is occurring around 120th subcarrier. In Figure.5.3 (b), the subcarrier allocation of the combined sub-optimal method allocates subcarriers within the range (1st subcarrier to 4th subcarrier and 25th subcarrier to 52nd subcarrier) to user 1, because user 1 has relatively higher channel gains than user 2 within this range. Beyond this, user 1 has reached the number of subcarriers required (32 subcarriers), so that subcarrier allocation to user 1 does not occur at the area containing the subcarrier with maximum channel gain. Oppositely, the subcarrier allocation of the proposed method shown in Figure.5.3 (c) assigns most of the subcarriers to the user possessing maximum D_n (i.e. user 1 around 120th subcarrier) where D_n is defined as the gain difference between the maximum and the next maximum users' channel gains for each subcarrier. The subcarriers around 120th subcarrier for user 1 all have large difference with user 2. Therefore these subcarriers are firstly selected for user 1.

3-User, 4-User, 5-User, 6-User and 7-User OFDM systems

We now show the improvement of proposed method in the OFDM systems with more than two users by the total transmit power over the allocated subcarriers for each user under the condition of unit receive power is assumed for each subcarrier. The transmit power of one user on one of allocated subcarriers is the reciprocal of this user' channel gain on this allocated subcarrier. The total transmit powers over the allocated subcarriers for each user in the 3-User, 4-User, 5-User, 6-User and 7-User OFDM system respectively are calculated by applying both combined sub-optimal method and proposed method. The frequency is divided to 128 subcarriers for all these systems. 5-path frequency selective fading channel is used, and the amplitude of each path varies independently of the others, according to a Rayleigh distribution with an exponential power-delay profile. The results are based on the 1000 times simulation for each system, and shown in the Table 5.1.

3-User OFDM system. User data rate ratio $R_1 : R_2 : R_3 = 1:2:1$

	User 1	User 2	User 3
Combined sub-optimal method	22.3710	58.5643	22.1395
Proposed method	21.0098	50.4119	20.9187

4-User OFDM system._User data rate ratio $R_1 : R_2 : R_3 : R_4 = 3:1:2:2$

	User 1	User 2	User 3	User 4
Combined sub-optimal method	39.6114	10.4479	22.5513	21.9255
Proposed method	34.4712	9.6062	20.9970	20.8266

5-User OFDM system. User data rate ratio $R_1 : R_2 : R_3 : R_4 : R_5 = 2:1:3:1:1$

	User 1	User 2	User 3	User 4	User 5
Combined sub-optimal method	22.0775	10.3862	41.2528	10.3240	10.3529
Proposed method	20.6283	9.5998	35.3139	9.5457	9.6940

6-User OFDM system

User data rate ratio $R_1 : R_2 : R_3 : R_4 : R_5 : R_6 = 4:2:6:1:2:1$

	User 1	User 2	User 3	User 4	User 5	User 6
Combined sub-optimal method	22.0810	10.3117	41.0346	5.2203	10.3269	5.1612
Proposed method	20.8509	9.6056	35.4518	4.6995	9.5584	4.6970

7-User OFDM system

User data rate ratio $R_1 : R_2 : R_3 : R_4 : R_5 : R_6 : R_7 = 3:1:4:2:1:2:3$

	User 1	User 2	User 3	User 4	User 5	User 6	User 7
Combined sub-optimal method	16.0933	5.1585	23.5373	10.1914	4.9926	10.3933	16.0821
Proposed method	14.9339	4.6699	21.1312	9.4951	4.6311	9.5321	14.8382

Table.5.1. The total transmit powers over the allocated subcarriers for users

As shown in Table.5.1, in these Multiuser (3 -7 users) OFDM systems, we find out the total transmit power of each user on the subcarriers allocated by the proposed method is always larger than that by combined sub-optimal method. Therefore it obviously shows that the total transmit power is always less in the systems applying proposed method than that applying combined sub-optimal method. Therefore according to the figure and tables explanation, the improvement of proposed method is clearly shown.

5.3.5.2. Average Bit SNR with Number of Users

The Figure.5.4 shows the average bit SNR (in dB) needed to achieve the same BER $P_e = 10^{-4}$ versus the number of users by applying the proposed method, combined sub-optimal method, Wong's method and some static multiple accesses with/without bit loading. The average required transmit power is defined as the ratio of overall transmit energy per OFDM symbol to the total number of bits transmitted per OFDM symbol. Then the average bit SNR is defined as the ratio of the average required transmit power to the noise PSD level N_0.

As shown in Figure.5.4, we find that the optimal bit allocation (OBA) leads better performance than the equal bit allocation (EBA) in the Fixed OFDM-FDMA systems with 2dB- 3.5dB advantage. Wong's method, combined sub-optimal method and proposed method apply the adaptive subcarrier allocation combined with OBA; thereby they all lead better performance than Fixed OFDM-FDMA systems. Wong's method is 3-5dB better than Fixed OFDM-FDMA with OBA and 5-8dB better than Fixed OFDM-FDMA with EBA. Compared with Wong's method, the combined sub-optimal method saves the transmit power around 0.5dB when number of users equals 4 and 7, and requires almost equal transmit power with Wong's method when number of users equals 3, 5 and 6. Thus it has similar overall performance with Wong's method. However, our proposed method has around 0.5-1dB advantage over Wong's method in saving the transmit power.

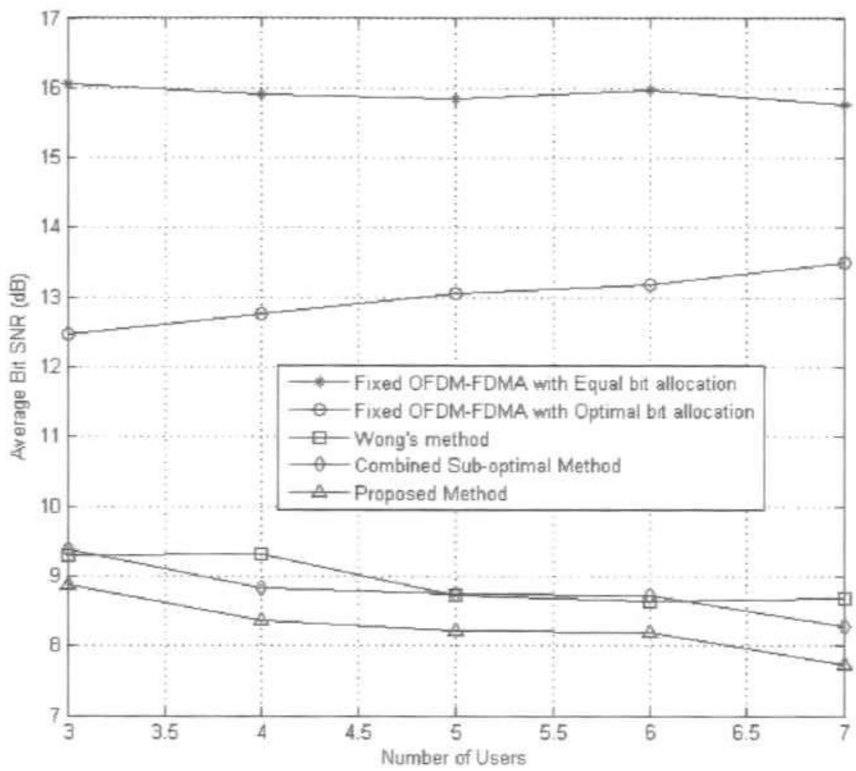

Figure.5.4. Average Bit SNR vs. Number of users

5.3.5.3. BER with Average Bit SNR

Figure.5.5 continuously shows the improvement with more familiar BER versus bit SNR curves. We assume a 5- user OFDM system. For different BER requirement ($P_e = 10^{-1} \sim 10^{-5}$), the relevant Average bit SNR (in dB) is calculated. Then we concluded that our proposed method outperforms other methods under the same operating environment, and that combined sub-optimal method also gives slightly better performance than Wong's method.

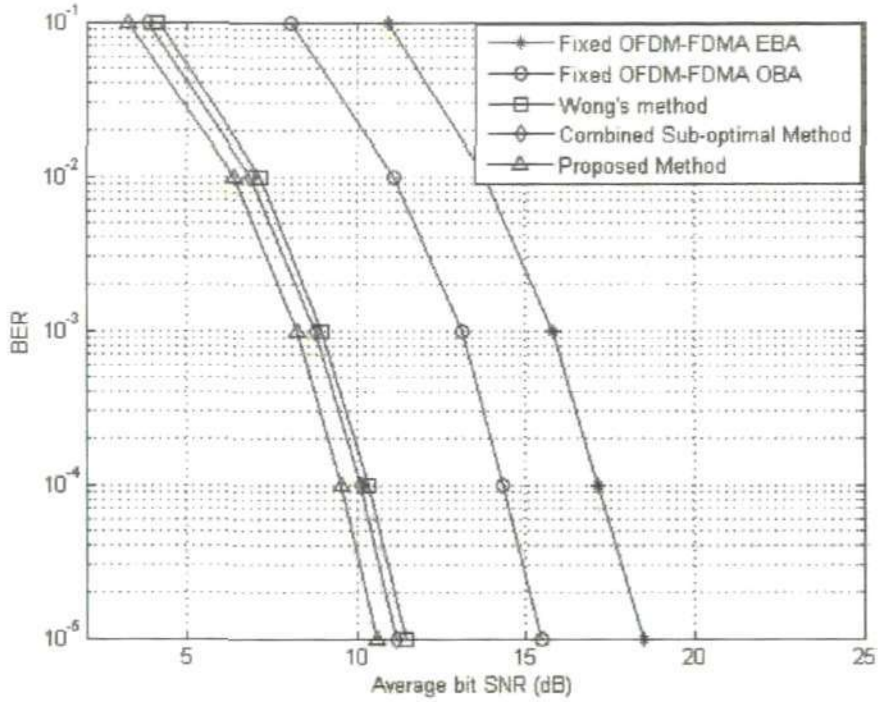

Figure.5.5. BER vs. Average Bit SNR in 5-users OFDM system

5.3.5.4. Probability of Total Transmit Power Distribution

Figure.5.6 shows the total transmit power (TTP) distribution in a five-user OFDM system by applying proposed method, combined sub-optimal method and Wong's method. The red line represents the proposed method, blue line represents the combined sub-optimal method, and the green line represents the Wong's method. We find out the TTP is distributed over 33.9-37dB, 34.2-39.6dB and 35.1-37.1dB in the system applying proposed method, combined sub-optimal method and Wong's method respectively. The proposed method gives the smallest TTP range. In addition, under the same probability, the system applying proposed method always require less TTP than the system applying combined sub-optimal method and Wong's method . Hence, these facts further prove the improvement of proposed method.

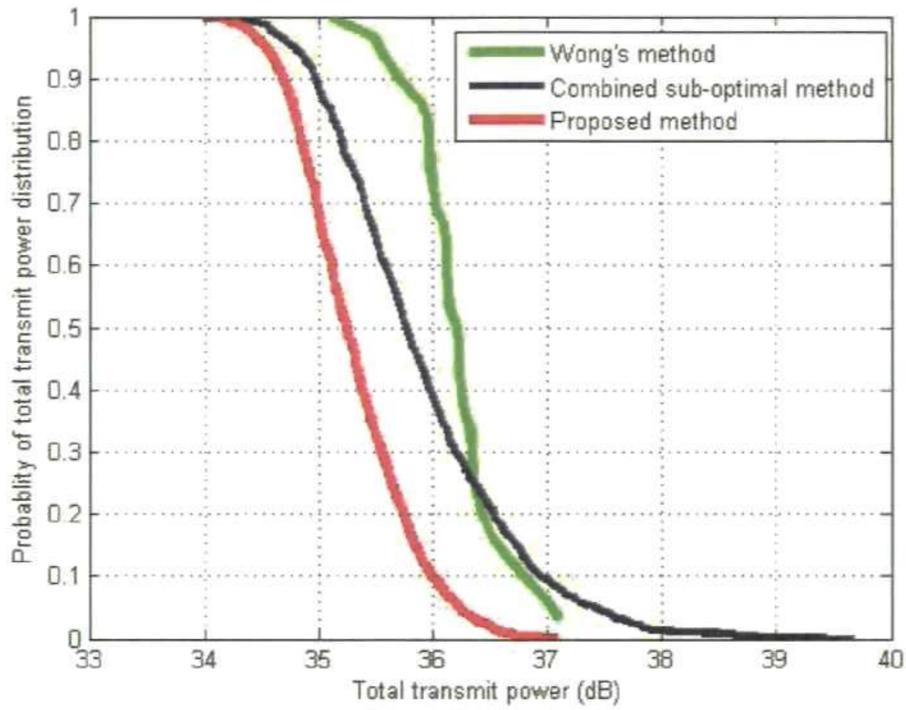

Figure.5.6. Probability and total transmit power

5.3.5.5. Computation Complexity

The computation complexities of the Wong's method, combined sub-optimal method and proposed method are calculated by the laboratory computer processor for 1000 times each under the 3-User system, the 4- User system, the 5- User system, the 6- User system and the 7- User system respectively. Then we calculate their average operation time in these multiuser systems to represent the computation complexity.

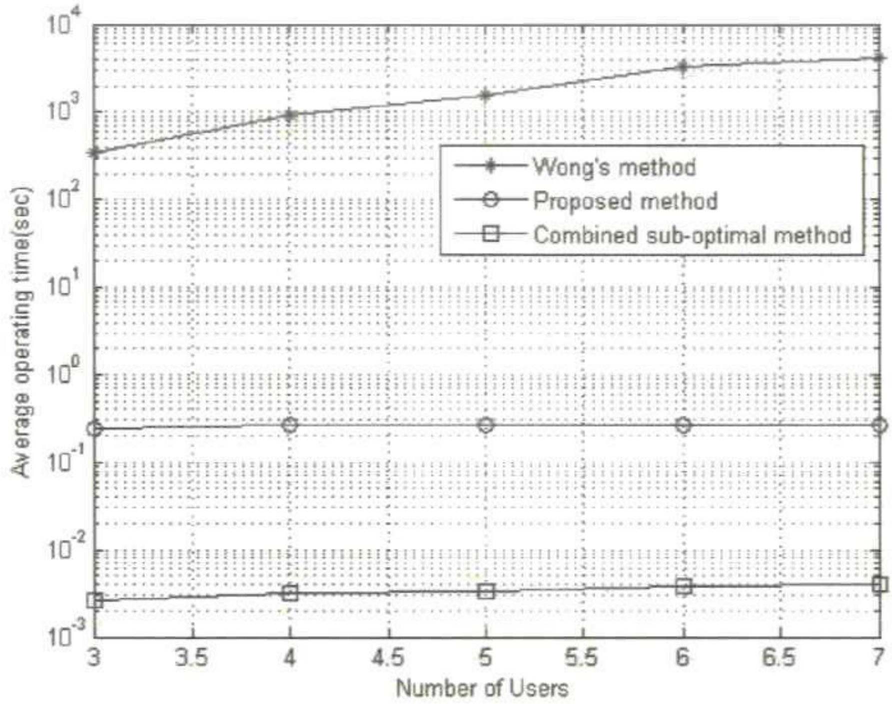

Figure.5.7. Average operation time vs. Number of users

As shown in the Figure.5.7, the required average operation time is increased for all three algorithms along with the increase of number of users. However the increase trend is relatively flat for proposed method and combined sub-optimal method, and quickly raising for Wong's method. In addition, the Wong's method has much higher complexity ($10^2 \sim 10^4$) than the combined sub-optimal method and the proposed method. And the proposed method has slightly higher complexity than the combined sub-optimal method because it required some computation to calculate and compare the channel gain differences. But its order of magnitude is below 10^0, so it is easy to be implemented with the current processors. Therefore both combined sub-optimal method and the proposed method are much more practical in real life than the Wong's method.

5.4. Resource Allocation in Multiuser MIMO-OFDM System

5.4.1. Multiuser MIMO System Model

In his section, we review two types of precoding techniques applied in the Multiuser MIMO systems. One is Lai's model [13] using Zero-forcing technique; another is Liu's model [14] using Singular Value Decomposition (SVD) technique. For both models, the base station has N_T transmit antennas and serves K mobile users, each user having N_k receive antenna. The frequency band is divided to N subcarriers. The channel matrix $\mathbf{H}_k$ for user k which is a $N_k \times N_T$ matrix is not varied during the symbol interval.

In addition, we denote a K -user system with N_T transmit antennas at the base station and N_k antennas at the k^{th} mobile user as a $(N_T, [N_1, N_2, ..., N_K])$ system, and also denote single-user system with N_T transmit antennas at the base station and N antennas at the mobile user as a (N_T, N) system.

5.4.1.1. Lai's Model

In the Lai's model [73], users' data are pre-processed before transmission at basestation. Let $\mathbf{d}_k$ is the $L_k \times 1$ transmit data symbol vector for user k , where $L_k (\le N_k)$ is the number of parallel data symbols transmitted simultaneously for user k . This data symbol is passed through a transmit precoder $\mathbf{F}_k$ which is a $N_T \times L_k$ matrix. At the receiver of user k , the received signals can be written by a vector of length N_k , and given by:

$$\mathbf{y}_k = \mathbf{H}_k \sum_{k=1}^{K} \mathbf{F}_k \mathbf{d}_k + \mathbf{w}_k \tag{5-20}$$

where $\mathbf{w}_k$ is the Gaussian noise vectors. In order to cancel the interference from other users, user k defines his precoder $\mathbf{F}_k$ to be:

$$\mathbf{F}_k = \mathbf{V}_k \mathbf{A}_k \tag{5-21}$$

where $\mathbf{V}_k$ is an orthonormal basis of the subspace $\bigcap_{i=1,i\neq k}^{K} \ker(H_i)$ with m_k the dimention, where $\ker(X)$ denotes the null space or kernel of X, and $\cap$ represents the intersection of the subspaces, and

$$m_k = N_T - \sum_{i=1,i\neq k}^{K} N_i \tag{5-22}$$

In addition, $\mathbf{A}_k$ is consisting of the right singular vectors of $\mathbf{H}_k \mathbf{V}_k$ if SVD technique is used. By substituting (5-21) to (5-20), we can obtain:

$$\mathbf{y}_k = \mathbf{H}_k \mathbf{F}_k \mathbf{d}_k + \mathbf{w}_k = \mathbf{H}_k \mathbf{V}_k \mathbf{A}_k \mathbf{d}_k + \mathbf{w}_k \tag{5-23}$$

Note that the multiuser MIMO system has been decoupled to K parallel single-user MIMO systems. We can think the equivalent single-user MIMO channel for user k as $\mathbf{H}_k \mathbf{V}_k$ and the equivalent transmit processor as $\mathbf{A}_k$. The multiuser MIMO decomposition has the following key properties:

1) The equivalent single-user system for user k is a system with m_k transmit antennas and N_k receive antennas.
2) Increasing N_T by one increases the m_k by one from equation (5-22). E.g. a (6,[2,2,2]) 3-user MIMO system is equivalent to a (m_k,2) single-user system with $m_k = 2$, then a (7,[2,2,2]) 3-user MIMO system is equivalent to a (m_k,2) single-user system with $m_k = 3$.

But this system has a drawback. The number of simultaneous users is restricted by the number of transmit antennas. If we have large number of users in the system, the efficient user selection algorithm is necessary to decide the users who can transmit data simultaneously.

5.4.1.2. Liu's Model

Liu's model [74] is SVD assisted transceiver design. At the base station, users' data are processed before transmission. Let $\mathbf{d}_k$ is the $N_k \times 1$ transmit data symbol vector for user k. It requires the number of transmit data symbol equals to the number of receive antennas for user k. This data symbol is passed through a transmit precoder $\mathbf{F}_k$ which is a $N_T \times N_k$ matrix. At the receiver of user k, the received signals can be written by a vector of length N_k, and given by:

$$\mathbf{y}_k = \mathbf{H}_k \sum_{k=1}^{K} \mathbf{F}_k \mathbf{d}_k + \mathbf{w}_k \tag{5-24}$$

By assuming $rank\,(H_k) = N_k$ and $N_T \geq \sum_{k=1}^{K} N_k$, channel matrix $\mathbf{H}_k$ for user k is decomposed by SVD and given by:

$$\begin{aligned} \mathbf{H}_k &= \mathbf{U}_k \left[\mathbf{\Sigma}_k^{1/2}, 0\right] \mathbf{V}_k^H \\ &= \mathbf{U}_k \left[\mathbf{\Sigma}_k^{1/2}, 0\right] \begin{bmatrix} \mathbf{V}_{k,s}^H \\ \mathbf{V}_{k,z}^H \end{bmatrix} \\ &= \mathbf{U}_k \mathbf{\Sigma}_k^{1/2} \mathbf{V}_{k,s}^H \end{aligned} \tag{5-25}$$

where $\mathbf{U}_k$ and $\mathbf{V}_k$ are the $N_k \times N_k$ and $N_T \times N_T$ left and right singular vectors of H_k respectively. $\mathbf{\Sigma}_k$ is the $N_k \times N_k$ diagonal matrix containing the singular values of $\mathbf{H}_k \mathbf{H}_k^H$. Furthermore, $\mathbf{V}_{k,s}$ is the matrix with size of $N_T \times N_k$, and containing the right singular vectors corresponding to the non-zero singular values of $\mathbf{H}_k$. $\mathbf{V}_{k,s}$ is the matrix with size of $N_T \times (N_T - N_k)$, and containing the right singular vectors corresponding to the zero singular values of $\mathbf{H}_k$.

If we let $\mathbf{F} = [\mathbf{F}_1, \mathbf{F}_2, ..., \mathbf{F}_K]$ and $\mathbf{d} = [\mathbf{d}_1^T, \mathbf{d}_2^T, ..., \mathbf{d}_K^T]^T$, then (5-24) can be written as:

$$\mathbf{y}_k = \mathbf{H}_k \mathbf{F}\mathbf{d} + \mathbf{w}_k = \mathbf{U}_k \mathbf{\Sigma}_k^{1/2} \mathbf{V}_{k,s}^H \mathbf{F}\mathbf{d} + \mathbf{w}_k \tag{5-26}$$

According to (5-26), the overall received signal $\mathbf{y}$ of all the K users can be expressed as:

$$\mathbf{y} = \mathbf{U}\mathbf{\Sigma}^{1/2}\mathbf{V}_s^H \mathbf{F}\mathbf{d} + \mathbf{w} \tag{5-27}$$

where

$$\mathbf{U} = diag\{\mathbf{U}_1, \mathbf{U}_2, ..., \mathbf{U}_k\}$$

$$\mathbf{\Sigma} = diag\{\mathbf{\Sigma}_1, \mathbf{\Sigma}_2, ..., \mathbf{\Sigma}_k\}$$

$$\mathbf{V}_s = [\mathbf{V}_{1,s}, \mathbf{V}_{2,s}, ... \mathbf{V}_{k,s}]$$

$$\mathbf{w} = [\mathbf{w}_1^T, \mathbf{w}_2^T, ... \mathbf{w}_k^T]^T \tag{5-28}$$

The base station transmit precoder $\mathbf{F}$ is designed to cancel the Multiuser Interference (MUI). As shown in (5-27), the MUI can be fully removed if $\mathbf{F}$ is chosen to be:

$$\mathbf{F} = [\mathbf{V}_s^H]^{+} \tag{5-29}$$

By substituting the overall transmit precoder (5-29) into (5-27), the overall receive signal $\mathbf{y}$ of all the K users can be simplified as:

$$\mathbf{y} = \mathbf{U}\mathbf{\Sigma}^{1/2}\mathbf{d} + \mathbf{w} \tag{5-30}$$

To be more specific, the receive signal of user k can be expressed as:

$$\mathbf{y}_k = \mathbf{U}_k \mathbf{\Sigma}_k^{1/2} \mathbf{d}_k + \mathbf{w}_k \tag{5-31}$$

Considering (5-31), we can see that the MUI is cancelled, but there may exist Inter-antenna Interference (IAI) among the antenna-specific symbols transmitted by the base station to the user k. The IAI can be suppressed by multiplying (5-31) by $\mathbf{U}_k^H$, and then the received data symbol $\hat{\mathbf{d}}_k$ can be expressed as:

$$\hat{\mathbf{d}}_k = \mathbf{\Sigma}_k^{1/2}\mathbf{d}_k + \mathbf{U}_k^H\mathbf{w}_k \tag{5-31}$$

or jointly as:

$$\hat{\mathbf{d}} = [\hat{\mathbf{d}}_1^T, \hat{\mathbf{d}}_2^T, ..., \hat{\mathbf{d}}_K^T]^T \tag{5-32}$$

5.4.1.3. Evaluation and Extension

According to the above analysis, the difference between Lai's model and Liu's model is the users' precoder design. In this section, we evaluate the BER performance of Lai's model and Liu' model over several SNR values. The model with better performance is extended to our MIMO-OFDM system. In the simulation, QPSK is utilized for data modulation. More than 10,000 independent flat fading MIMO channels are used to obtain BER simulation. And number of data streams transmitted by each user is equal to L $(L_1 = L_2 = ... = L_K = L)$.

First of all, we consider two types of Multiuser MIMO systems. One is having 6 transmit antennas in base station, and 2 receive antennas for each user. Another one is having 7 transmit antennas in base station, and 2 receive antennas for each user. In both systems, each user transmits $L = 2$ data symbols simultaneously. Under each system setting, Lai's model and Liu's model are applied, and the results are shown in Figure.5.8.

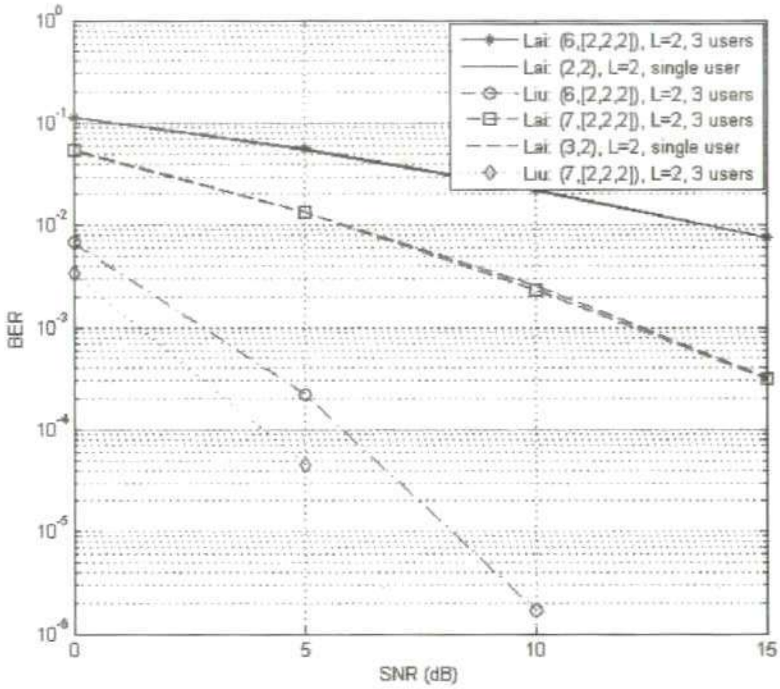

Figure.5.8. Performance comparison between single-user MIMO systems and Multiuser MIMO systems for Lai's model, and performance comparison between Lai's model and Liu's model in Multiuser MIMO systems

As shown in Figure.5.8, for Lai's model, it shows that (6, [2, 2, 2]) Multiuser MIMO system has similar performance with (2, 2) single-user MIMO system, and (7, [2, 2, 2]) Multiuser MIMO system has similar performance with (3, 2) single-user MIMO system. In both (6, [2, 2, 2]) and (7, [2, 2, 2]) Multiuser MIMO systems, Liu's model provides smaller BER than Lai's model over all SNR values.

Subsequently, since Multi-input single-output (MISO) system is a special case of an MIMO system, the decomposition approach is also applicable to Multiuser MISO systems. We consider two types of Multiuser MISO systems. One is having 3 transmit antennas in base station, and single receive antennas for each user. Another one is having 4 transmit antennas in base station, and single receive antennas for each user. In both systems, each user transmits $L = 1$ data symbol simultaneously. Under each system setting, Lai's model and Liu's model are applied, and the results are shown in Figure.5.9.

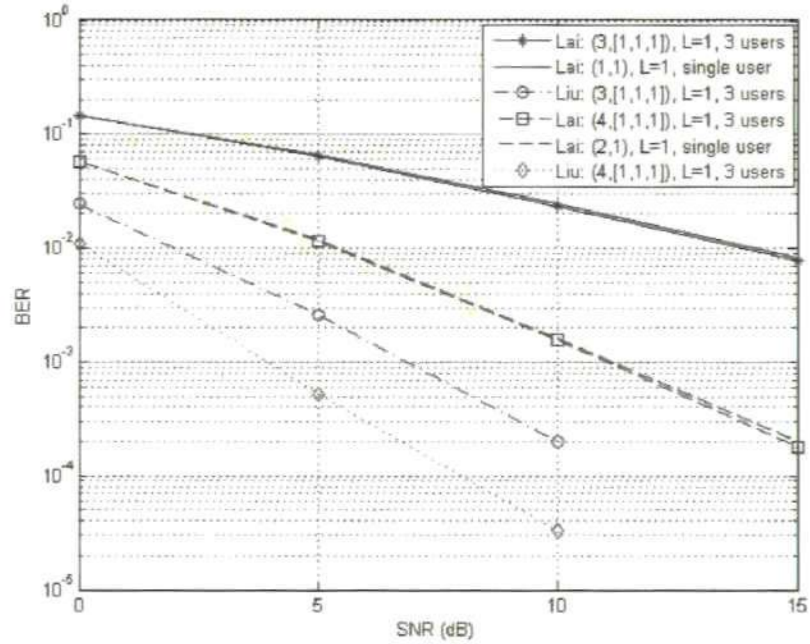

Figure.5.9. Performance comparison between single-user MISO systems and Multiuser MISO systems for Lai's model, and performance comparison between Lai's model and Liu's model in Multiuser MISO systems

As shown in Figure.5.9, for Lai's model, it shows that (3, [1, 1, 1]) Multiuser MISO system has similar performance with (1, 1) single-user MIMO system, and (4, [1, 1, 1]) Multiuser MISO system has similar performance with (2, 1) single-user MISO system. In both (3, [1, 1, 1]) and (4, [1, 1, 1]) Multiuser MISO systems, Liu's model provides smaller BER than Lai's model over all SNR values.

Summary

Both Lai's model and Liu's model proposed novel precoding technique in Multiuser MIMO systems in order to cancel the MUI. Liu's model can provide better performance as shown in our simulation results. We will extend Liu's SVD assisted model to Multiuser MIMO-OFDM system. However when the base station has large number of users to serve in real life, there will be large number of transmit antennas required to cover all users, which is impractical.

Therefore, in the extended Liu's model in our Multiuser MIMO-OFDM system, we propose a simple but efficient subcarrier allocation algorithm to decide the users who can transmit data simultaneously on each subcarrier so that the system flexibility can be better achieved.

5.4.2. Extended SVD assisted Multiuser MIMO-OFDM System

We consider a downlink multiuser MIMO-OFDM system with N subcarriers. The base station (BS) has N_T transmit antennas to serve K mobile users where each user having N_R receive antennas. We assume the users' channel matrix which is not varied during the coherence interval and is perfectly known in both BS and users' mobile units, and that $rank(H_{k,n}) = N_R$ and $N_T \geq \sum_{k=1}^{k \in S_n} N_R$ where S_n is the subset of users sharing the n^{th} subcarrier. The received signal of the user k on the n^{th} subcarrier is represented as:

$$\mathbf{y}_{k,n} = \mathbf{H}_{k,n} \sum_{k=1}^{k \in S_n} \mathbf{F}_{k,n} \sqrt{\mathbf{P}_{k,n}} \mathbf{d}_{k,n} + \mathbf{w}_{k,n}, k \in S_n \tag{5-33}$$

where $\mathbf{d}_{k,n}$ is the parallel N_R data of user k transmitted on the n^{th} subcarrier, $\mathbf{P}_{k,n} = diag\{P_{k,n,1}, P_{k,n,2}, ..., P_{k,n,N_R}\}$ is the $N_R \times N_R$ diagonal matrix, representing the transmit power level of user k on the n^{th} subcarrier for N_R data symbols, $\mathbf{F}_{k,n}$ is the $N_T \times N_R$ precoder matrix for user k on the n^{th} subcarrier, $\mathbf{H}_{k,n}$ is the $N_R \times N_T$ channel matrix for user k on the n^{th} subcarrier, and $\mathbf{w}_{k,n}$ is the complex Gaussian noise with zero mean for user k on the n^{th} subcarrier. As shown in the multiuser MIMO system of [74], the precoder is containing the transmit power level $\mathbf{P}_{k,n}$ which is pre-defined as constraints. In our work, $\mathbf{P}_{k,n}$ is a separate identity from the precoder because it is the factor which is unknown and needs to be minimized. According to the SVD based matrix decomposition method in [74], the $\mathbf{H}_{k,n}$ can be expressed as:

$$
\begin{aligned}
\mathbf{H}_{k,n} &= \mathbf{U}_{k,n}\left[\boldsymbol{\Sigma}_{k,n}^{1/2},0\right]\mathbf{V}_{k,n}^{H} \\
&= \mathbf{U}_{k,n}\left[\boldsymbol{\Sigma}_{k,n}^{1/2},0\right]\begin{bmatrix}\mathbf{V}_{k,n,s}^{H}\\ \mathbf{V}_{k,n,z}^{H}\end{bmatrix} \\
&= \mathbf{U}_{k,n}\boldsymbol{\Sigma}_{k,n}^{1/2}\mathbf{V}_{k,n,s}^{H}
\end{aligned}
\tag{5-34}
$$

where $\mathbf{U}_{k,n}$ and $\mathbf{V}_{k,n}$ are the $N_R \times N_R$ and $N_T \times N_T$ left and right singular vectors of $\mathbf{H}_{k,n}$ respectively. $\boldsymbol{\Sigma}_{k,n}$ is the $N_R \times N_R$ diagonal matrix containing the singular values of $\mathbf{H}_{k,n}\mathbf{H}_{k,n}^{H}$. Furthermore, $\mathbf{V}_{k,n,s}$ is the matrix with size of $N_T \times N_R$, and containing the right singular vectors corresponding to the non-zero singular values of $\mathbf{H}_{k,n}$. $\mathbf{V}_{k,n,z}$ is the matrix with size of $N_T \times (N_T - N_R)$, and containing the right singular vectors corresponding to the zero singular values of $\mathbf{H}_{k,n}$. Then we consider the system in overall view with the following definitions:

$$
\begin{aligned}
&\mathbf{d}_n = [\mathbf{d}_{1,n}^T, \mathbf{d}_{2,n}^T, \ldots \mathbf{d}_{k,n}^T]^T, k \in S_n \\
&\mathbf{F}_n = [\mathbf{F}_{1,n}, \mathbf{F}_{2,n}, \ldots \mathbf{F}_{k,n}], k \in S_n \\
&\mathbf{P}_n = diag\,\{\mathbf{P}_{1,n}, \mathbf{P}_{2,n}, \ldots \mathbf{P}_{k,n}\}, k \in S_n \\
&\mathbf{U}_n = diag\,\{\mathbf{U}_{1,n}, \mathbf{U}_{2,n}, \ldots, \mathbf{U}_{k,n}\}, k \in S_n \\
&\boldsymbol{\Sigma}_n = diag\,\{\boldsymbol{\Sigma}_{1,n}, \boldsymbol{\Sigma}_{2,n}, \ldots, \boldsymbol{\Sigma}_{k,n}\}, k \in S_n \\
&\mathbf{V}_{n,s} = [\mathbf{V}_{1,n,s}, \mathbf{V}_{2,n,s}, \ldots \mathbf{V}_{k,n,s}], k \in S_n \\
&\mathbf{w}_n = [\mathbf{w}_{1,n}^T, \mathbf{w}_{2,n}^T, \ldots \mathbf{w}_{k,n}^T]^T, k \in S_n
\end{aligned}
\tag{5-35}
$$

where $\mathbf{d}_n$ is the overall transmitted data vector on the n^{th} subcarrier, $\mathbf{F}_n$ is the overall precoder matrix on the n^{th} subcarrier, and P_n is the overall transmit power level matrix on the n^{th} subcarrier. Therefore according to [74], the overall received signal vector $\mathbf{y}_n$ of all the users sharing the n^{th} subcarrier can be expressed as:

$$
\mathbf{y}_n = \mathbf{U}_n\boldsymbol{\Sigma}_n^{1/2}\mathbf{V}_{n,s}^{H}\mathbf{F}_n\sqrt{\mathbf{P}_n}\mathbf{d}_n + \mathbf{w}_n \tag{5-36}
$$

As shown in (5-36), the MUI on the n^{th} subcarrier can be fully removed when $\mathbf{F}_n$ is chosen to be:

$$\mathbf{F}_n = [\mathbf{V}_{n,s}^H]^+ \tag{5-37}$$

where $[\mathbf{V}_{n,s}^H]^+$ denotes the psedo-inverse of $\mathbf{V}_{n,s}^H$. By substituting(5-37) into (5-36), $\mathbf{y}_n$ can be expressed as:

$$\mathbf{y}_n \;=\; \mathbf{U}_n \boldsymbol{\Sigma}_n^{1/2} \sqrt{\mathbf{P}_n}\, \mathbf{d}_n + \mathbf{w}_n \tag{5-38}$$

To be more specific, the received signal of user k on the n^{th} subcarrier can be expressed as:

$$\mathbf{y}_{k,n} \;=\; \mathbf{U}_{k,n} \boldsymbol{\Sigma}_{k,n}^{1/2} \sqrt{\mathbf{P}_{k,n}}\, \mathbf{d}_{k,n} + \mathbf{w}_{k,n}, k \in S_n \tag{5-39}$$

As shown in (5-39), user k has fully removed the MUI generated from other users sharing the n^{th} subcarrier. Furthermore, the IAI among the antenna-specific symbols can be suppressed by post-processing $\mathbf{y}_{k,n}$ with $\mathbf{U}_{k,n}^H$ and shown as:

$$\mathbf{U}_{k,n}^H \mathbf{y}_{k,n} = \hat{\mathbf{d}}_{k,n} = \boldsymbol{\Sigma}_{k,n}^{1/2} \sqrt{\mathbf{P}_{k,n}}\, \mathbf{d}_{k,n} + \mathbf{U}_{k,n}^H \mathbf{w}_{k,n}, k \in S_n \tag{5-40}$$

where $\hat{\mathbf{d}}_{k,n}$ is the $N_R \times 1$ received data for user k on the n^{th} subcarrier from the N_R antennas. Then we assume that users' unity power-normalized data $\mathbf{d}_{k,n}, k \in S_n$ transmitted on the n^{th} subcarrier are not correlated with each other, so $E(\mathbf{d}_{k,n}\mathbf{d}_{k,n}^H) = I$. According to (5-40), the required receive power $\mathbf{P}_{k,n}^r$ for user k on the n^{th} subcarrier is given by:

$$\begin{aligned} \mathbf{P}_{k,n}^r &= \hat{\mathbf{d}}_{k,n}\hat{\mathbf{d}}_{k,n}^H \\ &= E(\boldsymbol{\Sigma}_{k,n}^{1/2}\sqrt{\mathbf{P}_{k,n}}\,\mathbf{d}_{k,n}\mathbf{d}_{k,n}^H(\sqrt{\mathbf{P}_{k,n}})^H(\boldsymbol{\Sigma}_{k,n}^{1/2})^H) \\ &= \boldsymbol{\Sigma}_{k,n}^{1/2}\sqrt{\mathbf{P}_{k,n}}\,E(\mathbf{d}_{k,n}\mathbf{d}_{k,n}^H)(\sqrt{\mathbf{P}_{k,n}})^H(\boldsymbol{\Sigma}_{k,n}^{1/2})^H \\ &= \boldsymbol{\Sigma}_{k,n}^{1/2}\sqrt{\mathbf{P}_{k,n}}(\sqrt{\mathbf{P}_{k,n}})^H(\boldsymbol{\Sigma}_{k,n}^{1/2})^H \\ &= (\boldsymbol{\Sigma}_{k,n}^{1/2})^2\mathbf{P}_{k,n} \end{aligned} \tag{5-41}$$

thus,

$$\mathbf{P}_{k,n} = [(\boldsymbol{\Sigma}_{k,n}^{1/2})^{-1}]^2 \mathbf{P}'_{k,n}, k \in S_n \tag{5-42}$$

Here $\mathbf{P}'_{k,n} = diag\{P'_{k,n,1}, P'_{k,n,2}, \ldots, P'_{k,n,N_R}\}$ which is to support $c_{k,n} = [c_{k,n,1}, c_{k,n,2}, \ldots c_{k,n,N_R}]$ bits by satisfying target bit error rate (BER) P_e for user k on the n^{th} subcarrier over N_R receive antennas. According to [53], $P'_{k,n,i}, (k \in S_n, i = 1,2, \ldots, N_R)$ can be expressed as:

$$P'_{k,n,i} = f(c_{k,n,i}) = \frac{N_0}{3}[Q^{-1}(\frac{P_e}{4})]^2(2^{c_{k,n,i}} - 1) \tag{5-43}$$

where N_0 is the noise power spectral density, Q^{-1} is the inversed Q function. Because of the precoder $\mathbf{F}_{k,n}$, the actual transmit power $\mathbf{P}_{k,n}^F$ for user k on the n^{th} subcarrier is:

$$\begin{aligned} \mathbf{P}_{k,n}^F &= \sum_{i=1}^{N_R} \left\| F_{k,n,i} \right\|^2 P_{k,n,i} \\ &= trace\,(\mathbf{F}_{k,n}^H \mathbf{F}_{k,n} \mathbf{P}_{k,n}) \qquad , k \in S_n \\ &= trace\,(\mathbf{F}_{k,n}^H \mathbf{F}_{k,n} [(\boldsymbol{\Sigma}_{k,n}^{1/2})^{-1}]^2 \mathbf{P}'_{k,n}) \end{aligned} \tag{5-44}$$

where $F_{k,n,i}$ is the i^{th} column of $\mathbf{F}_{k,n}$. According to (5-44), the effective channel gains $\mathbf{g}_{k,n}$ of the user k on the n^{th} subcarrier can be expressed as:

$$\mathbf{g}_{k,n} = diag\,(\mathbf{F}_{k,n}^H \mathbf{F}_{k,n} [(\boldsymbol{\Sigma}_{k,n}^{1/2})^{-1}]^2), k \in S_n \tag{5-45}$$

We then denote the $g_{k,n,i}$ as the i^{th} diagonal element of $\mathbf{g}_{k,n}$. The total transmit power for users on all subcarriers are formulated as:

$$P_{total} = \sum_{n=1}^{N} \sum_{k \in S_n} \mathbf{P}_{k,n}^{F} = \sum_{n=1}^{N} \sum_{k \in S_n} \sum_{i=1}^{N_R} \frac{P_{k,n,i}^{r}}{g_{k,n,i}} \tag{5-46}$$

Then the optimization problem can be formulated as:

$$\min\ P_{total} = \min \sum_{n=1}^{N} \sum_{k \in S_n} \sum_{i=1}^{N_R} \frac{P_{k,n,i}^{r}}{g_{k,n,i}} \tag{5-47}$$

subject to the following conditions:

$$\sum_{n=1}^{N} \rho_{k,n} (\sum_{i=1}^{N_R} c_{k,n,i}) = R_k, \quad k = 1,\ldots, K \tag{5-48}$$

$$\rho_{k,n} = \begin{cases} = 1 & if \quad \sum_{i=1}^{N_R} c_{k,n,i} \neq 0 \\ = 0 & if \quad \sum_{i=1}^{N_R} c_{k,n,i} = 0 \end{cases} \tag{5-49}$$

where R_k is the data rate of user k and $\rho_{k,n} = 1$ means subcarrier n is allocated to user k .

5.4.3. Subcarrier and Bit Allocation

In this section, we focus on the subcarrier allocation algorithms in the extended SVD assisted multiuser MIMO-OFDM system. We review the maximum singular value-based subcarrier allocation algorithm proposed by Zhang in [79], and the Extended Correlation based subcarrier allocation algorithm (ECBA) extended from the correlation based user selection algorithm in multiuser MIMO systems proposed in [108]. The aim is to analyze these algorithms and their computational complexities for comparison with our proposed subcarrier allocation algorithm.

As a result of subcarrier allocation, the set of users S_n sharing the n^{th} subcarrier is applied to calculate the effective channel gains $\mathbf{g}_{k,n}$ of the user k on the n^{th} subcarrier. Then the single user OBA algorithm described in Section 5.2 is applied to allocate bits to the assigned subcarriers with minimum power for each user.

5.4.3.1. Zhang's Subcarrier Allocation Algorithm

Zhang's subcarrier allocation algorithm [79] is based on the maximum singular value of each user's channel, and each subcarrier can be allocated to only one user at most. The algorithm is composed of two steps which are the constructive initial allocation (CIA) and the iterative subcarrier swapping (ISS). For the CIA, we firstly order the maximum singular values of channel matrixes in all subcarriers for each user in descending order, then consider the first un-assigned subcarrier in the ordered lists of all users, one user at a time, subsequently consider the second un-assigned subcarrier in the ordered lists of all users. The process is repeated until all the subcarriers are assigned to users. Based on the initial allocation results, the ISS is carried out. The idea is that if for user pair (i, j), we can find a pair of subcarriers (n_i, n_j), so that allocating n_i to user j, and allocating n_j to user i leads a decrease in the total transmit power, then the subcarrier allocation is swapped. The process is iterative until the total transmit power cannot be further reduced.

In CIA step, sorting N maximum singular values for each user takes $O(N)$ running time. There are K users, thus CIA requires computation of $O(KN)$. In ISS step, the main computation comes from calculating the power deduction factors for all possible swapping subcarrier pairs. We assume each user is assigned approximately (N/K) subcarriers for each iteration on average. There are C_2^K user pairs where C_2^K is the 2-combination of the set K, thus $O(C_2^K(N/K)(N/K)) \approx O(N^2)$ possible swapping cases is required per iteration. Thus the total computational complexity is $O(KN + LN^2)$ where L is the number of iterations. Normally ISS step takes a pre-defined number of iterations in order to reduce the complexity.

5.4.3.2. Extended Correlation based Subcarrier Allocation Algorithm

In [108], the channel correlation metric between user i and user j is proposed for the user selection in multiuser MIMO systems and the channel correlation metric is defined as:

$$\eta_{i,j} = \frac{\left\| \mathbf{H}_i \mathbf{H}_j^H \right\|^2}{\left\| \mathbf{H}_i \right\|^2 \left\| \mathbf{H}_j \right\|^2} \tag{5-50}$$

where $\mathbf{H}_i$ is the channel matrix of user i. Here we modify the channel correlation metric as $\hat{\eta}_{i,j} = \frac{\left\| \mathbf{H}_{i,n} \mathbf{H}_{j,n}^H \right\|^2}{\left\| \mathbf{H}_{i,n} \right\|^2 \left\| \mathbf{H}_{j,n} \right\|^2}$ for the subcarrier n so that it can be used in the subcarrier allocation of multiuser MIMO-OFDM systems with the following definition:

1. Each subcarrier is allowed to be shared between multiple users.
2. The maximum number of users sharing one subcarrier is $\hat{K} = N_T / N_R$,
3. The subset of users in the n^{th} subcarrier is $S_n = \phi, \forall n \in N$,
4. The set of available users in the n^{th} subcarrier is $U1_n = \{1,2,...K\}, \forall n \in N$.
5. The number of subcarriers required by users $n_k, \forall k \in K$ is proportional to their data rate.

$$\begin{aligned} & n_1 : n_2 : ... : n_K = R_1 : R_2 : ... : R_K \\ & \sum_{k=1}^{K} n_k = NN_T \end{aligned} \tag{5-51}$$

Then the ECBA algorithm is executed as follows:

for each subcarrier $n \in [1,..., N]$

(a) Find $u = \arg \max\limits_{\substack{k \in U1_n \\ n_k > 0}} \left\| \mathbf{H}_{k,n} \right\|^2$

$S_n = S_n \cup u$, $U1_n = U1_n - u$ $n_u = n_u - N_R$, $\rho_{u,n} = 1$

(b) *while* $size(S_n) < \hat{K}$

Find a user $\hat{u}$, $\hat{u} = \arg \min\limits_{\substack{k \in U1_n \\ n_k > 0}} \sum\limits_{m \in S_n} \hat{\eta}_{m,k}$

If no $\hat{u}$ found, break the loop, otherwise

$\rho_{\hat{u},n} = 1, U1_n = U1_n - \hat{u}, n_{\hat{u}} = n_{\hat{u}} - N_R, S_n = S_n \cup \hat{u}$

end

end

For the n^{th} subcarrier, average $O(K)$ running time is required to find out the user with highest channel norm value, and maximum $O(\hat{K}K)$ running time is required to select rest of users for the n^{th} subcarrier. Therefore, the total computation complexity maximizes to $O(NK + N\hat{K}K)$.

5.4.3.3. Proposed Unit Power based Subcarrier Allocation Algorithm

We propose our modified subcarrier allocation algorithm. The definition of proposed algorithm is inherited from that in ECBA.

The Freobenius norm indicates the overall energy of the channel. We find out the maximum channel Freobenius norm (MCFN) among all users for each subcarrier and order the subcarriers by their MCFN values. The subcarrier allocation is from the first to the last ordered subcarrier so that the user having higher channel energy has the priority to be served. We denote T as the set of ordered N subcarriers. Then we assume unit received power required in each receive antenna among all users and all subcarriers, so that

$$P'_{k,n,i} = 1, (\forall k \in K, \forall n \in N, \forall i \in N_R) \tag{5-52}$$

For the n^{th} subcarrier in T, the user with MCFN is selected first, subsequently the user generating maximum effective channel gains $\mathbf{g}_{k,n}$ then requiring minimum transmit power ($\sum_{i=1}^{N_R} 1/g_{k,n,i}$) if assigned to this subcarrier is selected iteratively until $\hat{K}$ is reached. The detailed algorithm is described as follow:

for each subcarrier n in T

(a) Find $u = \arg \max_{\substack{k \in U1_n \\ n_k > 0}} \left\| \mathbf{H}_{k,n} \right\|^2$

$S_n = S_n \cup u \ , U1_n = U1_n - u \ , n_u = n_u - N_R \ , \rho_{u,n} = 1$

(b) *while* $size(S_n) < \hat{K}$

Find a user $\hat{u}$, $\hat{u} = \arg \min_{\substack{k \in U1_n \\ n_k > 0 \\ S_n = S_n \cup k}} \sum_{i=1}^{N_R} \frac{P^r_{k,n,i}}{g_{k,n,i}}$

If no $\hat{u}$ found, break the loop, otherwise

$\rho_{\hat{u},n} = 1 \ , U1_n = U1_n - \hat{u} \ , n_{\hat{u}} = n_{\hat{u}} - N_R \ , S_n = S_n \cup \hat{u}$

end

end

In the proposed algorithm, sorting N subcarriers requires $O(N)$ running time. Then for each subcarrier, average $O(K)$ running time is required to find out the user with highest channel norm value, and maximum $O(\hat{K}KM)$ running time is required to select the rest of users for the n^{th} subcarrier where M is the average computation required for the calculation of effective channel gains $\mathbf{g}_{k,n}$. Therefore, the total computation complexity maximizes to $O(N + NK + N\hat{K}KM)$.

5.4.4. Simulation and Performance Evaluation

In this section, we compare the performance of Zhang's algorithm, ECBA algorithm and proposed algorithm. The target BER is set to be 10^{-4}, the number of subcarriers is set to 32 and the number of iterations L of Zhang's algorithm is set to be 15. The wireless channel between a couple of transmit antenna and receive antenna is modeled as a 5-path frequency selective fading channel. The amplitude of each path varies independently of the others, according to a Rayleigh distribution with an exponential power-delay profile. The noise power spectral density level is assumed to be unity ($N_0 = 1$). Two situations are considered:

(a) Single receive antenna for all users $(N_R = 1)$

The sum of target data rate of users is 256 bits/symbol. The achieved results are shown in Figures.5.10, 5.11 and 5.12.

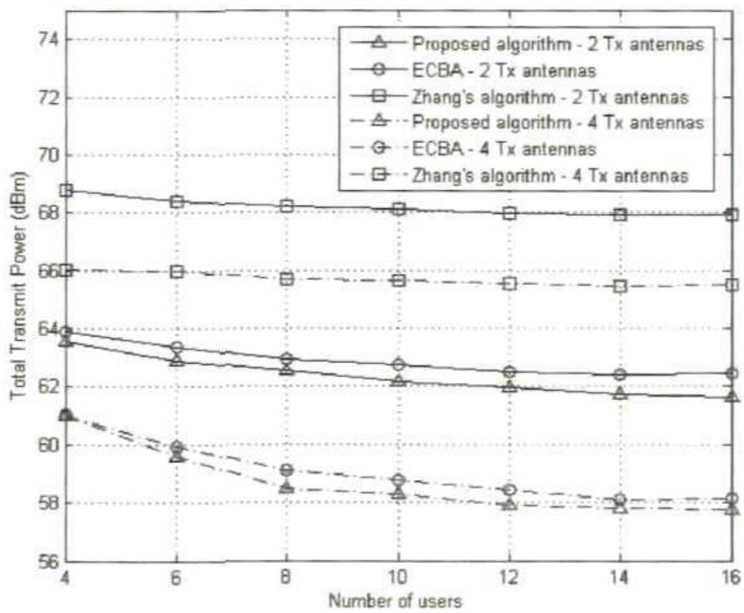

Figure.5.10.Total transmit power vs. Number of users $(N_R = 1)$

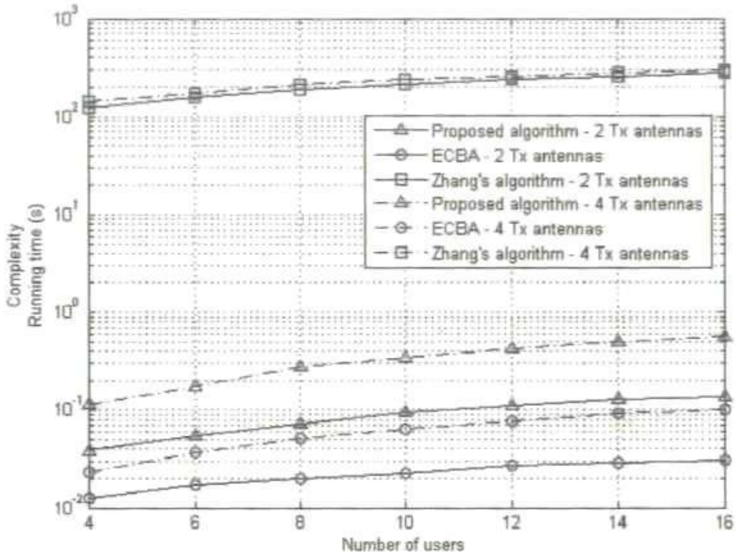

Figure.5.11. Running time vs. Number of users ($N_R = 1$)

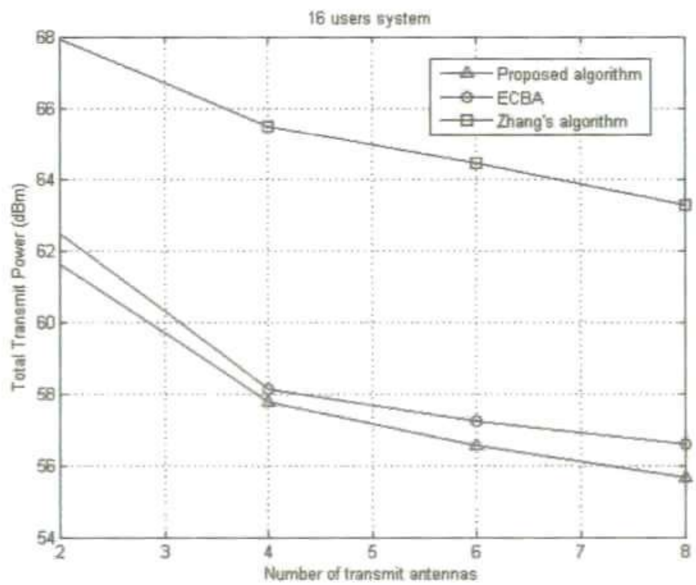

Figure.5.12.Total transmit power vs. number of antennas when number of users is 16 ($N_R = 1$)

(b) Multiple receive antenna for all users ($N_R = 2$)

The system capacity is increased with the growth of number of receive antennas, so the sum of target data rate of users is 512 bits/symbol. The achieved results are shown in Figures.5.13, 5.14 and 5.15.

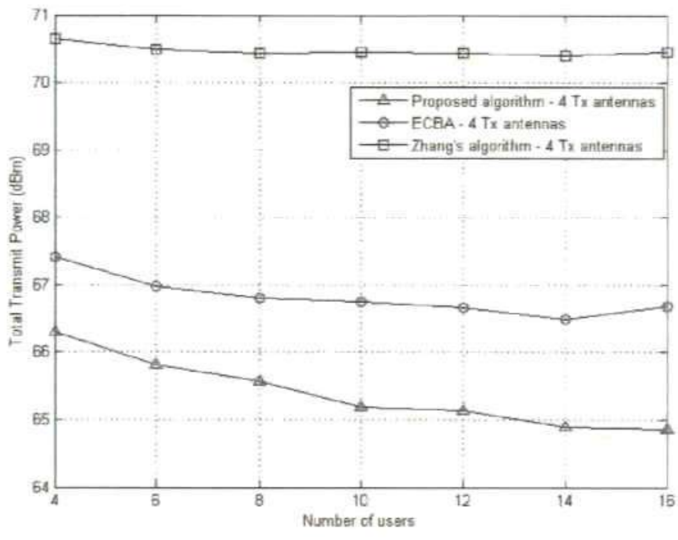

Figure.5.13.Total transmit power vs. Number of users ($N_R = 2$)

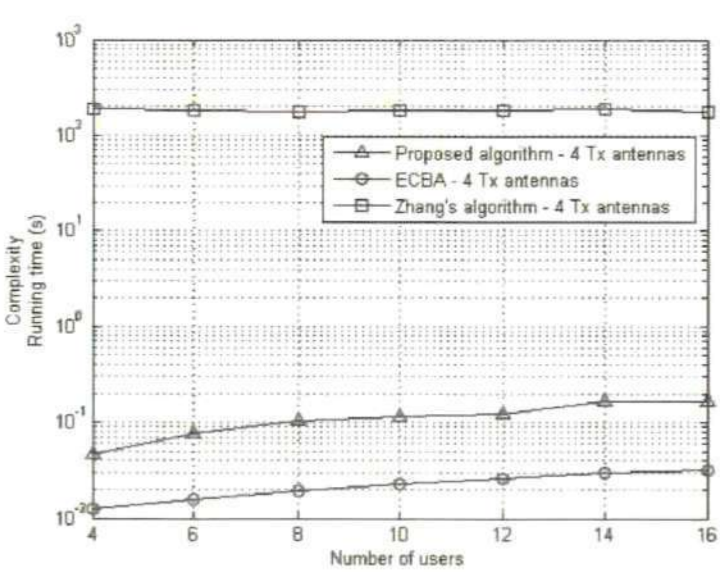

Figure.5.14.Running time vs. Number of users ($N_R = 2$)

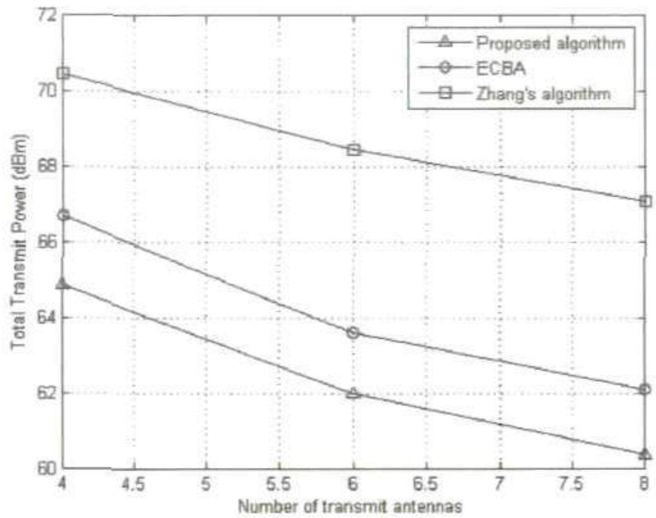

Figure.5.15.Total transmit power vs. number of antennas when number of users is 16 ($N_R = 2$)

Number of transmit antennas	4	6	8	10
Normalized Correlation between two receive antennas (ECBA)	0.3963	0.7062	1.0130	1.3791
Normalized Correlation between two receive antennas (Proposed algorithm)	0.3606	0.6722	0.9809	1.3409

Table.5.2. Normalized sub-channel correlations of users on their allocated subcarriers in a 16-user MIMO-OFDM system ($N_R = 2$)

With end-user using one or two receiving antennas, Figure.5.10 and Figure.5.13 show that proposed algorithm outperforms the Zhang's algorithm and the ECBA algorithm with lower total transmit power for various number of users. Increasing the number of receive antennas, the performance gap between ECBA and proposed algorithm is enlarged because the proposed algorithm reduces the correlation between sub-channels of users which is not considered by ECBA. The Table 5.2 shows this fact. As shown in Table 5.2, in the 16-user MIMO-OFDM system with different number of transmit antennas, the sum of sub-channel correlations of users on their allocated subcarriers given by proposed algorithm is always less than that given by ECBA.

Figure.5.11 and Figure.5.14 show the computing complexity required for these three algorithms, which is increased with the growth of number of users. The running time is computed using a laboratory computer processor. Faster processor may take shorter running time but the conclusion from the running time comparison for the algorithms does not change. Zhang's algorithm requires very high computation due to the iterations in ISS step. The proposed algorithm requires slightly higher computation than ECBA algorithm because of the calculation of effective channel gains. However the cost of the computation increase is in exchange of lowering the transmit power and is within limit of up to date processors.

Figure.5.12 and Figure.5.15 show that for all three algorithms, the required total transmit power is reduced as the number of transmit antennas increases under the condition of fixed number of users. And the proposed algorithm always outperforms Zhang's algorithm and ECBA algorithm as the number of transmit antennas increases.

Overall speaking, the proposed algorithm selects the users for each subcarrier, who is requiring minimum transmit power until the allowed maximum number of users is met. It has the similar idea with the greedy optimum algorithm; however it has much lower computation complexity.

5.5. Summary

In this chapter, the resource allocation in multiuser SISO/MIMO OFDM systems is explored. First of all, we review the single user optimal bit allocation algorithm in SISO-OFDM systems so that it can be applied in the followed multiuser solutions. Secondly, we analyze the optimal subcarrier and bit allocation in multiuser SISO-OFDM systems followed by two sub-optimal subcarrier allocation algorithms called Wong's sub-optimal algorithm and combined sub-optimal algorithm. And then we propose an efficient channel gain difference based subcarrier allocation algorithm with low complexity. The simulation results show that proposed algorithm outperforms the Wong's sub-optimal algorithm and combined sub-optimal algorithm. Third, we study two advanced precoding based transceiver design methodologies in multiuser MIMO systems and find out by computer simulation that the SVD assisted model has lower BER performance. Then the SVD assisted model is extended to multiuser MIMO-OFDM systems. Based on the extended SVD assisted multiuser MIMO-OFDM system, Zhang's and ECBA subcarrier allocation algorithms are reviewed and a unit power based subcarrier allocation is proposed. The simulation results show the significant improvement on the proposed subcarrier algorithm compared with Zhang's and ECBA subcarrier allocation algorithms.

Chapter 6

Conclusions and Future Work

6.1. Thesis Main Conclusions

The next generation (4G) OFDM based wireless systems are expected to be all-IP based and provide universal personal and multimedia communications services for heterogeneous classes of traffics such as voice, web browsing, teleconferencing and interactive games etc. The major challenges include the wireless channel, the synchronization, radio resources and diverse QoS requirements. This motivates the development of synchronization algorithms to provide smaller error variance and better estimation accuracy, and resource allocation techniques to provide subcarrier, power and bit allocation under guaranteed fairness to ensure the QoS for each user.

In this thesis, we firstly focus on the synchronization technique in classic single user OFDM system. The following work has been done.

- Comprehensive study of timing synchronization algorithms in OFDM system.
- Two accurate FFT-based Frequency Offset estimation algorithms in OFDM systems are proposed.
- Lower estimation error variance than Schmidl's method for FFT-based algorithm I in AWGN and time invariant channels
- Lower estimation error variance than Schmidl's method for FFT-based algorithm II in AWGN, time invariant/variant channels
- Both FFT-based algorithms have low computational complexity

Subsequently, we concentrate on the resource allocation algorithms for multiuser OFDM system and multiuser MIMO-OFDM system over downlink transmission. The following work has been done.

Multiuser OFDM system

- Review the single user optimal bit allocation algorithm.
- Analyze the optimal subcarrier and bit allocation in multiuser OFDM system followed by two sub-optimal subcarrier allocation algorithms called Wong's sub-optimal algorithm and combined sub-optimal algorithm.
- Propose an efficient channel gain difference based subcarrier allocation algorithm with low complexity.
- The proposed algorithm outperforms the Wong's sub-optimal algorithm and combined sub-optimal algorithm with lower total transmit power.
- The fairness among users and the overall power efficiency are guaranteed.

Multiuser MIMO-OFDM system

- Study two advanced precoding based transceiver design methodologies in multiuser MIMO systems and find out the SVD assisted model has lower BER performance through computer simulation.
- The SVD assisted model is extended to multiuser MIMO-OFDM systems.
- Based on the extended SVD assisted multiuser MIMO-OFDM system, Zhang's and ECBA subcarrier allocation algorithms are reviewed and a unit power based subcarrier allocation is proposed.
- The simulation results show the significant improvement on the proposed subcarrier algorithm compared with Zhang's and ECBA subcarrier allocation algorithms.
- The fairness among users and the overall power efficiency are guaranteed.

6.2. Suggested Future Work

The work presented in this thesis can be extended in many ways. We give some suggested aspects for potential future research.

- Synchronization in uplink multiuser OFDM / MIMO-OFDM systems

  The proposed frequency offset estimation algorithms are based on the classic single user OFDM architecture. They can be extended to the uplink multiuser OFDM/MIMO-OFDM systems. The training sequence transmitted from each mobile user is perfectly known by base station so that the accurate frequency offset estimation can be achieved by proposed methods.

- Rate adaptive resource allocation in multiuser OFDM/MIMO-OFDM systems

  We have explored the Margin adaptive resource allocation scheme in this thesis. It is interesting to investigate the best assignment of subcarrier and power among users under the constraint of fixed total transmit power, so that the total data rate of system is maximized and each user's minimum required data rate is also achieved.

- Resource allocation with imperfect channel status information

  The proposed algorithms in multiuser OFDM/MIMO-OFDM systems make the assumption that the perfect channel information is available for adaptive resource allocation. In real life, the estimated channel is not accurate due to the estimation error or the time delay between estimation and transmission. Therefore the transmitter optimisation with noisy channel estimates is still largely an unresolved research problem. It is of interest to explore the resource allocation schemes in the presence of channel mismatch.

- MAC-PHY based cross layer resource allocation in OFDM systems

  Most existing resource allocation algorithms focus on the physical layer of the overall network protocol stack. These algorithms are based on the assumption of deterministic traffic arrival and do not consider the dynamic queuing behaviours in MAC layer. In practice, traffics arrive at the receiver randomly so that dynamic queuing should be considered. Comparing with the PHY layer resource allocation, the MAC layer seeks the QoS specialized in packet delay, packet scheduling and throughput instead of those observed in PHY layer such as user's data rate and BER. Therefore, cross-layer approaches jointly considering physical layer and MAC layer issues hold significant potential for improving the system performance. To date, little work has been done to investigate cross-layer resource allocation algorithms for OFDM systems, when the constraints such as imperfect channel estimation, random traffic arrival, and various QoS requirements are considered. It is of interest to explore the low complexity joint PHY-MAC resource allocation algorithms under the real wireless environments.

  The future communication systems have high demands on the real-time services such as teleconferencing, online video etc. These applications introduce a maximum allowed delay for each packet. The joint PHY-MAC resource allocation algorithms, which not only consider each user's channel status information and QoS requirements, but also the waiting time and the maximum allowable packet delay, will bring the benefit for developing the efficient and intelligent wireless communication systems.

- Intelligent resource allocation implementation

  In current work, the optimization is carried out independently in every frame. For the real systems, the channel and queuing status are correlated in consecutive frames. The resource allocation algorithms where the resource allocation in one frame is obtained by the updates from the previous frames can significantly reduce the computational complexity.

- Resource allocation in wireless ad-hoc networks

  In this thesis, the central base station is serving the mobile users with aim of allocating subcarrier, bit and power efficiently among users. However the ad-hoc networks require the peer to peer communications, therefore it is a big challenge to allocate the resources in a distributed manner for the future WLANs and wireless sensor networks.

- Next generation WLANs development

  The next generation WLANs are expected to provide services parallel to their wired counterparts. MIMO techniques have been applied in the current IEEE 802.11WLAN standards. For example, the MIMO-based IEEE 802.11n promises an average data rate of 200Mbit/sec. Although MIMO techniques have been applied at the PHY layer, its impact on network capacity and protocol design is still not well investigated. It is of interest to further research the MIMO techniques and WLANs by concentrating on the network and protocol aspects.

Appendixes

I. Single user Optimal Bit Allocation algorithm

Initialization:

For the n^{th} subcarrier, let $c_n = 0, \forall n$, m bits are assigned at a time, $\Delta P_n = [f(m) - f(0)] / \alpha_n^2$, where $f(c)$ is required received power for reception of c bits/symbol when channel gain equals to unity which can be calculated by equation (2-2).

Iterations:

Repeat the following R/m times:

$n' = \arg\min_n \Delta P_n$;

$c_{n'} = c_{n'} + m$;

$\Delta P_{n'} = [f(c_{n'} + m) - f(c_{n'})] / \alpha_{n'}^2$

End;

Finish:

$\{c_n\}_{n=1}^{N}$ is the final bit allocation solution.

The initialization stage computes, for each subcarrier, the additional power needed to transmit an additional bit. For each bit assignment iteration, the subcarrier that needs the minimum additional power is assigned m more bits, and the new additional power for that subcarrier is updated. Finally, it gives the optimal bits assignment for each subcarrier.

II. Combined Sub-optimal Subcarrier Allocation algorithm

Step I:

Assign the number of subcarriers n_k to user k based on the proportionality given in (5-16).

Step II:

For each subcarrier n

1) Order the channel gains of all users for subcarrier n in descending order so that the users are ordered from highest channel gain to lowest channel gain.
2) If the user k with the highest channel gain doesn't meet the required number of subcarriers n_k, this subcarrier is assigned to this user,
3) Otherwise procedure 2) is applied to the user $k+1$.

End

Finally all users are assigned the subcarriers according to their own required number of subcarriers.

Step III:

Now the subcarrier allocation between users has been obtained through Step II.

For each user k

The single user OBA algorithm described in Appendix I is applied for the bit and power allocation in the assigned subcarriers.

End

III. Proposed Channel Gain Difference based Subcarrier Allocation Algorithm

Modified Step II:

Initialise the allocated subcarrier set B which is empty but can have maximum N elements, user set U which contains all K users.

While the number of elements in B is less than total number of subcarriers N, do the following:

A:

For each unallocated subcarrier n

1) Order the channel gains of users in U in descending order.
2) Calculate the difference D_n between the maximum channel gain and the next maximum channel gain for subcarrier n

End

B:

Find out maximum D_n, and its corresponding subcarrier $n^{'}$, and then find out the user $k^{'}$ with maximum channel gain in subcarrier $n^{'}$.

C:

If user $k^{'}$ hasn't met the required number of subcarriers $n_{k^{'}}$, assign subcarrier $n^{'}$ to user $k^{'}$, and then update the allocated subcarrier set B. Otherwise remove user $k^{'}$ from user set U.

End

Finally all users are assigned the subcarriers according to their own required number of subcarriers.

The advantage of the proposed method is introducing the channel gain difference factor D_n to ensure users have the largest chance to occupy their best subcarriers.

Bibliography

[1] A. Goldsmith, "Wireless Communications," *Cambridge University Press*, 2005

[2] Y. Kim, B. J. Jeong, J. Chung, C.-S. Hwang, J. S. Ryu, K.-H. Kim, and Y. K. Kim, "Beyond 3G: Vision, requirements, and enabling technologies," *IEEE Communication. Magazine*, vol. 41, no. 3, pp. 120-124, March 2003.

[3] "Defining 4G: Understanding the ITU Processfor the Next Generation of Wireless Technology", *3G Americas*, July 2007

[4] S. Kano, "Technical Innovations, Standardization and Regional Comparison:- A case study in mobile communications", *Telecommunications Policy Journal,* May 2000

[5] M. Ulema and B. Kozbe, "Management of next-generation wireless networks and services," *IEEE Communication Magazine.* vol. 41, no. 2, pp. 86-87, Feb. 2003.

[6] R. Berezdivin, R. Breinig, and R. T. Raytheon, "Next-generation wireless communications concepts and technologies," *IEEE Communication Magazine.*, vol. 40, no. 3, pp. 108-116, March 2002.

[7] W. Wohr, "The WINNER (Wireless World Initiative New Radio) project – development of a radio interface for systems beyond 3G", International Journal of Wireless Information Networks 14(2): pp. 67–78, 2007.

[8] Wireless World Research Forum. http://www.wireless-worldresearch.org/, 2007.

[9] X.H. Yu, G. Chen, M. Chen & X. Gao, "Toward beyond 3G: The FuTURE project in China", IEEE Communication. Magazine. 43(1): pp.70– 75, 2007

[10] P. Zhang, X. Tao, J. Zhang, Y. Wang, L. Li & Y. Wang, "A vision from the future: beyond 3G TDD", IEEE Communication. Magazine. 43(1): pp. 38– 44, 2005.

[11] H. Sampath, S. Talwar, J. Tellado, V. Erceg & A. Paulraj, "A fourth generation MIMO-OFDM broadband wireless system: Design, performance, and field trial results", IEEE Communication Magazine. 40(9): 143–149, 2002.

[12] "IEEE 802.11n," http://grouper.ieee.org/groups/802/11.

[13] A. Van Zelst and T. C. W. Schenk, "Implementation of a MIMO OFDM based wireless LAN system," IEEE Transaction On Signal Processing, vol. 52, no. 2, pp. 483–494, Feb. 2004.

[14] S. Weinstein and P. M. Ebert, "Data transmission by frequency-division multiplexing using the discrete Fourier transform". *IEEE Transaction on Communication,* vol. 40, pp. 628-634, 1971.

[15] S. Ohmori, Y. Yamao, and N. Nakajima, "The future generations of mobile communications based on broadband access technologies," IEEE Communication Magazine., vol. 38, no. 12, pp. 134-142, Dec. 2000

[16] W. W. Lu, "Technologies on broadband wireless mobile: 3Gwireless and beyond," IEEE Communication Magazine., vol. 38, no. 10, pp. 57, Oct. 2000

[17] E.P. Lawrey, PhD thesis, "Adaptive Techniques for Multiuser OFDM", James Cook University, Dec 2001

[18] R. W. Chang, "Synthesis of band-limited orthogonal signals for multichannel data transmission", Bell System Technology Journal, vol. 45, pp. 1775–1796, Dec. 1966

[19] D. Tse & P. Viswanath, "Fundamentals of Wireless Communication", *Cambridge University Press*, Cambridge, UK, 2005

[20] A.J. Paulraj, D.A. Gore, R.U. Nabar & H. Bolcskei, "An overview of MIMO communications: A key to gigabit wireless", *Proceeding of the IEEE 92(2):* 198–218, 2004

[21] B. R. Saltzberg, "Performance of an efficient parallel data transmission system", IEEE Transaction on Communication, vol. COM-15, no. 6, pp. 805–811, Dec. 1967

[22] R. W. Chang, "Orthogonal frequency division multiplexing", U.S. Patent 3488445, Nov. 14, 1966, issued Jan. 6, 1970.

[23] R. W. Chang and R. A. Gibby, "A theoretical study of performance of an orthogonal multiplexing data transmission scheme", IEEE Transaction on Communication, vol. COM-16, no. 4, pp. 529–540, Aug. 1968.

[24] G. J. Foschini, "Layered space-time architecture for wireless communication in a fading environment when using multiple antennas," *Bell Laboratory Technology Journal*, vol. 1, no. 2, pp. 41-59, 1996.

[25] G.J. Foschini and M.J. Gans, "On limits of wireless communications in a fading environment when using multiple antennas," *Wireless Personal Communication*, vol.6, pp.311-335, March 1998

[26] R. D. Murch and K. B. Letaief, "Antenna systems for broadband wireless access," *IEEE Communication. Magazine.*, vol. 40, pp. 76–83, Apr. 2002

[27] A. Goldsmith, S.A. Jafar, N.Jindal and S. Vishwanath, " Capacity limits of MIMO channels ," *IEEE Journal on Selected Areas in Communications*, vol.21, no.5, pp.684-702, June 2003

[28] Y.J Zhang, "Adaptive Multiple Access and Resource Allocation with Guaranteed QoS for Broadband OFDM Wireless Networks," PhD thesis , *The Hong Kong University of Science & Technology* , Nov 2004

[29] Gesbert D., Shafi M., Shiu D. S., Smith P. and Naguib A "From theory to practice: An overview of mimo space-time coded wireless systems." *IEEE Journal on Selected Areas in Communications*, 2003, *21*(3): 281-302.

[30] M. Jiang and L. Hanzo, "Multiuser MIMO-OFDM for Next Generation Wireless Systems" *Proceedings of the IEEE*, Vol. 95, No. 7, pp1430-1469, July 2007

[31] L. Hanzo, C. Wong & M. Yee, "Adaptive Wireless Transceivers", John Wiley & Sons, Ltd, 1st edition, 2002.

[32] J. Winters, J. Salz, and R. D. Gitlin, "The impact of antenna diversity on the capacity of wireless communication systems," IEEE Transaction on Communication. vol. 42. pp. 1740-1751, Feb/Mar/Apr 1994.

[33] T. Pollet, M. Van Bladel, and M. Moeneclaey, "Ber sensitivity of OFDM systems to carrier frequency offset and wiener phase noise," *IEEE Transaction on Communication.*, vol. 43, pp. 191–193, Feb./Mar/Apr1995

[34] Z.K. Shen,, "Multiuser Resource Allocation in Multichannel Wireless Communication Systems", PhD thesis, *The University of Texas at Austin*, May 2006

[35] T. Schmidl and D. Cox, "Robust frequency and timing synchronization for OFDM," *IEEE Transaction on Communication*, vol. 45, no.12, pp. 1613-1621, 1997

[36] H. Minn, M. Zeng, and V. K. Bhargava, Fellow, IEEE, "On Timing Offset Estimation for OFDM Systems" *IEEE Communication Letters*, vol. 4, no. 7, pp 242-244, July 2000

[37] B. Park, H. Cheon, C. Kang, and D. Hong, "A Novel Timing Estimation Method for OFDM Systems", *IEEE Communication Letters*, vol. 7, no. 5, pp.239-241, May 2003

[38] C.N. Kishore, V.U. Reddy, "A Frame Synchronization and Frequency Offset Estimation Algorithm for OFDM System and its Analysis", EURASIP Journal on Wireless Communications and Networking, Vol.2006, pp. 1-16, Jan. 2006

[39] S.D. Choi, J.M. Choi, and J.H. Lee, "An Initial Timing Offset Estimation Method for OFDM Systems in Rayleigh Fading Channel", *Proceeding of IEEE Vehicle Technology Conference 2006-fall*, Montreal, Canada, Sept. 2006

[40] P. Moose, "A technique for orthogonal frequency-division multiplexing frequency offset correction," *IEEE Transactions on Communication*, vol.10: pp. 2908-2914, 1994

[41] F. Classen, H. Meyr. "Synchronization algorithms for an OFDM system for mobile communication," *ITG-Fachtagung*, pp.105-113, Oct. 26-28, 1994

[42] U. Lambrette, M. Speth, H. Meyr, "OFDM burst frequency synchronization by single carrier training data", *IEEE Communications Letters*, 1(2): pp. 46-48, 1997

[43] Y.H. Kim, Y.K. Hahm, H.J. Jung, I. Song, "An Efficient Frequency offset Estimator for Timing and Frequency Synchronization in OFDM system" *IEEE Pacific Rim Conference on Communications, Computers and Signal Processing*, pp. 580 – 583, 22-24 Aug. 1999

[44] M. Morelli, U. Mengali. An improved frequency offset estimator for OFDM applications, *IEEE Communications Letters*, 3(3): pp. 75-77, 1999

[45] J. Li, G.Q. Liu, and G.B. Giannakis, "Carrier Frequency Offset Estimation for OFDM-Based WLANs" *IEEE Signal Processing Letters*, vol. 8, no. 3, pp.80-82, Mar 2001

[46] K. Shi, E. Serpedin, "Coarse Frame and Carrier Synchronization of OFDM Systems: A New Metric and Comparison", *IEEE Transactions on Wireless Communications*, 2004, 3(4): 1271-1284

[47] D. Hughes-Hartogs, "Emsemble Modem Structure for Imperfect Transmission Media", U.S. Patents Nos. 4679227 (July 1987), 4731816 (March 1988) and 4833706 (May 1989)

[48] P.S. Chow, J.M.Cioffi, and J.A.C. Bingham, "A Practical Discrete Multitone Transceiver Loading Algorithm for Data Transmission over Spectrally Shaped Channels", *IEEE Transactions on Communications,* 43: pages 773-775, Feb/Mar/Apr 1995

[49] R.F.H. Fischer, and J.B. Huber, " A new loading algorithm for discrete multitone transmission", *IEEE Global Telecommunications Conference*, London, pp. 724-728, Nov 1996

[50] A. Czylwik, "Adaptive OFDM for wideband radio channels", *IEEE Global Telecommunications Conference*, London, pp. 713-718, Nov 1996

[51] M. Wahlqvist, C. Ostberg, J.J.V.D. Beek, O. Edfors, and P.O. Borjesson, "A Conceptual Study of OFDM-based Multiple Access Schemes - Part 1: Air Interface Requirements", *Technical Report, Telia Research*, Sweden, Jun. 1996

[52] H. Rohling, R. Gruneid "Performance comparison of different multiple access schemes for the downlink of an OFDM communication system", *IEEE Vehicular Technology Conference*, Vol.3, pp. 1365-1369, May 1997

[53] C. Y. Wong, R. S. Cheng, K. B. Lataief, and R. D. Murch, "Multiuser OFDM System with Adaptive Subcarrier, Bit, and Power Allocation", *IEEE Journal on Selected Areas in Communications*, vol. 17, pp. 1747-1758, Oct 1999

[54] C.Y. Wong, C. Y. Tsui, Roger *S.* Cheng, "A Real-time Sub-carrier Allocation Scheme for Multiple Access Downlink OFDM Transmission." *IEEE International Vehicular Technology Conference,* 1999

[55] D. Kivanc, H. Liu. "Subcarrier Allocation and Power Control for OFDMA." *IEEE International Vehicular Technology Conference,* 2000

[56] W. Rhee and J. M. Cioffi, "Increasing in Capacity of Multiuser OFDM System Using Dynamic Subchannel Allocation," *IEEE International Vehicular Technology Conference*, vol. 2, pp. 1085-1089, May 2000.

[57] H. Yin and H. Liu, "An Efficient Multiuser Loading Algorithm for OFDM-based Broadbank Wireless Systems", *IEEE Global Telecommunications Conference*, pp. 103-107, 2000

[58] J. Jang and K. B. Lee, "Transmit Power Adaptation for Multiuser OFDM Systems", *IEEE Journal on Selected Areas in Communications*, vol. 21, no. 2, pp. 171-178, Feb. 2003.

[59] I. Kim, H. L. Lee, B. Kim, and Y. H. Lee, "On the use of linear programming for dynamic subchannel and bit allocation in multiuser OFDM," *IEEE Global Telecommunications Conference*, vol. 6, pp. 3648-3652, Nov. 2001

[60] Z. Li, G.Q. Zhu, W.H. Wang, J. Song, " Improved Algorithm of Multiuser Dynamic Subcarrier Allocation in OFDM System", *IEEE International Conference on Communication Technology*,2003

[61] G.D. Zhang, "Subcarrier and Bit Allocation for Real-time Services in Multiuser OFDM Systems" , *IEEE International Conference on Communications*, Jun 2004

[62] G. Münz, S. Pfletschinger, J. Speidel," An Efficient Water-filling Algorithm for Multiple Access OFDM", *IEEE Global Telecommunications Conference 2002*, Nov. 2002.

[63] Z. Shen, J. G. Andrews, and B. L. Evans, "Adaptive Resource Allocation in Multiuser OFDM Systems with Proportional Fairness", *IEEE Transactions on Wireless Communications*, Nov 2005.

[64] C. Mohanram and S. Bhashyam, "A Sub-optimal Joint Subcarrier and Power Allocation Algorithm for Multiuser OFDM", *IEEE Communications Letters*, Vol. 9, No. 8, Aug 2005

[65] A. Ahrens and C. Lange, "Modulation-Mode and Power Assignment in SVD equalized MIMO Systems." *Facta Universitatis (Series Electronics and Energetics)*, vol. 21, no. 2, pp. 167–181, Aug. 2008

[66] S. Vishwanath, N. Jindal & A. Goldsmith, "Duality, achievable rates, and sum-rate capacity of Gaussian MIMO broadcast channels" *IEEE Transactions on Information Theory* 49(10): pp. 2658–2668, 2003

[67] H. Weingarten, Y. Steinberg & S. Shamai, "The capacity region of the Gaussian multiple-input multiple-output broadcast channel", *IEEE Transactions on Information Theory* 52(9): pp. 3936–3964, 2006

[68] W. Yu & J. Cioffi, "Sum capacity of Gaussian vector broadcast channels", *IEEE Transactions on Information Theory* 50(9): pp. 1875–1892, 2004

[69] Z. Tu & R. Blum, "Multiuser diversity for a dirty paper approach", *IEEE Communication Letter* 7(8): pp. 370–372, 2003

[70] P. Tejera, W. Utschick, G. Bauch & J.A. Nossek, "Subchannel allocation in multiuser multiple-input–multiple-output systems", *IEEE Transactions on Information Theory* 52(10): pp. 4721–4733, 2006

[71] M. Sharif & B. Hassibi, "A comparison of time-sharing, DPC, and beamforming for MIMO broadcast channels with many users", *IEEE Transactions on Communications* 55(1): pp. 11–15, 2007

[72] T. Yoo & A. Goldsmith, "On the optimality of multiantenna broadcast scheduling using zero-forcing beamforming", *IEEE Journal on Selected Areas in Communications* 24(3): pp. 528–541, 2006

[73] L.U. Choi and R. D. Murch, "A Transmit Preprocessing Technique for Multiuser MIMO Systems Using a Decomposition Approach", *IEEE Transaction on Wireless Communications*, vol. 3, no. 1, Jan 2004

[74] W. Liu, L.L. Yang and L. Hanzo, "SVD Assisted Joint Transmitter and Receiver Design for the Downlink of MIMO Systems", *The 68th IEEE Vehicular Technology Conference (VTC 2008)*, pp.1-5, Sept.2008

[75] G. Dimic & N. Sidiropoulos, "On downlink beamforming with greedy user selection: Performance analysis and a simple new algorithm", *IEEE Transactions on Signal Processing* 53(10): pp.3857–3868, 2005

[76] Y.M. Tsang, and R.S. Cheng, "Rate Maximization in Space-Division Multiple Access (SDMA) /Multi-Input-Single Output (MISO) /OFDM system under QoS and total power constraint", *IEEE International Conference on Communications (ICC '04)*, June 2004.

[77] Y.M. Tsang, and R.S. Cheng, "Optimal resource allocation in SDMA/Multi-Input-Single Output (MISO) /OFDM system under QoS and total power constraint" *IEEE Wireless Communications & Networking Conference (WCNC)* , pp.1595-1600, 2004

[78] A. Wiesel, Y.C. Eldar & S. Shamai, "Linear precoding via conic optimization for fixed MIMO receivers", *IEEE Transactions on Signal Processing* 54(1): 161–176, 2006

[79] Y.J. Zhang, "An Efficient Resource-Allocation Scheme for Spatial Multiuser Access in MIMO/OFDM Systems," *IEEE Transactions on Communications*, vol. 53, no. 1, pp.107-116, Jan 2005

[80] Y.J. Zhang and K.B. Letaief, "Adaptive Resource Allocation for Multiaccess MIMO/OFDM Systems With Matched Filtering," *IEEE Transactions on Communications*, vol. 53, no. 11, pp. 1810-1816, Nov 2005

[81] X. Xiao, Z.P. Hu, G.X. Zhu and L. Li, "Adaptive subcarrier allocation for increasing the capacity of multiuser spatial multiplexing based OFDM systems". *IEEE Personal, Indoor and Mobile Radio Communications Symposium 2005*, Berlin, Germany, pp.377-381, Sep. 12-14, 2005

[82] Y. Hu, C.C. Yin and G.X Yue, "Multiuser MIMO-OFDM with adaptive antenna and subcarrier allocation". *IEEE Vehicular Technology Conference-2006 Spring*. Melbourne, Australia, PP.2873-2877, May 7-10, 2006.

[83] Peter W. C. Chan, and Roger S. K. Cheng, "Optimal Power Allocation in Zero-forcing MIMO-OFDM Downlink with Multiuser Diversity", the *14th IST Mobile & Wireless Communications Summit*, Jun 2005

[84] P. Chan & R. Cheng, "Capacity maximization for zero-forcing MIMOOFDMA downlink systems with multiuser diversity", *IEEE Transactions on Wireless Communications* 6(3): pp. 1880–1889, 2007

[85] M.S Maw, I. Sasase, "Resource Allocation Scheme in MIMO-OFDMA System for User's Different Data Throughput Requirements" *IEEE Wireless Communications & Networking Conference (WCNC)*, pp. 1708-1712, 2007

[86] Y.I. Shin, T.S. Kang and H.M. Kim, "An Efficient Resource Allocation For Mulituser MIMO-OFDM Systems with Zero-forcing Beamformer", *The 18th Annual IEEE International Symposium on Personal, Indoor and Mobile Radio Communications (PIMRC'07)*, pp. 1-5, 3-7 Sept. 2007

[87] H. Karaa, R.S. Adve, and A. J. Tenenbaum, "Linear Precoding for Multiuser MIMO-OFDM Systems", *IEEE International Conference on Communications (ICC 07)*, pp. 2797-2802, Jun 2007

[88] T. Keller, L. Piazzo, P. Mandarini, L. Hanzo, "Orthogonal Frequency Division Multiplex Synchronization Techniques for Frequency-Selective Fading Channels", *IEEE Journal on Selected Areas in Communications*, vol. 19, June 2001, no 6, pp. 999-1008.

[89] B. Park, H. Cheon, E. Ko, C.E. Kang, D.S. Hong, "A Blind OFDM Synchronization Algorithm Based on Cyclic Correlation", *IEEE Signal Processing Letters*, vol. 11, no 2, pp.83-85, February 2004

[90] F. Gini, G. Giannakis, "Frequency Offset and Symbol Timing Recovery in Flat-Fading Channels- A Cyclostationary Approach", *IEEE Transaction on Communications*, vol. 46, no 3, pp.400-411, March 1998

[91] F.F. Gao, A. Nallanathan, "Blind Maxumum Likelihood CFO Estimation for OFDM System via Polynomial Rooting", *IEEE Signal Processing Letters*, vol. 13, no 2, February 2006

[92] H. Bolcskei, "Blind Estimation of Symbol Timing and Carrier Frequency Offset in Wireless OFDM Systems", *IEEE Transactions on Communications,* vol. 49, pp.988-999, June 2001

[93] J. H. Winters, "Optimum combining in digital mobile radio with cochannel interference", *IEEE Journal on Selected Areas in Communications*, vol. SAC-2, no. 4, pp. 528–539, Jul. 1984.

[94] J. H. Winters, "On the capacity of radio communication systems with diversity in a Rayleigh fading environment", *IEEE Journal on Selected Areas in Communications,* vol. SAC-5, no. 5, pp. 871–878, Jun. 1987.

[95] J. H. Winters, "Optimum combining for indoor radio systems with multiple users", *IEEE Transactions on Communications*, vol. COM-35, no. 11, pp. 1222–1230, Nov. 1987.

[96] J. Salz, "Digital transmission over cross-coupled linear channels", *AT&T Technical Journal*, vol. 64, pp. 1147–1159, Jul.–Aug. 1985.

[97] J. H. Winters, J. Salz, and R. D. Gitlin, "The impact of antenna diversity on the capacity of wireless communication systems", *IEEE Transactions on Communications.*, vol. 5, no. 234, pp. 1740–1751, Feb./Mar./Apr. 1994.

[98] G. J. Foschini, "Layered space-time architecture for wireless communication in a fading environment when using multi-element antennas", *Bell Labs Technology Journal*, vol. autumn, pp. 41–59, Oct. 1996.

[99] G. G. Raleigh and J. M. Cioffi, "Spatio-temporal coding for wireless communications", *IEEE Global Telecommunications Conf*erence, vol. 3, pp. 1809–1814, Nov 1996

[100] J. H. Winters, "The diversity gain of transmit diversity in wireless systems with Rayleigh fading", *IEEE Transaction on Vehicle Technology*, vol. 47, no. 1, pp. 119–123, Feb. 1998.

[101] V. Tarokh, N. Seshadri, and A. R. Calderbank, "Space-Time Codes for High Data Rate Wireless Communication: Performance Criterion and Code Construction," *IEEE Transactions on Information Theory*, vol. 44, pp.744-765, Mar 1998

[102] V. Tarokh, H. Jafarkhani, and A. R. Calderbank, "Space-Time Block Codes from Orthogonal Designs", *IEEE Transactions on Information Theory*, vol.45, pp. 1456-1467, July 1999

[103] C. Masouros and E. Alsusa, "Dynamic Linear Precoding for the Exploitation of Known Interference in MIMO Broadcast Systems", *IEEE Transactions on Wireless Communications,* vol.8, no.3, pp.1396-1404, March 2009

[104] Y.H.R. Zheng and C.S. Xiao, "Simulation Models With Correct Statistical Properties for Rayleigh Fading Channels", *IEEE Transactions on Communications*, Vol.51, No.6, June 2003

[105] W. C. Jakes, "Microwave Mobile Communications", Piscataway, NJ: IEEE Press, 1994.

[106] M.F. Pop and N.C. Beaulieu, "Limitations of Sum-of-Sinusoids Fading Channel simulators", *IEEE Transactions on Communications*, Vol.49, No.4, April 2001

[107] J. Li, A. Bose and Yiqiang Q.Zhao "Rayleigh Flat Fading Channels' Capacity", *Proceedings of the 3rd Annual Communication Networks and Services Research Conference),*May2005, Canada

[108] T.X Ji, C.H Zhou, S.D Zhou, Y. Yao, "Low Complex User Selection Strategies for Multi-user MIMO Downlink Scenario", *IEEE Wireless Communications & Networking Conference*, pp.1534-1539, Mar 2007

[109] D. C. Rife and R. R. Boorstyn, -, "Multiple tone parameter estimation from discrete time observations," *Bell System Technology Journal.,* vol. 55, pp. 1389-1410, Nov.1976.

[110] S. Sadr, A. Anpalagan, K. Raahemifar, "Radio Resource Allocation Algorithms for the Downlink of Multiuser OFDM Communication Systems", *IEEE Communications Surveys & Tutorials*, vol.11, pp.92-106, Aug 2009

[111] T.W. Hwang, C.Y. Yang, G. Wu, S.Q. Li, Y. Li. G, "OFDM and Its Wireless Applications: A Survey", *IEEE Transactions on Vehicular Technology*, vol.58, pp.1673-1694, May 2009

[112] X.J. Tong, T. Luo, "Theory and application of OFDM wireless communication technique" *People Post press, China*, May 2003

An Efficient Sub-Optimal Subcarrier Allocation Algorithm for Multiuser OFDM System

Fan Wu
Mobile Communications Network Research
School of Computing, Communications & Electronics
University of Plymouth, UK
fan.wu@plymouth.ac.uk

Mosa Ali Abu-Rgheff
Mobile Communications Network Research
School of Computing, Communications & Electronics
University of Plymouth, UK
mosa@plymouth.ac.uk

Abstract— **this paper investigates the allocation of subcarriers and power in the downlink channels of multiuser OFDM systems. The goal is to minimize the total transmit power under the constraints of user data rates and bit error rate (BER). We propose a sub-optimal algorithm to achieve the goal in this paper. We introduce a new factor which is the gain difference between the maximum and the next maximum users' channel gains for each subcarrier. Then the subcarriers are allocated to different users according to this factor. The simulation results show this algorithm outperforms the multiuser OFDM systems with static Frequency Division Multiple Access (FDMA) technique, also it outperforms the sub-optimal method proposed by Wong. We quantify the improvement in terms of total required transmit power and BER.**

Keywords: Multiuser OFDM, Subcarrier Allocation

I. INTRODUCTION

RESOURCE management including subcarrier, power and bit allocation has raised the hot discussion in Multiuser OFDM system optimization. Simple but efficient optimization algorithms are required for the practical use. In Multiuser OFDM-FDMA systems, users have multipath fading but each has independent fading parameters due to different locations. A subcarrier in deep fade for one user may not be in deep fade for other users. Therefore it is necessary to find out a method to allocate subcarriers efficiently between users according to the channel state information (CSI) which can be analyzed from the uplink received symbols in time division duplex (TDD) wireless communication system. In this paper, the perfect CSI of each user is assumed to be known by the base station.

Generally speaking, there are two classes of optimization techniques: margin adaptive (MA) [1], [2], [3] which is to achieve the minimum overall transmit power given the constraints on the users' data rate or bit error rate (BER), and rate adaptive (RA) [4], [5], [6] which is to adapt the transmit power with water-filling policy for each user in each subcarrier and to maximize the overall data rate with a total transmit power constraint. We focus on Margin Adaptive optimization.

Wong et al. proposed an optimal optimization algorithm based on Lagrange relaxation in order to minimize the total transmission power with satisfying all users' rate requirement [1]. He applied this algorithm to allocate the subcarrier first, and then applied a single user optimal bit allocation (OBA) for each user on the assigned subcarriers. The algorithm outperforms the fixed allocation schemes (e.g., OFDM-TDMA, OFDM-FDMA etc) a lot, but it is very complex and has heavy computation. To cope with this problem, Wong et al. proposed a simplified sub-optimal algorithm which performs closely with optimal solution [2]. But it has fixed the number of assigned subcarriers of each user which is not a good strategy in practical systems. Kivanc et al. proposed the famous Graving Greedy subcarrier and power allocation algorithm [3]. The algorithm was separated into two stages: the first step is determining the number of subcarriers based on *SNR* and users' rate requirement, the second step allocates the appropriate subcarrier to each user by using amplitude craving greedy (ACG) subcarrier assignment algorithm in order to minimize the total transmit power. To reduce the computational complexity, Kim et al. converted the nonlinear optimization problem into a linear integer-programming problem [7]. However, the complexity still grows exponentially with the number of subcarriers and users. Zhang at el. proposed a novel dynamic subcarrier and bit allocation algorithm for real-time services in multiuser OFDM systems, which takes advantage of the instantaneous channel gain in subcarrier and bit allocation properly without relying on the nonlinear optimization technique like algorithm in [1], in order to reduce the computation complexity [8].

In this paper, we propose a two-step subcarrier and power allocation algorithm. We introduce a factor which is the gain difference between the maximum and the next maximum users' channel gains for each subcarrier. The subcarriers are allocated to different users according to this factor. Then single user OBA as described in section III (A) is applied to each user on the assigned subcarriers to minimize the total transmit power. The rest of the paper is organized as follows. Section II describes the Multiuser OFDM System Model and MA optimization problem formulation. Section III describes the single user OBA method, Wong's method in [1] and combined sub-optimal method from [6] and [9]. Section IV describes the proposed method. Section V presents the performance according to the simulation results. Finally, Section VI concludes the paper.

II. SYSTEM MODEL

The Multiuser OFDM system has K users and N subcarriers. The base station assigns subcarriers to each user and determines the number of bits on each subcarrier according to the CSI of each user. Subcarrier sharing between users is not allowed. This paper focuses on the MA optimization. Mathematically, the original problem can be formulated as [1]:

$$P = \min_{C_{k,n} \in D} \sum_{n=1}^{N} \sum_{k=1}^{K} \frac{1}{\alpha_{k,n}^2} \cdot f_k(c_{k,n}) \tag{1}$$

where P is the total power, $c_{k,n}$ is the number of bits for k^{th} user on n^{th} subcarrier in one OFDM symbol, $\alpha_{k,n}^2$ is the channel power gain for k^{th} user on n^{th} subcarrier, and $D \in [0, M]$ is the set of all possible constellation values for $c_{k,n}$ with maximum allowed value M .

In addition, $f(c)$ is the required received power for reception of c bits/symbol when channel gain equals to unity; here we consider the system employing MQAM, therefore $f(c)$ is expressed as [1]:

$$f(c) = \frac{N_0}{3}[Q^{-1}(\frac{P_e}{4})]^2(2^c - 1) \tag{2}$$

where N_0 is the noise power spectral density, P_e is the given BER, and Q represents Q-function. And the minimization is subject to the following constraints:

$$R_k = \sum_{n=1}^{N} c_{k,n} \tag{3}$$

$$c_{k',n} \neq 0, \text{ then } c_{k,n} = 0 \text{ for } k \neq k' \tag{4}$$

R_k is the required data rate for user k.

III. ALGORITHMS IN THE LITERATURE

In this section, we present the review of the published algorithms of subcarrier, bit and power allocations.

A. Single user OBA Method

The Single user OBA method proposed in [1] will be applied after subcarrier allocation to minimize the total transmit-power. In a Single user OFDM system optimization, the problem in (1) can be rewritten as:

$$P = \min_{C_n \in D} \sum_{n=1}^{N} \frac{1}{\alpha_n^2} \cdot f_k(c_n) \tag{5}$$

Subject to

$$R = \sum_{n=1}^{N} c_n \tag{6}$$

A greedy approach is optimal by assigning bits to the subcarrier that requires the least additional power until all R bits are assigned. The algorithm is described in Table I.

Initialization:
For all n , let $c_n = 0$, m bits are assigned each time, $\Delta P_n = [f(m) - f(0)]/\alpha_n^2$, $f(c)$ can be calculated by (2)
Iterations:
Repeat the following (R/m) times:
$n' = \arg\min_n \Delta P_n$;
$c_{n'} = c_{n'} + m$;
$\Delta P_n = [f(c_{n'} + m) - f(c_{n'})]/\alpha_n^2$
Finish:
$\{c_n\}_{n=1}^{N}$ is the final bit allocation solution.

Table I. Single user OBA Algorithm

B. Wong's Method

Wong proposed the optimal solution in [1] by relaxing the requirement $c_{k,n} \in D$ to allow $c_{k,n}$ being a real number within $[0, M]$. The detailed algorithm is briefly described in [1]. But the optimal solution requires a complex converging process, and results cannot be used immediately in the original problem (1) because $c_{k,n}$ may not be an integer. So Wong proposed a sub-optimal method to use the optimal solution to obtain the subcarrier allocation, and then the single user OBA method is applied to each user on the allocated subcarriers.

C. Combined Sub-optimal Method

In [6], Jang et al proposed the maximum bit-rate method which is allocating the subcarrier to the user with the best channel condition. For each subcarrier, by comparing the channel gains of all the users, the subcarrier is allocated to the user with the highest channel gain. This process is repeated until all the subcarriers are distributed. But this method doesn't take into account the fairness between users. A user may have high channel gains on all subcarriers, thereby dominating the subcarriers. Then in [9], the fairness among the users is considered. The constraint (7) is added to determine the number of subcarriers S_k required for user k by the proportion of the required data rate R_k . As shown in (7), the proportionality of left hand side of (7) is equal to the proportionality of right hand side.

$$S_1 : S_2 : ... : S_k = R_1 : R_2 : ... R_k \tag{7}$$

Assign the number of subcarriers S_k to user k based on the proportionality given in (7).
Step I :

For each subcarrier n

1) Order the channel gains of all users for subcarrier n in descending order so that the users are ordered from highest channel gain to lowest channel gain.
2) If the user k with the highest channel gain doesn't meet the required number of subcarriers S_k, this subcarrier is assigned to this user.
3) Otherwise procedure 2) is applied to the user $k+1$

End
Finally all users are assigned the subcarriers according to their own required number of subcarriers.

Step II:

Now we have the subcarrier allocation between users given in Step I.
For each user k

The single user bit-loading algorithm described in Section III (A) is applied for the bit and power allocation in the assigned subcarriers.

End

Table II. Combined sub-optimal method

Here, we combined the maximum bit-rate method proposed in [6] and the constraint in [9]. Finally the bit and power allocation is done by Single user OBA method. The algorithm is briefly described in Table II.

IV. PROPOSED METHOD

In this paper, we proposed a simple but efficient sub-optimal subcarrier allocation method. A new factor D_n, which is the gain difference between the maximum and the next maximum users' channel gains for each subcarrier, is introduced. The subcarriers are allocated to different users according to this factor. Finally the bit and power allocation is also done by the single user OBA method. The proposed method makes some modification on the Step I of combined sub-optimal method for the subcarrier allocation based on the new factor. The modification is briefly described in Table III.

The advantage of the proposed method is introducing D_n to ensure users have the largest chance to occupy their best subcarriers. Fig.1 shows the comparison

Initialize the allocated subcarrier set B which is empty but can have maximum N elements. The user set U contains all K users.

While the number of elements in B is less than total number of subcarriers N, do the following:

A.
For each unallocated subcarrier n

1) Order the channel gains of users in U in descending order.
2) Calculate the difference D_n between the maximum and the next maximum users' channel gains for subcarrier n

End

B. Find out maximum D_n, and its corresponding subcarrier n', and then find out the user k' with maximum channel gain in subcarrier n'.

C. If user k' hasn't met the required number of subcarriers $S_{k'}$, assign subcarrier n' to user k', and then update the allocated subcarrier set B. Otherwise remove user k' from user set U.

End

Finally all users are assigned the subcarriers according to their own required number of subcarriers.

Table III. Proposed method

of subcarrier allocation between the proposed method and the combined sub-optimal method. We assume a 2-user OFDM system with 128 subcarriers, and data rate ratio between user 1 and user 2 is $R_1 : R_2 = 1:3$, therefore user 1 requires 32 subcarriers and user 2 requires 96 subcarriers. The channel gains of these two users are shown in Fig.1 (a), and the subcarrier allocation in combined sub-optimal method and proposed method are shown in Fig.1 (b) and Fig.1 (c) respectively. The stars represent the subcarriers allocated to user 1, and the circles represent the subcarriers allocated to user 2.

As shown in Fig.1 (a), the maximum channel gain for user 1 is occurring around 120th subcarrier. In Fig.1 (b), the subcarrier allocation of the combined sub-optimal method allocates subcarriers within the range (1st subcarrier to 4th subcarrier and 25th subcarrier to 52nd subcarrier) to user 1,

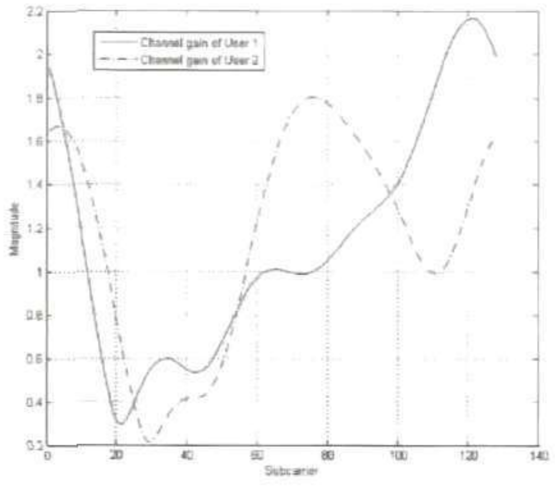

(a) Channel gains of two users in a 2-user OFDM System

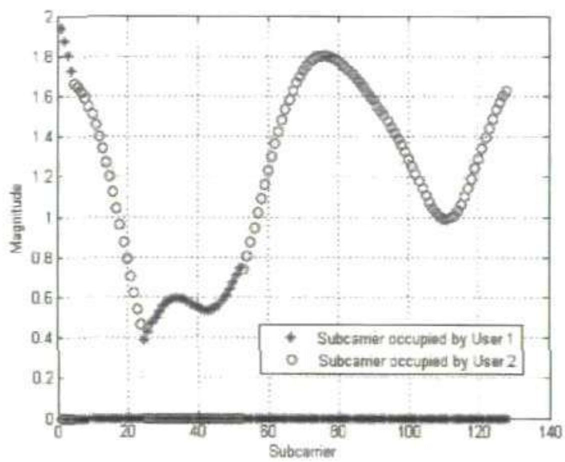

(b) Subcarrier allocation in combined sub-optimal method

because user 1 has relatively higher channel gains than user 2 within this range. Beyond this, user 1 has reached the number of subcarriers required (32 subcarriers), so that subcarrier allocation to user 1 does not occur in the area containing the subcarrier with maximum channel gain. Oppositely, the subcarrier allocation of the proposed method shown in Fig.1 (c) assigns most of the subcarriers to the user possessing maximum D_n (i.e. user 1 around 120th subcarrier) where D_n is defined as the gain difference between the maximum and the next maximum users' channel gains for each subcarrier. The subcarriers around the 120th subcarrier for user 1 all have large difference with user 2. Thus these subcarriers are firstly selected for user 1.

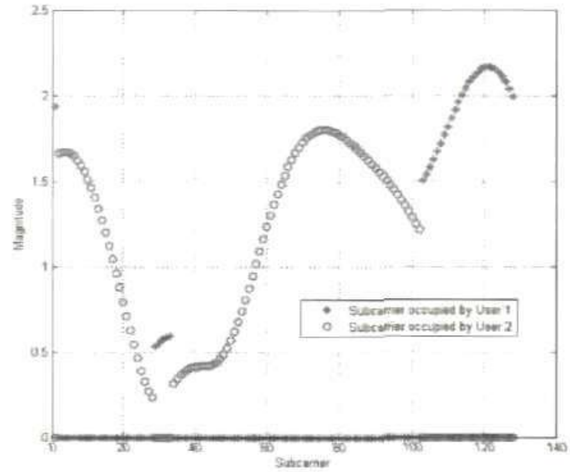

(c) Subcarrier allocation in proposed method

Fig.1. Subcarrier allocation comparison

V. PERFORMANCE

In this section, we compare the performance of the proposed method with currently available schemes such as the Static subcarrier allocation method (Fixed OFDM-FDMA), the Wong' method and the combined sub-optimal method.

We assume the Multiuser OFDM operates with 128 subcarriers, and the characteristics of users' channels are five-path frequency selective Rayleigh fading channels with exponential power delay profile. We quantify the improvement in terms of the Average bit SNR and BER. The Average bit SNR is defined as the ratio of the average required transmit power to the noise PSD level N_0, while the average required transmit power is defined as the ratio of overall transmit energy per OFDM symbol to the total number of bits transmitted per OFDM symbol.

The Fig.2 shows the average bit SNR (in dB) needed to achieve the same BER $P_e = 10^{-4}$ plotted versus the number of users for the proposed method, combined sub-optimal method, Wong's method and Fixed OFDM-FDMA with OBA and equal bit allocation (EBA). We find that the OBA leads better performance than EBA in the Fixed OFDM-FDMA systems with 2dB-3.5dB advantage. Wong's method, combined sub-optimal method and proposed method apply the adaptive subcarrier allocation combined with OBA; thereby they all lead better performance than Fixed OFDM-FDMA systems. Wong's method is 3-5dB better than Fixed OFDM-FDMA with OBA and 5-8dB

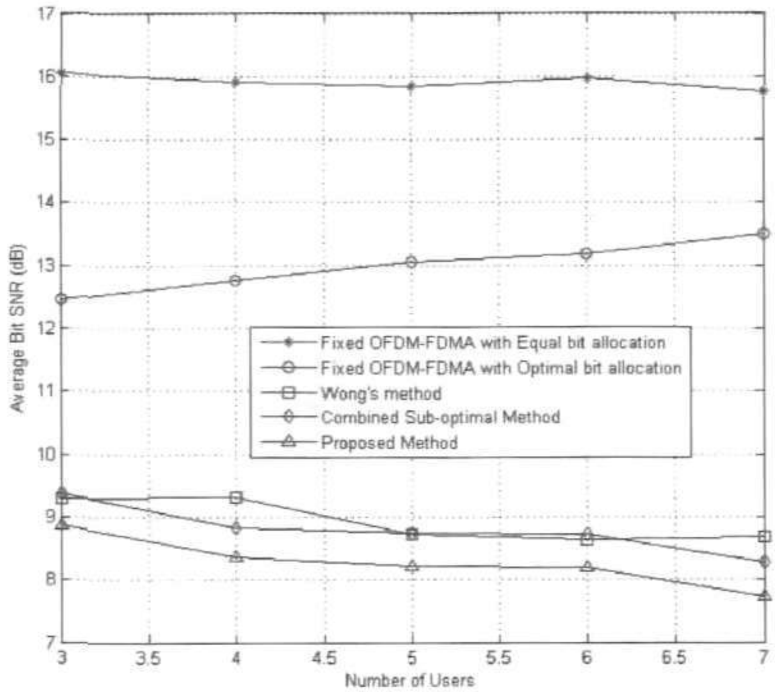

Fig.2 Number of users vs. average bit SNR

better than Fixed OFDM-FDMA with EBA. Compared with Wong's method, the combined sub-optimal method saves the transmit power around 0.5dB when number of users equals 4 and 7, and requires almost equal transmit power with Wong's method when number of users equals 3, 5 and 6. Thus it has similar overall performance with Wong's method. However, our proposed method has around 0.5-1dB advantage over Wong's method in saving the transmit power.

Fig.3 continuously shows the improvement with more familiar BER versus bit SNR curves. We assume a five user OFDM system. For different BER requirement ($P_e = 10^{-1} \sim 10^{-5}$), the relevant Average bit SNR (in dB) is calculated. Then we concluded that our proposed method outperforms other methods under the same operating environment, and that combined sub-optimal method also gives slightly better performance than Wong's method.

Additionally, in the aspect of algorithm's computation complexity, both combined sub-optimal method and proposed method require much less computation than Wong's method because they don't have the complex converging process like Wong's method, therefore they are much more practical in real life.

VI. CONCLUSION

In this paper, we investigate the subcarrier and power allocation in Downlink of Multiuser OFDM Systems. The proposed method not only considers the fairness of subcarrier allocation between users, but also introduces a factor which is the difference between the maximum channel gain and second maximum channel gain for each subcarrier. Then the subcarrier allocation is carried out according to the factor.

Simulation results show it outperforms the Fixed OFDM-FDMA, Wong's method and the combined sub-optimal method. In addition, the proposed method has much less computation complexity than the optimal solution proposed in [1] because it doesn't require the complex converging process. For large number of users, the proposed method may require relatively large computation for comparison between user's channel gains to determine D_n for each subcarrier. However, with the increasing processors, this should not be difficult to achieve. Thereby it is much more useful in practice systems.

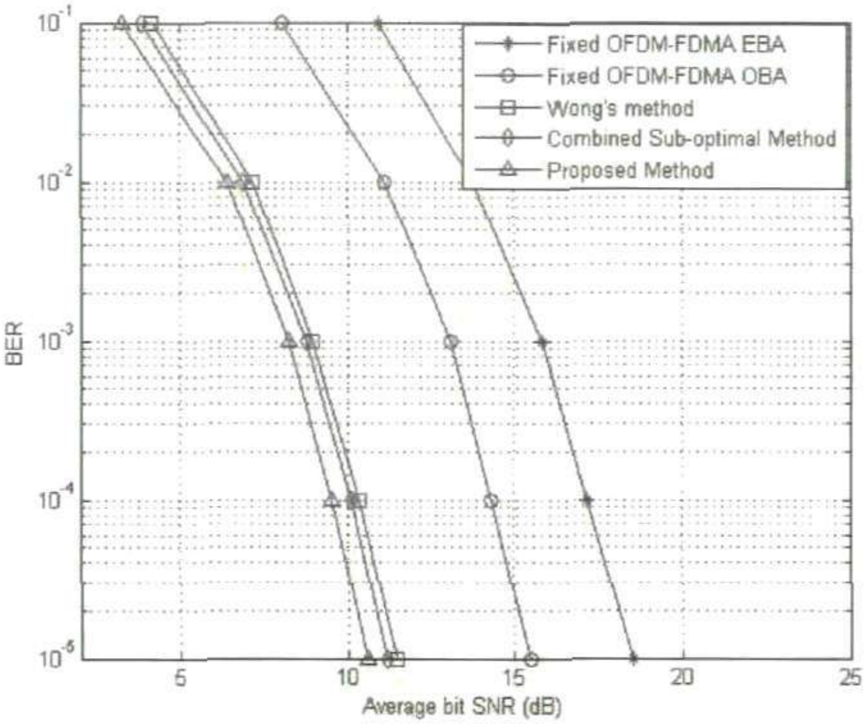

Fig.3 Average bit SNR vs. BER

REFERENCES

[1] C. Y. Wong, R. S. Cheng, K. B. Lataief, and R. D. Murch, "Multiuser OFDM System with Adaptive Subcarrier, Bit, and Power Allocation", *IEEE Journal on Selected Areas in Communication*, Vol. 17, pp. 1747-1758, Oct. 1999.

[2] C.Y. Wong, C. Y. Tsui, Roger S. Cheng, "A Real-time Sub-carrier Allocation Scheme for Multiple Access Downlink OFDM Transmission." *Proc. IEEE International Vehicular Technology Conference*, vol. 2, pp. 1124-1128, Sep 1999.

[3] Didem Kivanc, Hui Liu. "Subcarrier Allocation and Power Control for OFDMA." *Proc. Asilomar Conference on Signals, Systems and Computers*, Vol. 1, pp. 147-151, 2000

[4] W. Rhee and J. M. Cioffi. "Increasing in Capacity of Multiuser OFDM System Using Dynamic Subchannel Allocation," in *Proc. IEEE International Vehicular Technology Conference*, vol. 2, pp. 1085-1089,, Tokyo, Japan, May 2000.

[5] H. Yin and H. Liu, "An Efficient Multiuser Loading Algorithm for OFDM-based Broadband Wireless Systems", *IEEE Global Telecommunications Conference*, vol. 1, pp. 103-107, 2000

[6] J. Jang and K. B. Lee, "Transmit Power Adaptation for Multiuser OFDM Systems", *IEEE Journal on Selected Areas in Communications*, vol. 21, no. 2, pp. 171-178, Feb. 2003.

[7] I. Kim, H. L. Lee, B. Kim, and Y. H. Lee, "On the use of linear programming for dynamic subchannel and bit allocation in multiuser OFDM," *IEEE Global Telecommunications Conference*, vol. 6, pp. 3648-3652, Nov. 2001.

[8] Guodong Zhang, "Subcarrier and Bit Allocation for Real-time Services in Multiuser OFDM Systems" , *IEEE International Conference on Communications*, vol. 5, pp. 2985-2989. NY, USA, June 2004

[9] I. C. Wong, Z. Shen, L. Evans, and J. G. Andrews, "A Low Complexity Algorithm for Proportional Resource Allocation in OFDMA Systems," *IEEE workshop on Signal Processing Systems*, pp. 1-6, Texas, USA, Oct 2004

FFT-based Frequency Offset Estimation in OFDM Systems

Fan Wu
Mobile Communications Network Research
School of Computing and Mathmetics
University of Plymouth, UK
fan.wu@plymouth.ac.uk

Mosa Ali Abu-Rgheff
Mobile Communications Network Research
School of Computing and Mathmetics
University of Plymouth, UK
mosa@plymouth.ac.uk

Abstract—**In this paper, two fast and accurate FFT-based frequency offset estimation methods for OFDM systems are proposed. We analyze and simulate proposed methods in both Gaussian and multipath fading channels, and compare the results with those obtained using well known Schmidl's method. The simulation results are presented in terms of Error Variance (EV). Both proposed FFT-based methods have significantly smaller EV than Schmidl's method in AWGN and Multipath static fading channel and the proposed FFT method-II also has smaller EV than Schmidl's method in multipath time-varying fading channel.**

Index Terms— OFDM, synchronization, frequency offset, FFT, *Error Variance*

I. INTRODUCTION

SYCHRONIZATION is one of the crucial research topics in orthogonal frequency division multiplexing (OFDM) system because of its sensitivity to the timing and frequency errors [1].

To guarantee fast and accurate data transmission, Inter Carrier Interference (ICI) caused in the transmission has to be eliminated as much as possible which can be achieved by *maintaining the orthogonality of carriers such that the* transmitter and the receiver have the exact same carrier frequency. But in the real world, frequency offsets will be arising from the frequency mismatch of the transmitter and the receiver oscillators and the existence of Doppler shift in the channel. So it is important to be able to estimate the frequency offset to minimize its impact on system performance.

Moose [2] described a technique to estimate the frequency offset using two repeated OFDM symbols but the estimation range is limited within half sub carrier interval. Jan [3] proposed a maximum likelihood (ML) frequency offset estimation method for OFDM systems by using the cyclic prefix. However, the most popular method is that proposed by Schmidl [4], using a preamble consisting of two OFDM training symbols with specific design.

In this paper, Schmidl's method is reviewed, and then two fast and efficient FFT-based frequency offset estimation methods are proposed. The performance of proposed methods is evaluated through comparing the actual frequency offset with that estimated together with the EV of estimated results. The results obtained are compared with those obtained using Schmidl's method [4]. Finally, the computational complexities are computed and compared with Schmidl's method. The rest of paper is organized as follow. Section II briefly describes the *OFDM system model. Section III reviews Schmidl's method* and introduces our proposed FFT-based methods. Section IV presents the simulation results. Section V concludes the paper.

II. OFDM SYSTEM MODEL

The block diagram of a typical OFDM transceiver is shown in Figure 1. A block of input information data bits is encoded and mapped to PSK or QAM symbol c_n, and converted by the serial to parallel converter to a number of parallel streams which go through the Inverse Fast Fourier Transform (IFFT) processor and a cyclic prefix (CP) is inserted to the IFFT output. The CP consists of the output own last N_g samples. The baseband OFDM symbol S_k can be expressed as:

$$S_k = \frac{1}{\sqrt{N}} \sum_{n=0}^{N_c - 1} c_n . e^{j2\pi nk/N} (-N_g \le k \le N-1) \quad (1)$$

where N is the number of IFFT points. N_c is number of subcarriers ($N_c \le N$). These symbols are filtered, up-converted and then transmitted.

The research was supported by University of Plymouth, UK

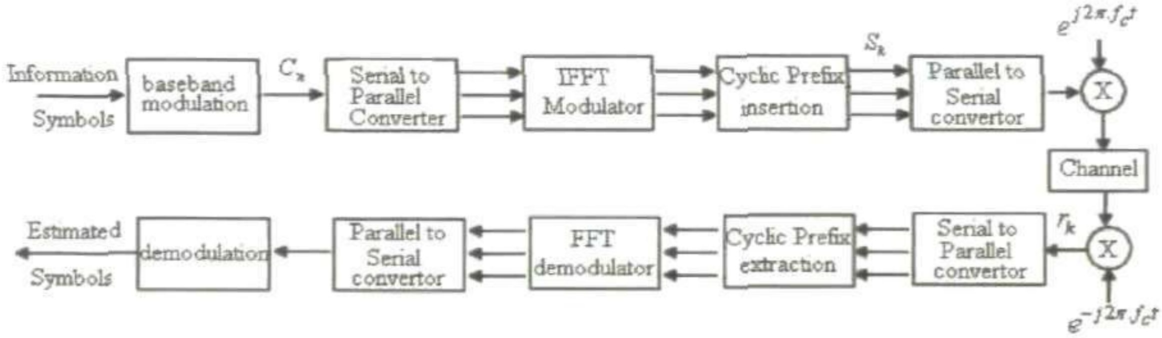

Figure.1. Block Diagram of OFDM Transceiver

At the receiver, the timing offset is modelled as a delay in the received signal and frequency offset is modelled as a phase distortion of the received data in the time domain [5]. The received samples of the OFDM symbol can be expressed as:

$$r_k = e^{j2\pi \varepsilon.k/N}.\sum_{m=0}^{v-1} S_{k-te-m}.h_m + \eta_k \tag{2}$$

Here, h_m is the channel impulse response with length v, te is the delay of a symbol, ε is the frequency offset f_e normalized to the subcarrier spacing $1/(NT_s)$, where T_s is the sample interval, and η_k is the white Gaussian noise. The boundary of preamble and the frequency offset will be estimated by timing and frequency synchronization algorithms respectively and then the OFDM symbols inside the frame needs to be compensated for the frequency offset before carrying out demodulation.

III. FREQUENCY OFFSET ESTIMATORS

In this section, we review the Schmidl's method first, and then propose two FFT-based frequency offset estimation methods. All training symbols are QPSK modulated, and then multiplied by $\sqrt{2}$ in frequency domain in order to maintain approximately constant signal power.

3.1. Schmidl method

Schmidl [4] designed two training symbols as preamble. The first one has two identical parts $s_{1,n}$ and $s_{1,n+L}$ with $N/2$ samples each and L (= $N/2$) delay between identical samples. They will remain identical after passing through the channel, except the phase difference ϕ between them due to the frequency offset.

$$\phi = 2\pi.\Delta f_c LT_s = \pi.f_e NT_s \tag{3}$$

where ϕ can be estimated from the timing metric given in [4] at the optimum timing point . Then if $|\phi|$ is less then π, the frequency offset will be:

$$f_e = \phi/(\pi NT_s) \tag{4}$$

Otherwise

$$f_e = \frac{\phi}{\pi NT_s} + \frac{2\hat{l}}{NT_s} \tag{5}$$

where $\bar{\ell}$ is an integer. We correct the two training symbols with the computed frequency offset ($\frac{\phi}{\pi NT_s}$). All we have to do now is to find the unknown second term in (5). Let the FFT's of received first and second corrected training symbols be ($F_{1,k}$, $F_{2,k}$) and the differentially modulated PN sequence on the even frequencies of the second training symbol be (u_k). Then the sliding correlation between the FFTs and (u_k) is given by

$$B(\ell) = \frac{|\sum_{k\in X} F^*_{1,k+2\ell}.u^*_k.F_{2,k+2\ell}|^2}{2(\sum_{k\in X}|F_{2,k}|^2)^2} \tag{6}$$

where X is the set of indices for even frequency components of the second training symbol. Finally, the l corresponding to the maximum value of $B(l)$ is used to calculate integral frequency offset in (5).

3.2. Proposed FFT-based methods

Frequency offset estimation comes after a precise timing estimation, the received training symbol r_n after removing the CP is multiplied with the conjugate of the known training symbol to get the modified signal d_n, and then processed by N-point FFT as shown in (7) for frequency offset search. The training symbol can be the one applied for timing offset estimation in Schmidl's method so that only one training symbol is required for both time and frequency synchronization in OFDM systems.

$$F_k = \sum_{n=0}^{N-1} d_n . e^{-j2\pi.nk/N} (0 \le k \le N-1) \quad (7)$$

$$d_n = r_n . A_n^* \quad (8)$$

where A_n is the training sequence which is assumed to be known to the receiver, A_n^* is its conjugate. The coarse frequency offset f_{coarse} is given by (9) where $k_{\max}$ is the bin number of the largest magnitude in the FFT outputs.

$$f_{coarse} = \frac{k_{\max}}{NT_s} \quad (9)$$

Normally equation (9) gives the exact frequency when the largest magnitude falls at the centre of the $|F(k_{\max})|$. However, when it is offset to the right or the left of the centre due to noise or distortion, equation (9) will give an incorrect frequency. To alleviate this problem, we propose two methods for fine frequency search.

3.2.1. FFT method-I

We use the largest magnitude $|F(k_{\max})|$, and two magnitudes on both sides of largest magnitude $|F(k_{\max}-1)|$ and $|F(k_{\max}+1)|$. Define a switching function α as:

$$\begin{aligned} \alpha &= 1 \quad if \quad |F(k_{\max}-1)| \le |F(k_{\max}+1)| \\ \alpha &= -1 \quad if \quad |F(k_{\max}-1)| > |F(k_{\max}+1)| \end{aligned} \quad (10)$$

It can be shown that the fine frequency offset is given by:

$$f_{fine} = \frac{1}{NT_s} . \frac{\alpha}{F(k_{\max})/F(k_{\max}+\alpha)+1} \quad (11)$$

Then the frequency offset is given by:

$$\begin{aligned} f_e &= f_{corse} + f_{fine} \\ &= \frac{1}{NT_s}(k_{\max} + \frac{\alpha}{F(k_{\max})/F(k_{\max}+\alpha)+1}) \end{aligned} \quad (12)$$

3.2.2. FFT method-II

We define the phase θ_0, which is caused by the coarse frequency offset operating on the CP of training symbol as:

$$\theta_0 = angle(e^{j2\pi.f_{coarse}N_gT_s}) \quad (13)$$

The first step is the spectrum shifting, which is shifting the maximum bin $k_{\max}$ to zero frequency position to achieve the spectrum of the signal distorted by fine frequency offset only. And then IFFT is applied to transform signal back to time domain given by:

$$d_n' = \sum_{n=0}^{N-1} F_k' . e^{j2\pi.nk/N} (0 \le k \le N-1) \quad (14)$$

where F_k' is the shifted FFT output. Then d_n' can be represented in polar coordinates as equation (15) with magnitude M_n and phase α_n, which is the same as the expected training sequence subject to fine frequency offset f_{fine} only as shown in equation (16)

$$s_n = M_n . e^{j\alpha_n} \quad (15)$$

$$s_n' = |A_n|^2 e^{j2\pi.f_{fine}.(n+N_g)T_s} \quad (16)$$

The match filter (MF) output is given by autocorrelation of s_n and s_n', and the real MF out is given by:

$$y_n = \sum_{n=0}^{N-1} M_n . |A_n|^2 \cos([\alpha_n - \theta_0]_{2\pi} - 2\pi f_{fine}(n+N_g)T_s) \quad (17)$$

The estimate of this fine frequency offset derived in [6] is:

$$f_{fine} = \frac{\sum_{n=0}^{N-1} M_n |A_n|^2 .(n+N_g).[\alpha_n - \theta_0]_{2\pi}}{2\pi T_s \sum_{n=0}^{N-1} (n+N_g)^2 .M_n |A_n|^2} \quad (18)$$

The frequency offset is given by:

$$f_e = f_{coarse} + f_{fine}$$

$$= \frac{k_{\max}}{NT_s} + \frac{\sum_{n=0}^{N-1} M_n |A_n|^2 .(n+N_g).[\alpha_n - \theta_0]_{2\pi}}{2\pi T_s \sum_{n=0}^{N-1} (n+N_g)^2 .M_n |A_n|^2} \quad (19)$$

Note: α_n needs the phase compensation with θ_0 and 2π phase correction denoted as $[.]_{2\pi}$ to achieve accurate estimation.

IV. SIMULATION RESULTS

4.1 Simulation Parameters

Simulations are carried out to evaluate the proposed methods. Table I and II show the necessary simulation parameters and the multipath time-varying fading channel model respectively. The multipath static fading channel has zero Doppler shift, and fixed path gains which are the same as those of the multipath time-varying fading channel model.

Number of subcarriers (N_c)	1000
IFFT points (N)	1024
Date rate (R_d) (Mbits/s)	18
CP length	10% of OFDM symbol
Frequency offset	2.4 subcarrier spacing

Table I. Simulation Parameters

Maximum Doppler shift (Hz)	60
Number of Paths	3
Delays of the paths in samples	[0,6,11]
Path gain	[0.9,0.36,0.29]

Table II. Multipath time-varying Fading channel

4.2 Performance of Frequency estimators

The simulations are carried out to evaluate the proposed methods and compared with the Schmidl's method.

First of all, a series of frequency offsets are assumed, then for each one, the value f_e estimated by the proposed methods is compared with the actual value in AWGN channel and multipath time-varying fading channel with SNR in both channels fixed at 10dB. Results are shown in Figure.2.

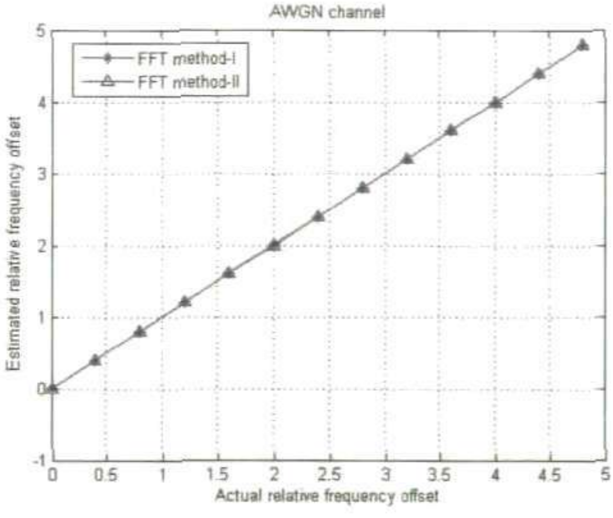

(a)

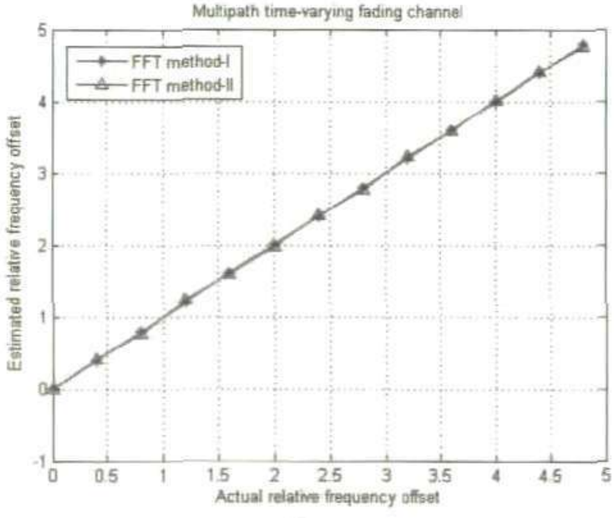

(b)

Figure.2. Proposed FFT-based estimators' performance in (a) AWGN (b) Multipath time-varying fading channel

Figure.2 shows the estimated versus assumed frequency offset of the proposed methods when system is operating in AWGN channel and multipath time-varying fading channel. The results show the excellent agreement of estimated with assumed frequency offset values.

Subsequently, the EV is evaluated and compared for the proposed methods. Here the frequency offset is assumed as 2.4 subcarrier spacing. The SNR is set in the range of 0 to 24dB with 3 dB intervals. The EVs of different SNR for these estimators are evaluated in AWGN channel, multipath static fading channel and multipath time-varying fading channel respectively. Results are shown in Figure.3. Obviously, in AWGN Channel and multipath static fading channel, proposed FFT method-I and FFT method-II all have smaller EV than Schmidl' method, and FFT method-II has smaller EV than FFT method-I. In the multipath time-varying fading channel, FFT method-II still has smaller EV than the other two, however FFT method-I has slightly higher EV than Schmidl's method because the lack of consideration on signal phase leads the un-stabled estimation.

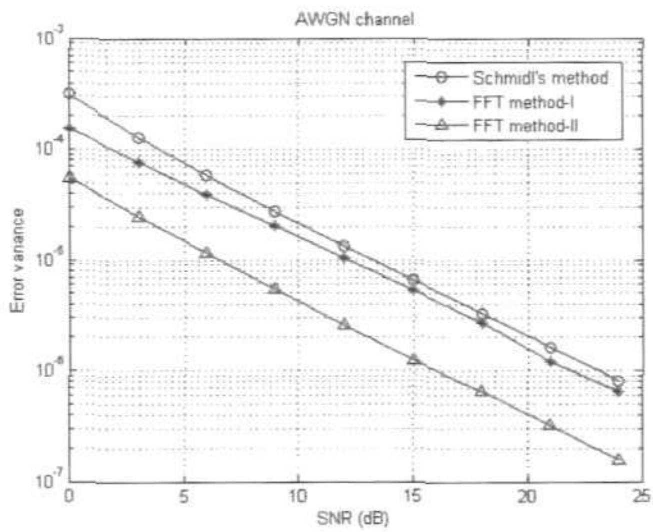

(a)

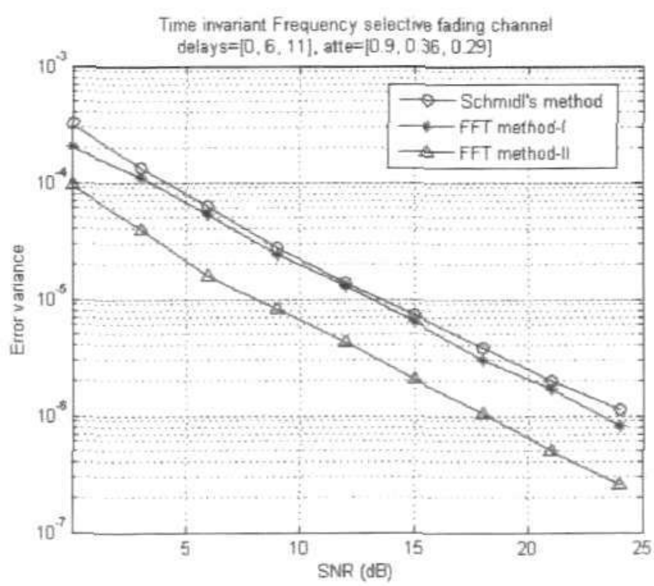

(b)

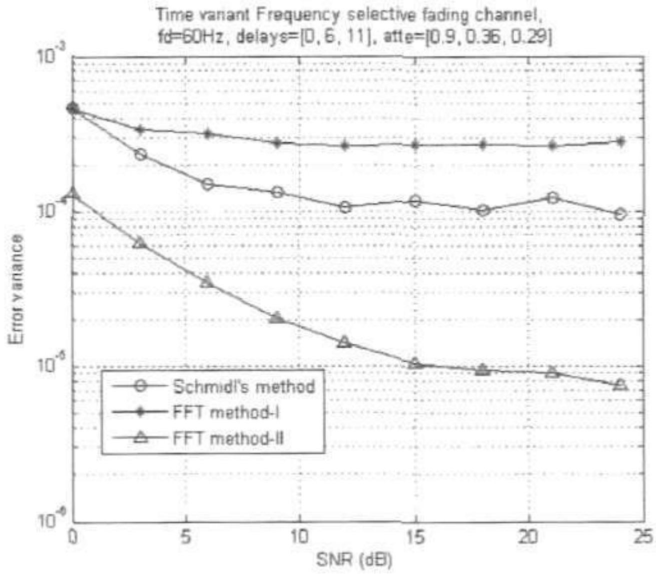

(c)

Figure.3. EV of Proposed methods and Schmidl method in
(a) AWGN channel
(b) Multipath static fading channel
(c) Multipath time-varying fading channel

4.3 The Computational Complexity

This section presents the comparison of the computational complexity of proposed methods with that of Schmidl's method. We assume the training symbol used for estimation has 1024 samples, and Radix-2 FFT is applied when needed. The results are shown in Table III.

As shown in Table III, the proposed methods have less computational requirement than Schmidl' method. Both proposed methods can be practically implemented in real life.

	Addition	Product	Exponent Evaluation	Magnitude Evaluation
Schmidl method	23445	48131	4524	5868
FFT method-I	13	1099	10	1024
FFT method-II	5142	15507	1044	4096

Table III. Computational Complexity

V. CONCLUSIONS

Frequency offset estimation in OFDM system is presented in this paper. The popular Schmidl's method is reviewed, and two fast and efficient FFT-based methods are proposed. Simulation results from the proposed FFT-based methods show excellent frequency estimates, and even provide better performance than Schmidl's method in both AWGN channel and multipath static fading channel. In the multipath time-varying fading channel, FFT method-II still outperforms Schmidl's method, but FFT method-I has slightly higher EV than Schmidl's method because of the lack of consideration on signal phase. Additionally, they all require small computation complexity so that the estimates can be computed in short time using available fast processors. Therefore, the proposed methods can provide good performance with low complexity.

REFERENCES

[1] T. Pollet, M. Van Bladel, and M. Moeneclaey, "Ber sensitivity of OFDM systems to carrier frequency offsetand wiener phase noise," *IEEE Trans. Commun.*, vol. 43, pp. 191–193, Feb./Mar/Apr1995

[2] P. Moose, "A technique for orthogonal frequency-division multiplexing frequency offset correction," *IEEE Trans. Commun*, 1994,10: 2908-2914

[3] J. J. van de Beek, M. Sandell, and P. O. Borjesson, "ML estimation of time and frequency offset in OFDM systems," *IEEE Trans. Signal Processing*, vol. 43, pp. 761–766, Aug. 1997

[4] T. Schmidl and D. Cox, "Robust frequency and timing synchronization for OFDM," *IEEE Trans. Commun*, vol. 45, no.12, 1997:1613-1621

[5] Byungjoon Park, Hyunsoo Cheon, Changeon Kang, and Daesik Hong "A Novel Timing Estimation Method for OFDM Systems", *IEEE Communications Letters*, VOL. 7, NO. 5, MAY 2003, pp.239-241

[6] F.Wu and M. Ali Abu-Rgheff, "FFT-based Frequency offset Estimators in OFDM Systems", Research Report

Efficient Subcarrier Allocation in Downlink Multiuser MIMO-OFDM Systems

Fan Wu
Centre for Security, Communications and Network Research
University of Plymouth, UK
fan.wu@plymouth.ac.uk

Mosa Ali Abu-Rgheff
Centre for Security, Communications and Network Research
University of Plymouth, UK
mosa@plymouth.ac.uk

***Abstract*—this paper proposes a unit power based subcarrier allocation algorithm with the aim of minimizing the total transmit power in the downlink multiuser MIMO-OFDM systems, and compares its performance and complexity with Zhang's algorithm and extended Correlation-based algorithm (ECBA). By applying Singular Value Decomposition (SVD), the inter-antenna interference (IAI) and multiple user interference (MUI) can be minimized. Our proposal is combined with the single user optimal bit allocation (OBA) algorithm to achieve the aim. We verify the proposal by simulation of the performance of total transmit power and calculating the computation complexity. The simulation results show our modification has significant improvement compared with Zhang's algorithm and the ECBA.**

Index terms — Multiuser MIMO-OFDM, SVD, subcarrier allocation

I. Introduction

OFDM converts a frequency-selective channel into a set of parallel flat-fading channels, and consequently makes MIMO-related algorithms easy to implement [1]. Recently, there have been heated discussions for efficient resource allocation in multiuser MIMO-OFDM systems. Consequently, several resource allocation algorithms were proposed in multiuser SISO-OFDM system [2-4]. In [5], the resource allocation was extended to MIMO-OFDM systems based on SVD by utilizing the selection diversity gain. The user with maximum singular mode is selected during subcarrier allocation. In [6], Liu et al. proposed a novel SVD based downlink multiuser MIMO system, which takes into account the specific characteristics of the individual users channel matrix, instead of treating all the users' channels jointly, as in the traditional multiuser transmission (MUT) technique. In [7], Ji et al. proposed the channel correlation metric between users and used it to select users in the multiuser MIMO systems.

In downlink MIMO-OFDM systems, each subcarrier has multiple spatial layers; therefore multiple users can share one subcarrier for transmission. The problem raised is the MUI. In this paper, we extend the SVD based multiuser MIMO system in [6] to multiuser MIMO-OFDM system so that the MUI in each subcarrier can be minimized or cancelled. Subsequently, we review the Zhang's subcarrier allocation algorithm proposed in [5] and describe the ECBA extended from the correlation based user selection algorithm in multiuser MIMO systems proposed in [7]. Because Zhang's algorithm requires large computation and only one user is assigned in each subcarrier and ECBA algorithm does not consider the correlation among the spatial sub-channels within individual user. Therefore, we propose a unit power based subcarrier allocation algorithm which alleviates these problems. After the subcarrier allocation, the users' effective channel gains for each subcarrier are calculated. Each user's effective channel gains on the assigned subcarriers are applied to the single user OBA algorithm described in [3] to allocate bits on each assigned subcarrier, and finally achieve system optimization.

The rest of the paper is organized as follows. Section II describes the multiuser SVD based MIMO-OFDM system model. Section III describes the previous algorithms and our proposed modification algorithm for subcarrier allocation. Section IV presents the simulation results. Finally, Section V concludes the paper.

II. System Model

We consider a downlink multiuser MIMO-OFDM system with N subcarriers. The basestaion (BS) has N_T transmit antennas to serve K mobile users where each user having N_R receive antennas. We assume the users' channel matrix which *is not varied during the one frame time and is perfectly known* in both BS and users' mobile units, and that $N_T \geq \sum_{k=1}^{k\in S_n} N_R$ where S_n is the subset of users sharing the n^{th} subcarrier.The received signal of the user k on the n^{th} subcarrier is represented as:

$$\begin{aligned} \mathbf{y}_{k,n} &= \mathbf{H}_{k,n}\sum_{k=1}^{k\in S_n}\mathbf{F}_{k,n}\sqrt{\mathbf{P}_{k,n}}\mathbf{d}_{k,n} + \mathbf{w}_{k,n}, k\in S_n \\ &= \mathbf{H}_{k,n}\mathbf{F}_{k,n}\sqrt{\mathbf{P}_{k,n}}\mathbf{d}_{k,n} + \mathbf{H}_{k,n}\sum_{j=1,j\neq k}^{j\in S_n}\mathbf{F}_{j,n}\sqrt{\mathbf{P}_{j,n}}\mathbf{d}_{j,n} + \mathbf{w}_{k,n} \end{aligned} \quad (1)$$

where $\mathbf{d}_{k,n}$ is the parallel N_R data of user k transmitted on the n^{th} subcarrier , $\mathbf{P}_{k,n} = diag\{P_{k,n,1}, P_{k,n,2}, ..., P_{k,n,N_R}\}$ is the $N_R \times N_R$ diagonal matrix, representing the transmit power level of user k on the n^{th} subcarrier for N_R data symbols, $\mathbf{F}_{k,n}$ is the $N_T \times N_R$ precoder matrix for user k on the

n^{th} subcarrier, $\mathbf{H}_{k,n}$ is the $N_R \times N_T$ channel matrix for user k on the n^{th} subcarrier, and $\mathbf{w}_{k,n}$ is the complex Gaussian noise with zero mean for user k on the n^{th} subcarrier. As shown in the multiuser MIMO system of [6], the precoder is containing the transmit power level $\mathbf{P}_{k,n}$ which is pre-defined as constraints. In our paper, $\mathbf{P}_{k,n}$ is separated with precoder because it is the factor which is unknown and needs to be minimized. According to the SVD based matrix decomposition method in [6], the $\mathbf{H}_{k,n}$ can be expressed as

$$\begin{aligned}\mathbf{H}_{k,n} &= \mathbf{U}_{k,n}\left[\mathbf{\Sigma}_{k,n}^{1/2},0\right]\mathbf{V}_{k,n}^{H} \\ &= \mathbf{U}_{k,n}\left[\mathbf{\Sigma}_{k,n}^{1/2},0\right]\begin{bmatrix}\mathbf{V}_{k,n,s}^{H} \\ \mathbf{V}_{k,n,z}^{H}\end{bmatrix} \\ &= \mathbf{U}_{k,n}\mathbf{\Sigma}_{k,n}^{1/2}\mathbf{V}_{k,n,s}^{H}\end{aligned} \tag{2}$$

where $\mathbf{U}_{k,n}$ and $\mathbf{V}_{k,n}$ are the $N_R \times N_R$ and $N_T \times N_T$ left and right singular vectors of $\mathbf{H}_{k,n}$ respectively. $\mathbf{\Sigma}_{k,n}$ is the $N_R \times N_R$ diagonal matrix containing the singular values of $\mathbf{H}_{k,n}\mathbf{H}_{k,n}^{H}$. Furthermore, $\mathbf{V}_{k,n,s}$ is the matrix with size of $N_T \times N_R$, and containing the right singular vectors corresponding to the non-zero singular values of $\mathbf{H}_{k,n}$. $\mathbf{V}_{k,n,z}$ is the matrix with size of $N_T \times (N_T - N_R)$, and containing the right singular vectors corresponding to the zero singular values of $\mathbf{H}_{k,n}$.

Then we consider the system in overall view with the following definitions:

$$\mathbf{d}_n = [\mathbf{d}_{1,n}^T, \mathbf{d}_{2,n}^T, \dots \mathbf{d}_{k,n}^T]^T, k \in S_n \tag{3}$$

$$\mathbf{F}_n = [\mathbf{F}_{1,n}, \mathbf{F}_{2,n}, \dots \mathbf{F}_{k,n}], k \in S_n \tag{4}$$

$$\mathbf{P}_n = diag\{\mathbf{P}_{1,n}, \mathbf{P}_{2,n}, \dots \mathbf{P}_{k,n}\}, k \in S_n \tag{5}$$

$$\mathbf{U}_n = diag\{\mathbf{U}_{1,n}, \mathbf{U}_{2,n}, \dots, \mathbf{U}_{k,n}\}, k \in S_n \tag{6}$$

$$\mathbf{\Sigma}_n = diag\{\mathbf{\Sigma}_{1,n}, \mathbf{\Sigma}_{2,n}, \dots, \mathbf{\Sigma}_{k,n}\}, k \in S_n \tag{7}$$

$$\mathbf{V}_{n,s} = [\mathbf{V}_{1,n,s}, \mathbf{V}_{2,n,s}, \dots \mathbf{V}_{k,n,s}], k \in S_n \tag{8}$$

$$\mathbf{w}_n = [\mathbf{w}_{1,n}^T, \mathbf{w}_{2,n}^T, \dots \mathbf{w}_{k,n}^T]^T, k \in S_n \tag{9}$$

where $\mathbf{d}_n$ is the overall transmitted data on the n^{th} subcarrier, $\mathbf{F}_n$ is the overall precoder on the n^{th} subcarrier, and P_n is the overall transmit power level on the n^{th} subcarrier. Therefore the overall received signal vector $\mathbf{y}_n$ of all the users sharing the n^{th} subcarrier can be expressed as:

$$\mathbf{y}_n = \mathbf{U}_n\mathbf{\Sigma}_n^{1/2}\mathbf{V}_{n,s}^{H}\mathbf{F}_n\sqrt{\mathbf{P}_n}\mathbf{d}_n + \mathbf{w}_n \tag{10}$$

As shown in (10), the MUI on the n^{th} subcarrier can be fully removed when $\mathbf{F}_n$ is chosen to be:

$$\mathbf{F}_n = [\mathbf{V}_{n,s}^{H}]^{+} \tag{11}$$

where $[\mathbf{V}_{n,s}^{H}]^{+}$ denotes the psedo-inverse of $\mathbf{V}_{n,s}^{H}$. By substituting(11) into (10), $\mathbf{y}_n$ can be expressed as:

$$\mathbf{y}_n = \mathbf{U}_n\mathbf{\Sigma}_n^{1/2}\sqrt{\mathbf{P}_n}\mathbf{d}_n + \mathbf{w}_n \tag{12}$$

To be more specific, the received signal of user k on the n^{th} subcarrier can be expressed as:

$$\mathbf{y}_{k,n} = \mathbf{U}_{k,n}\mathbf{\Sigma}_{k,n}^{1/2}\sqrt{\mathbf{P}_{k,n}}\mathbf{d}_{k,n} + \mathbf{w}_{k,n}, k \in S_n \tag{13}$$

As shown in (13), user k has fully removed the MUI generated from other users sharing the n^{th} subcarrier. Furthermore, the IAI among the antenna-specific symbols can be suppressed by post-processing $\mathbf{y}_{k,n}$ with $\mathbf{U}_{k,n}^{H}$ and shown as:

$$\mathbf{U}_{k,n}^{H}\mathbf{y}_{k,n} = \hat{\mathbf{d}}_{k,n} = \mathbf{\Sigma}_{k,n}^{1/2}\sqrt{\mathbf{P}_{k,n}}\mathbf{d}_{k,n} + \mathbf{U}_{k,n}^{H}\mathbf{w}_{k,n}, k \in S_n \tag{14}$$

where $\hat{\mathbf{d}}_{k,n}$ is the $N_R \times 1$ received data for user k on the n^{th} subcarrier from the N_R antennas. Then we assume that users' unity power-normalized data $\mathbf{d}_{k,n}, k \in S_n$ transmitted on the n^{th} subcarrier are not correlated with each other, so $E(\mathbf{d}_{k,n}\mathbf{d}_{k,n}^{H}) = I$. According to (14), the required receive power $\mathbf{P}_{k,n}^{r}$ for user k on the n^{th} subcarrier is given by:

$$\begin{aligned}\mathbf{P}_{k,n}^{r} &= \hat{\mathbf{d}}_{k,n}\hat{\mathbf{d}}_{k,n}^{H} \\ &= E(\mathbf{\Sigma}_{k,n}^{1/2}\sqrt{\mathbf{P}_{k,n}}\mathbf{d}_{k,n}\mathbf{d}_{k,n}^{H}(\sqrt{\mathbf{P}_{k,n}})^{H}(\mathbf{\Sigma}_{k,n}^{1/2})^{H}) \\ &= \mathbf{\Sigma}_{k,n}^{1/2}\sqrt{\mathbf{P}_{k,n}}E(\mathbf{d}_{k,n}\mathbf{d}_{k,n}^{H})(\sqrt{\mathbf{P}_{k,n}})^{H}(\mathbf{\Sigma}_{k,n}^{1/2})^{H} \\ &= \mathbf{\Sigma}_{k,n}^{1/2}\sqrt{\mathbf{P}_{k,n}}(\sqrt{\mathbf{P}_{k,n}})^{H}(\mathbf{\Sigma}_{k,n}^{1/2})^{H} \\ &= (\mathbf{\Sigma}_{k,n}^{1/2})^2\mathbf{P}_{k,n}\end{aligned} \tag{15}$$

So,

$$\mathbf{P}_{k,n} = [(\mathbf{\Sigma}_{k,n}^{1/2})^{-1}]^2\mathbf{P}_{k,n}^{r}, k \in S_n \tag{16}$$

Here $\mathbf{P}_{k,n}^{r} = diag\{P_{k,n,1}^{r}, P_{k,n,2}^{r}, \dots, P_{k,n,N_R}^{r}\}$ is the required receive power to support $c_{k,n} = [c_{k,n,1}, c_{k,n,2}, \dots c_{k,n,N_R}]$ bits by satisfying target bit error rate (BER) P_e for user k on the n^{th} subcarrier over N_R receive antennas. According to [2], $P_{k,n,i}^{r}, (k \in S_n, i = 1,2,\dots,N_R)$ can be expressed as:

$$P_{k,n,i}^{r} = f(c_{k,n,i}) = \frac{N_0}{3}[Q^{-1}(\frac{P_e}{4})]^2(2^{c_{k,n,i}} - 1) \tag{17}$$

where N_0 is the noise power spectral density, and Q^{-1} is the inversed Q function. Because of the precoder $\mathbf{F}_{k,n}$, the actual transmit power $\mathbf{P}_{k,n}^{F}$ for user k on the n^{th} subcarrier is:

$$\begin{aligned}\mathbf{P}_{k,n}^{F} &= \sum_{i=1}^{N_R}\left\|F_{k,n,i}\right\|^2 P_{k,n,i} \\ &= trace(\mathbf{F}_{k,n}^{H}\mathbf{F}_{k,n}\mathbf{P}_{k,n}) \qquad ,k \in S_n \\ &= trace(\mathbf{F}_{k,n}^{H}\mathbf{F}_{k,n}[(\mathbf{\Sigma}_{k,n}^{1/2})^{-1}]^2\mathbf{P}_{k,n}^{r})\end{aligned} \tag{18}$$

where $F_{k,n,i}$ is the i^{th} column of $\mathbf{F}_{k,n}$. According to (18), the effective channel gains $\mathbf{g}_{k,n}$ of the user k on the n^{th} subcarrier can be expressed as:

$$\mathbf{g}_{k,n} = diag(\mathbf{F}_{k,n}^{H}\mathbf{F}_{k,n}[(\mathbf{\Sigma}_{k,n}^{1/2})^{-1}]^{2}), k \in S_n \quad (19)$$

We then denote the $g_{k,n,i}$ as the i^{th} diagonal element of $\mathbf{g}_{k,n}$. The total transmit power for users on all subcarriers are formulated as:

$$P_{total} = \sum_{n=1}^{N}\sum_{k\in S_n}\mathbf{P}_{k,n}^{F} = \sum_{n=1}^{N}\sum_{k\in S_n}\sum_{i=1}^{N_R}\frac{P_{k,n,i}^{r}}{g_{k,n,i}} \quad (20)$$

Then the optimization problem can be formulated as:

$$\min P_{total} = \min\sum_{n=1}^{N}\sum_{k\in S_n}\sum_{i=1}^{N_R}\frac{P_{k,n,i}^{r}}{g_{k,n,i}} \quad (21)$$

subject to the following conditions:

$$\sum_{n=1}^{N}\rho_{k,n}(\sum_{i=1}^{N_R}c_{k,n,i}) = R_k, \quad k = 1,...,K \quad (22)$$

$$\rho_{k,n} = \begin{cases} = 1 & if \ \sum_{i=1}^{N_R}c_{k,n,i} \neq 0 \\ = 0 & if \ \sum_{i=1}^{N_R}c_{k,n,i} = 0 \end{cases} \quad (23)$$

where R_k is the data rate of user k and $\rho_{k,n} = 1$ means subcarrier n is allocated to user k.

III. SUBCARRIER AND BIT ALLOCATION

In this section, we focus on the subcarrier allocation algorithms in multiuser MIMO-OFDM systems based on the review of previous algorithms and our proposed algorithm.

3.1. Reviews of Subcarrier allocation algorithms

We will review the maximum singular value-based subcarrier allocation algorithm proposed by Zhang in [5], and the ECBA subcarrier allocation algorithm extended from the correlation based user selection algorithm in multiuser MIMO systems proposed in [7].

3.1.1. Zhang's subcarrier allocation algorithm

Zhang's subcarrier allocation algorithm is based on the maximum singular value of each user's channel, and each subcarrier can be allocated to only one user at most. The detailed algorithm is described in [5].

3.1.2. Extended Correlation-based subcarrier allocation Algorithm (ECBA)

In [7], the channel correlation metric between user i and user j is proposed for the user selection in multiuser MIMO systems and defined by:

$$\eta_{i,j} = \frac{\|\mathbf{H}_i\mathbf{H}_j^{H}\|^2}{\|\mathbf{H}_i\|^2\|\mathbf{H}_j\|^2} \quad (24)$$

Here the channel correlation metric is extended to the subcarrier allocation of multiuser MIMO-OFDM systems with the following definition.

Definition

1. Each subcarrier is allowed to be shared between multiple users.
2. The maximum number of users sharing one subcarrier is $\hat{K} = N_T / N_R$,
3. The subset of users in the n^{th} subcarrier is $S_n = \phi, \forall n \in N$,
4. The set of available users in the n^{th} subcarrier is $U1_n = \{1,2,...K\}, \forall n \in N$.
5. The number of subcarriers required by users $n_k, \forall k \in K$ is proportional to their data rate.

$$n_1 : n_2 : ... : n_K = R_1 : R_2 : ... : R_K$$
$$\sum_{k=1}^{K} n_k = NN_T \quad (25)$$

Then the ECBA algorithm is executed as follows:

for each subcarrier $n \in [1,..., N]$

(a) Find $u = \arg\max_{\substack{k\in U1_n \\ n_k>0}}\|\mathbf{H}_{k,n}\|^2$

$S_n = S_n \cup u$, $U1_n = U1_n - u$

$n_u = n_u - N_R$, $\rho_{u,n} = 1$

(b) *while* $size(S_n) < \hat{K}$

Find a user $\hat{u}$, $\hat{u} = \arg\min_{\substack{k\in U1_n \\ n_k>0}}\sum_{m\in S_n}\eta_{m,k}$

If no $\hat{u}$ found, break the loop, otherwise

$\rho_{\hat{u},n} = 1$, $U1_n = U1_n - \hat{u}$,

$n_{\hat{u}} = n_{\hat{u}} - N_R$, $S_n = S_n \cup \hat{u}$

end

end

3.2. Proposed subcarrier allocation algorithm

We propose our unit power based subcarrier allocation algorithm. The definition of proposed algorithm is inherited from that in ECBA.

We modify the ECBA as follow. The Freobenius norm indicates the overall energy of the channel. We find out the maximum channel Frobenius norm (MCFN) among all users for each subcarrier and order the subcarriers by their MCFN values. The subcarrier allocation is from the first to the last ordered subcarrier so that the user having higher channel energy has the priority to be served. We denote T as the set of ordered N subcarriers. Then we assume unit received power required in each receive antenna among all users and all subcarriers, so that

$$P_{k,n,i}^{r} = 1, (\forall k \in K, \forall n \in N, \forall i \in N_R) \quad (26)$$

For each subcarrier in T, the user with MCFN is selected first, subsequently the users generating maximum effective channel gains $g_{k,n}$ then requiring minimum transmit power if added in this subcarrier are selected until $\hat{K}$ is reached. The detailed algorithm is described as follow:

for each subcarrier n in T

(a) Find $u = \arg\max_{\substack{k \in U1_n \\ n_k > 0}} \left\| \mathbf{H}_{k,n} \right\|^2$

$S_n = S_n \cup u$, $U1_n = U1_n - u$

$n_u = n_u - N_R$, $\rho_{u,n} = 1$

(b) *while* $size(S_n) < \hat{K}$

Find a user $\hat{u}$, $\hat{u} = \arg \min_{\substack{k \in U1_n, \\ n_k > 0 \\ S_n = S_n \cup k}} \sum_{i=1}^{N_R} \frac{P^r_{k,n,i}}{g_{k,n,i}}$

If no $\hat{u}$ found, break the loop, otherwise

$\rho_{\hat{u},n} = 1$, $U1_n = U1_n - \hat{u}$,

$n_{\hat{u}} = n_{\hat{u}} - N_R$, $S_n = S_n \cup \hat{u}$

end

end

3.3. Bit allocation

As a result of subcarrier allocation, the set of users S_n sharing the n^{th} subcarrier is applied to calculate the effective channel gains $\mathbf{g}_{k,n}$ of the user k on the n^{th} subcarrier. Then the single user OBA algorithm described in [3] is applied to allocate bits to the assigned subcarriers with minimum power for each user.

IV. Performance Evaluation

In this section, we compare the performance of Zhang's algorithm, ECBA algorithm and proposed algorithm. The target BER is set to be 10^{-4} , the number of subcarriers is set to 32 and the number of iterations L of Zhang's algorithm is set to be 15. The noise power spectral density level is assumed to be unity ($N_0 = 1$). Two situations are considered:

(a) Single receive antenna for all users ($N_R = 1$)

The sum of target data rate of users is 256 bits/symbol. The achieved results are shown in Fig.1, 2 and 3.

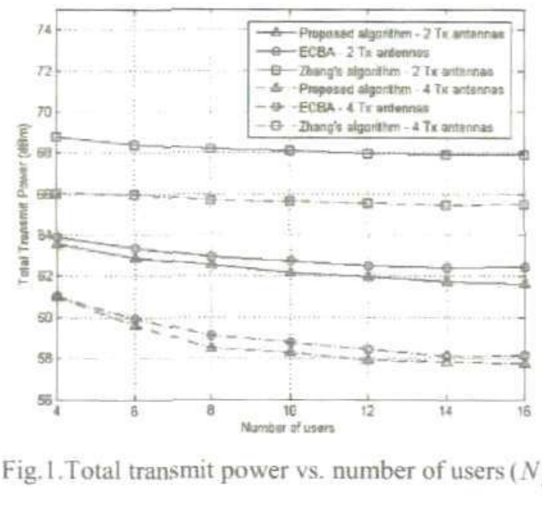

Fig.1.Total transmit power vs. number of users ($N_R = 1$)

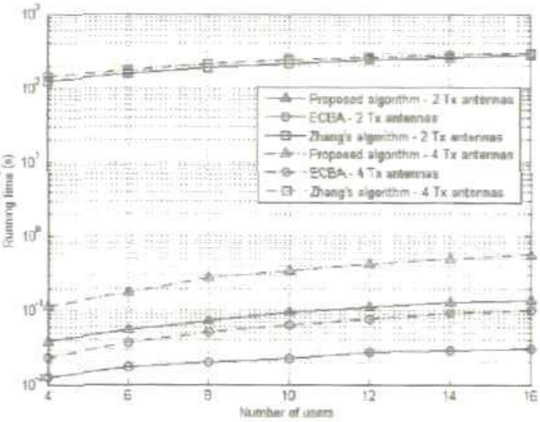

Fig.2. Running time vs. number of users ($N_R = 1$)

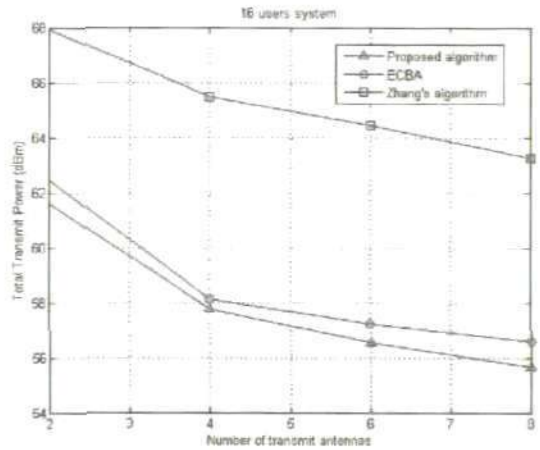

Fig.3.Total transmit power vs. number of antennas when number of users is 16 ($N_R = 1$)

(b) Multiple receive antenna for all users ($N_R = 2$)

The system capacity is increased with the growth of number of receive antennas, so the sum of target data rate of users is 512 bits/symbol. The achieved results are shown in Fig.4, 5 and 6.

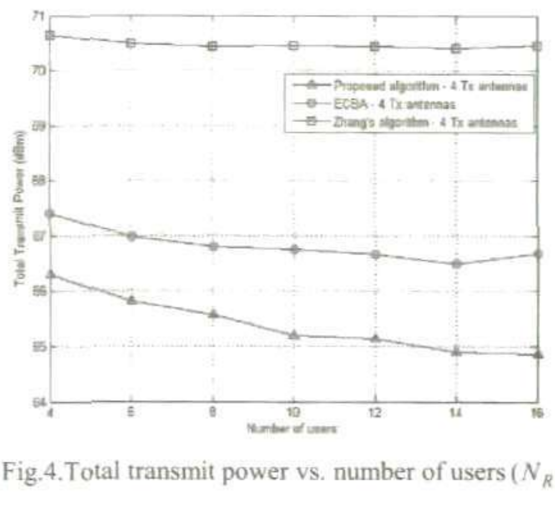

Fig.4.Total transmit power vs. number of users ($N_R = 2$)

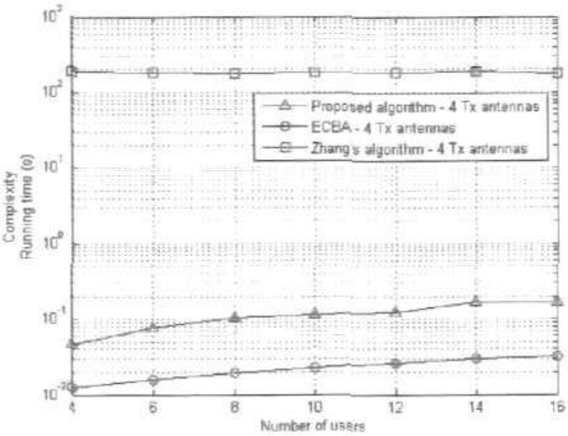

Fig.5.Running time vs. number of users ($N_R = 2$)

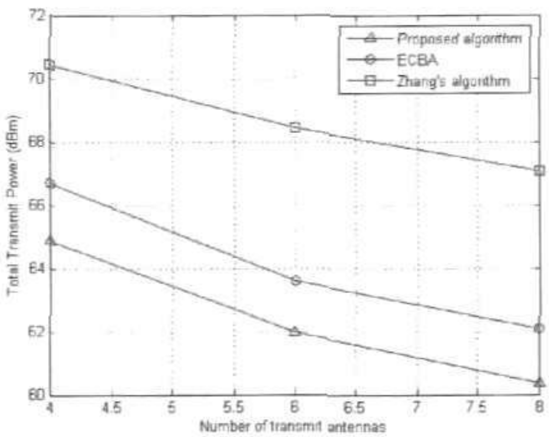

Fig.6.Total transmit power vs. number of antennas when number of users is 16 ($N_R = 2$)

Number of transmit antennas	4	6	8	10
ECBA	0.3963	0.7062	1.0130	1.3791
Proposed algorithm	0.3606	0.6722	0.9809	1.3409

Table.1. Normalized sub-channel correlations of users on their allocated subcarriers in a 16-user MIMO-OFDM system ($N_R = 2$)

With end-user using one or two receiving antennas, Fig.1 and Fig.4 show that proposed algorithm outperforms the Zhang's algorithm and the ECBA algorithm with lower total transmit power for various number of users. Increasing the number of receive antennas, the performance gap between ECBA and proposed algorithm is enlarged because the proposed algorithm reduces the correlation between sub-channels of users which is not considered by ECBA. The Table.1 shows this fact. As shown in Table.1, in the 16-user MIMO-OFDM system with different number of transmit antennas, the sum of sub-channel correlations of users on their allocated subcarriers given by proposed algorithm is always less than that given by ECBA.

Fig.2 and Fig.5 show the computing complexity required for these three algorithms, which is increased with the growth of number of users. The running time is computed using a laboratory computer processor. Faster processor may take shorter running time but the conclusion from the running time comparison for the algorithms does not change. Zhang's algorithm requires very high computation due to the iteration process. The proposed algorithm requires slightly higher computation than ECBA algorithm because of the calculation of effective channel gains. However the cost of the computation increase is in exchange of lowering the transmit power and is within limit of up to date processors.

Fig.3 and Fig.6 show that for all three algorithms, the required total transmit power is reduced as the number of transmit antennas increases under the condition of fixed number of users. And the proposed algorithm still outperforms Zhang's algorithm and ECBA algorithm as the number of transmit antennas increases.

V. CONCLUSION

In this paper, we propose a simple but efficient subcarrier allocation algorithm in the multiuser MIMO-OFDM systems. The SVD method is applied to cancel the interference among the users sharing the same subcarrier. Through comparison between proposed algorithm, Zhang's algorithm and ECBA algorithm, the proposed algorithm keeps outperforming the Zhang's algorithm and ECBA algorithm with lower total transmit power when increasing the number of transmit antennas and number of users. This lowering of transmit power comes at the cost of a slight increase in the computation complexity of proposed algorithm. However it is accepted in nowadays processors for real use.

REFERENCES

[1] Peter W. C. Chan and Roger S. K. Cheng, "Optimal Power Allocation in Zero-forcing MIMO-OFDM Downlink with Multiuser Diversity," *14th IST Mobile & Wireless Communications Summit*, 19-23 June 2005

[2] C. Y. Wong, R. S. Cheng, K. B. Lataief, and R. D. Murch, "Multiuser OFDM System with Adaptive Subcarrier, Bit, and Power Allocation", *IEEE Journal on Selected Areas in Communication*, Vol. 17, pp. 1747-1758, Oct. 1999.

[3] Fan Wu, Mosa Ali Abu-Rgheff, "An Efficient Sub-Optimal Subcarrier Allocation Algorithm for Multiuser OFDM System", *The 5th International Conference on Wireless and Mobile Communications*, pp.190-195, Cannes, La Bocca, France, Aug 2009.

[4] J. Jang and K. B. Lee, "Transmit Power Adaptation for Multiuser OFDM Systems", *IEEE Journal on Selected Areas in Communications*, vol. 21, no. 2, pp. 171-178, Feb. 2003.

[5] Ying Jun Zhang and Khaled Ben Lataief, "An Efficient resource allocation scheme for spatial multiuser access in MIMO/OFDM systems," in *IEEE Trans. Commun.*,vol. 53, pp.107-116, Jan. 2005.

[6] W.Liu, L.L. Yang and L. Hanzo, "SVD Assisted Joint Transmitter and Receiver Design for the Downlink of MIMO Systems", *The 68th IEEE Vehicular Technology Conference (VTC 2008)*, pp.1-5, Sept.2008

[7] Tianxiong Ji, Chunhui Zhou, Shidong Zhou, Yan Yao, "Low Complex User Selection Strategies for Multi-user MIMO Downlink Scenario", *IEEE Wireless Communications & Networking Conference(WCNC 2007)*, pp.1534-1539, Mar 2007